

Aus der Kinderklinik und Kinderpoliklinik im Dr. von Haunerschen Kinderspital
Klinikum der Ludwig-Maximilians-Universität München



Dissertation

zum Erwerb des Doctor of Philosophy (Ph.D.)

an der Medizinischen Fakultät der
Ludwig-Maximilians-Universität München

The role of IL-10 and TLR2 in the neonatal mouse model of obstructive nephropathy.

vorgelegt von:

Maja Agnieszka Wyczanska

aus:

Warschau / Polen

Jahr:

2025

Mit Genehmigung der Medizinischen Fakultät der
Ludwig-Maximilians-Universität München

Erstes Gutachten von: Prof. Dr. Bärbel Lange-Sperandio

Zweites Gutachten von: Prof. Dr. Markus Sperandio

Drittes Gutachten von: Priv. Doz. Dr. Monika Merkle

Viertes Gutachtes: Prof. Dr. Maciej Lech

Dekan: Prof. Dr. med. Thomas Gudermann

Datum der Verteidigung:

29.01.2025

Affidavit



Affidavit

Wyczanska, Maja

Surname, first name

Lindwurmstr. 2a

Street

80337, München, Germany

Zip code, town, country

I hereby declare, that the submitted thesis entitled:

The role of IL-10 and TLR2 in the neonatal mouse model of obstructive nephropathy.

.....

is my own work. I have only used the sources indicated and have not made unauthorised use of services of a third party. Where the work of others has been quoted or reproduced, the source is always given.

I further declare that the dissertation presented here has not been submitted in the same or similar form to any other institution for the purpose of obtaining an academic degree.

Munich, 31.01.2025

place, date

Maja Wyczanska

Signature doctoral candidate

Confirmation of congruency



LUDWIG-
MAXIMILIANS-
UNIVERSITÄT
MÜNCHEN

Promotionsbüro
Medizinische Fakultät



**Confirmation of congruency between printed and electronic version of
the doctoral thesis**

Wyczanska, Maja

Surname, first name

Lindwurmstr. 2a

Street

80337, München, Germany

Zip code, town, country

I hereby declare, that the submitted thesis entitled:

The role of IL-10 and TLR2 in the neonatal mouse model of obstructive nephropathy.
.....

is congruent with the printed version both in content and format.

Munich, 31.01.2025

place, date

Maja Wyczanska

Signature doctoral candidate

Table of content

Affidavit	1
Confirmation of congruency	2
Table of content	3
List of abbreviations	4
List of publications	5
Your contribution to the publications	6
1.1 Contribution to paper I.....	6
1.2 Contribution to paper II.....	7
2. Introductory summary	8
2.1 Congenital obstructive uropathies.....	8
2.2 UUO in neonatal mice	9
2.3 Pathophysiology of UUO.....	9
2.3.1 Inflammation	10
2.3.2 Cell death mechanisms.....	10
2.3.3 Interstitial fibrosis	11
2.4 Interleukin-10	12
2.5 Toll-like receptor 2	13
2.6 The importance of neonatal UUO research.....	13
3. Paper	16
4. Paper II	30
References	50
Acknowledgements	56

List of abbreviations

- Bax – Bcl2 associated X protein
- Bcl-2 – B-cell lymphoma 2
- CA 19-9 – Carbohydrat-Antigen 19-9
- DAMPs – Damage-associated molecular patterns
- ECM – extracellular matrix
- EGF - Epidermal growth factor
- ER - endoplasmic reticulum
- GRP78 - 78-kDa glucose-regulated protein
- HMGB1 – high mobility group box 1
- IGF-1 - Insulin-like growth factor 1,
- IL-10 – Interleukin-10
- IP-10 – Interferon gamma-induced protein 10
- JAK-2 - Janus kinase-2
- MCP1 - Monocyte Chemoattractant Protein-1
- MIP-2 α – Macrophage inflammatory protein 2
- NGAL - Neutrophil gelatinase-associated lipocalin
- RAGE - Receptor for advanced glycation end products
- STAT3 - Signal Transducer and Activator of Transcription-3
- TGF- β - Transforming growth factor β
- TH – T helper cell
- TLR2 – Toll-like receptor 2
- TNF – Tumor necrosis factor
- UPJO – Ureteropelvic junction obstruction
- UUO – unilateral ureteral obstruction

List of publications

Wyczanska M, Thalmeier F, Keller U, Klaus R, Narasimhan H, Ji X, Schraml BU, Wackerbarth LM, Lange-Sperandio B. Interleukin-10 enhances recruitment of immune cells in the neonatal mouse model of obstructive nephropathy. *Sci Rep.* 2024 Mar 6;14(1):5495. doi: 10.1038/s41598-024-55469-9. PMID: 38448513; PMCID: PMC10917785.

Wyczanska M, Rohling J, Keller U, Benz MR, Kirschning C, Lange-Sperandio B. TLR2 mediates renal apoptosis in neonatal mice subjected experimentally to obstructive nephropathy. *PLoS One.* 2023 Nov 28;18(11):e0294142. doi: 10.1371/journal.pone.0294142. PMID: 38015955; PMCID: PMC10684073.

Wyczanska M, Wacker K, Dyer PS, Werth S. Local-scale panmixia in the lichenized fungus *Xanthoria parietina* contrasts with substantial genetic structure in its *Trebouxia* photobionts. *The Lichenologist.* 2023;55(2):69-79.

Rollins RE, Yeyin Z, Wyczanska M, Alig N, Hepner S, Fingerle V, Margos G, Becker NS. Spatial variability in prevalence and genospecies distributions of *Borrelia burgdorferi* sensu lato from ixodid ticks collected in southern Germany. *Ticks Tick Borne Dis.* 2021 Jan;12(1):101589. doi: 10.1016/j.ttbdis.2020.101589. Epub 2020 Oct 10. PMID: 33096511.

Kubik MJ, Wyczanska M, Gasparitsch M, Keller U, Weber S, Schaefer F, Lange-Sperandio B. Renal developmental genes are differentially regulated after unilateral ureteral obstruction in neonatal and adult mice. *Sci Rep.* 2020 Nov 9;10(1):19302. doi: 10.1038/s41598-020-76328-3. PMID: 33168884; PMCID: PMC7653944.

Wyczanska M, Lange-Sperandio B. DAMPs in Unilateral Ureteral Obstruction. *Front Immunol.* 2020 Oct 7;11:581300. doi: 10.3389/fimmu.2020.581300. PMID: 33117389; PMCID: PMC7575708.

Your contribution to the publications

1.1 Contribution to paper I

This chapter delineates my individual contributions to the research article included in this cumulative dissertation. The publication represents a collaborative effort, and it is imperative to clarify the specific roles and responsibilities I undertook to ensure transparency and to highlight the impact of my work. The following section provides a detailed account of my involvement in the conception, execution, analysis, and writing processes for this publication.

- **Conceptualization:** I supported my supervisor in adapting the study framework in response to new questions and findings.
- **Literature Review:** I conducted a comprehensive review of existing literature to identify gaps and contextualize our research.
- **Data Collection:** I conducted the experiments and gathered the primary data, ensuring adherence to the methodological standards. This included surgery on neonatal mice and harvest of mice kidneys, serum, and biomaterial from mice tails.
- **Experimentation:** I led the laboratory work, including sample preparation, data acquisition, and troubleshooting technical issues. This included following: PCR analysis for mice genotyping, cell lysis and protein extraction including ELISA analysis of protein concentration of samples, serum sample ELISA, FACS analysis, chemokine and cytokine LUMINEX assay, western blot analysis. I also provided support in the immunohistochemical analysis.
- **Methodology Development:** I defined the experimental protocol for neonatal mouse surgery, PCR mouse genotyping, and the chemokine and cytokine LUMINEX assay used in the study.
- **Data Analysis:** I performed the statistical analyses, interpreted the results, and created the visual representations of the data for all experiments that were conducted by myself.
- **Manuscript Writing:** I wrote the initial draft of the manuscript and coordinated revisions based on feedback from co-authors and peer reviewers.

1.2 Contribution to paper II

This chapter outlines my individual contributions to the publication included in this dissertation. This paper has a shared first authorship. By providing a clear and detailed account of my roles and responsibilities, I aim to demonstrate the extent of my involvement and the value of my work within this collaborative research project.

- **Literature Review:** I conducted a comprehensive review of existing literature to identify gaps and contextualize our research.
- **Experimentation:** I led the laboratory work, including sample preparation, data acquisition, and troubleshooting technical issues. This included: Western blot analysis of TLR2, Bcl-2, Bax, GSDMD, GSMDE, HMGB1, and TNF; immunohistochemical analysis of apoptosis, tubular atrophy, fibrosis with Masson's Trichrome analysis, and α -SMA analysis.
- **Data Analysis:** I performed the statistical analyses, interpreted the results, and created the visual representations of the data. Statistical analysis was performed for all the experiments by myself. Visual representation and interpretation of the data was performed for all published results.
- **Manuscript Writing:** I wrote the initial draft of the manuscript and coordinated revisions based on feedback from co-authors and peer reviewers.

The decision on shared authorship was made based on equal contributions regarding experimental methodology for this publication.

2. Introductory summary

2.1 Congenital obstructive uropathies

Congenital obstructive uropathy, a significant contributor to chronic renal disease, refers to renal system injury, including the ureters and bladder resulting from urinary tract blockage [1]. Congenital obstructive uropathy is a urinary outflow obstruction that, without adequate therapy, limits renal developmental potential and leads to progressive deterioration of renal function [2, 3]. Congenital urinary tract obstructions are a frequent contributor to chronic kidney failure in pediatric patients [1, 4, 5]. The progression of uropathy in the developing kidney depends on the timing, intensity, and length of the obstruction [6]. Congenital obstructive uropathies are a diverse group of malformations affecting the upper and lower urinary tract, either unilaterally or bilaterally. These conditions frequently present as prenatal hydronephrosis and vary in severity. They can range from self-limiting pyelectasis and/or megaureter to a persistent physical blockage at the ureteropelvic/-vesical junction, or urethra, leading to kidney damage [1]. Urinary tract disorders detected through imaging are among the most common congenital defects, occurring in approximately 1 out of every 250 to 1,000 pregnancies [7]. Within these cases, congenital obstructive uropathies constitute the majority, accounting for around 1 out of every 2,000 pregnancies [8]. Renal malformations occur at an average rate of 1.6 per 1,000 births. With over 80% of cases identified before birth, hydronephrosis is a prevalent diagnosis [8]. Reported incidences of hydronephrosis attributed to ureteropelvic junction obstruction (UPJO) range from 39% to 64%, making UPJO the most frequent cause [9]. UPJO is generally seen as a functional issue caused by abnormalities in the smooth muscle of the pelvis and ureter [10]. UPJO is defined by a blockage at the proximal ureter where it narrows near the pelvis. This obstruction can be categorized as extramural, mural, and also as intramural, which are extremely rare in children. The most common type, mural obstruction, results from a dysfunctional ureteral segment with an irregular arrangement of smooth muscle cells and connective tissue. Mural UPJO development is primarily attributed to mechanisms such as inadequate development of the renal pelvis, irregular innervation of the pyeloureteral region, and impaired differentiation of smooth muscle cells [1, 11]. While surgery effectively prevents short-term renal lesions, growing evidence from both experimental and human studies suggests that UPJO leads to permanent changes in the renal parenchyma.

2.2 UUU in neonatal mice

In the study of obstructive uropathies, the model of unilateral ureteral obstruction (UUO) in neonatal mice and rats has proven successful, as the timing, duration and severity of the obstruction can be specifically varied as decisive factors in obstructive uropathy [1, 12, 13]. Depending on the intended severity, in adult mice, a partial or complete ligation of the ureter is performed surgically [14]. Partial ligation tends to reflect better the clinical reality of obstructive uropathies [10]. The neonatal mouse model has its limitations here, as the reproducibility of partial ligation in neonatal mice weighing 1-2 g represents a technical challenge [15]. However, the neonatal model reflects the effect of an obstruction on the still ongoing kidney development. In humans, nephrogenesis starts at the fourth or fifth week of gestation and finishes around 34–36 weeks of gestation. After this point, no additional nephrons will be formed for the individual's lifetime [16]. Conversely, in mice and rats, only one-tenth of fully developed glomeruli are present initially at birth, with the majority of kidney units maturing over the subsequent 10-14 days [17, 18]. Postnatal unilateral ureteral obstruction in rodents and congenital obstructive uropathy in humans therefore occur in the same vulnerable phase of nephrogenesis. Considering the timeline of nephrogenesis, the neonatal mouse or rat aligns with the human fetus during the middle trimester [2]. During this period, obstructive uropathies often initiate in the developing human fetus. Furthermore, since the histologic changes of experimental UUO-kidneys and human kidney biopsies of patients with ureteropelvic junction obstruction are comparable, direct conclusions can be drawn from the neonatal mouse model to the pathophysiology and effects of obstructive uropathies in the human developing kidney [10, 19, 20].

2.3 Pathophysiology of UUO

Ureteral obstruction significantly impacts renal physiology by modifying hemodynamics, altering glomerular filtration and renal metabolism, and prompting structural abnormalities in the kidney parenchyma, particularly renal fibrosis [21]. The massive dilatation of the tubules, exposed to acutely increased hydrostatic pressure following UUO, leads to mechanical stretching of the tubular epithelial cells [2, 20]. These damaged epithelial cells, together with inflammatory cells migrating into the interstitium, promote tubulointerstitial inflammation [22, 23]. Proximal tubules react early to the injury by cell death [24, 25]. This results in dysfunctional atubular glomeruli [26].

Chronic tubulointerstitial inflammation leads to the progressive development of interstitial fibrosis. Fibrosis is characterized by excessive buildup of extracellular matrix (ECM) components, such as collagens and fibronectin, primarily facilitated by activated myofibroblasts [12, 23]. Regardless of the underlying cause, fibrosis ultimately leads to the deterioration of organ structure and function.

2.3.1 Inflammation

Sterile inflammation is a result of UUO. Sterile inflammation occurs in reaction to acute or chronic tissue damage in the absence of any involvement of pathogens [22]. Following UUO, leukocytes migrate chemokine-mediated (e.g. IP-10, MIP-2 α) into the interstitium [27-29]. Together with the damaged cells, the inflammatory cells secrete cytokines, which further promote inflammation and fibrosis, like IL-1 alpha, IL-6, IL-17A, and TNF, resulting in the kidney being in an inflammatory state [23, 28, 30, 31]. This inflammatory condition contributes to tubular atrophy and interstitial fibrosis, that is typical of obstructive nephropathy [2, 23]. The recruitment and proliferation of leukocytes in the renal interstitium is closely linked to the advancement of renal injury. The activation of JAK2/STAT3 facilitates the recruitment of white blood cells to neonatal kidneys following UUO. When inhibited it leads to a significant reduction of inflammation, as shown by our lab [29]. Different leukocyte subtypes, like monocytes/macrophages, T-cells, dendritic cells and neutrophils are involved in this inflammatory state of the neonatal kidney after UUO [23]. Activated macrophages can have different impacts on the renal injury [32]. Upon activation, they can undergo differentiation at the site into pro-inflammatory M1 macrophages, triggering Th1-type adaptive immune responses and harming healthy tissues. Conversely, anti-inflammatory M2 macrophages elicit Th2-type immune responses, suppress immune responses, and foster wound healing and tissue fibrosis [33]. Macrophage accumulation and polarization play a pivotal function in the progression of a number of kidney diseases encompassing neonatal obstructive nephropathy.

2.3.2 Cell death mechanisms

One of the key characteristics of UUO is the occurrence of various forms of cell death mechanisms. Apoptosis, a type of regulated cell death, is markedly increased in the obstructed kidney during nephrogenesis [24, 34]. Apoptosis is governed by intracellular gene regulation and usually relies on the activity of non-inflammatory caspases [35]. The cleavage of PARP-1 by caspases is recognized as a distinctive feature of

apoptosis [36]. Bcl-2 was the initial gene identified to play a distinct role in natural cell death processes. It has the ability to hinder apoptosis. Bax, sharing structural similarities with Bcl-2, can counteract the protective effects provided by Bcl-2 [37]. Apoptotic characteristics encompass cytoplasmic condensation, along with phosphatidylserine exposure, membrane blebbing, and the formation of apoptotic bodies [38]. It has been shown recently that apoptosis is also regulated by endoplasmic reticulum (ER) stress, as evidenced by the enhancement of its indicators such as GRP78 [39, 40]. Apart from apoptosis, alternative types of controlled cell death also contribute to neonatal UUO. Our lab was able to demonstrate that the necrotic cell death form necroptosis is activated and contributes to inflammation following UUO in neonatal mice [24]. The necrotic cell death pathway, necroptosis, in contrast to apoptosis, induces inflammation. It is driven by receptor-interacting serine/threonine-protein kinase-3. Necroptosis is triggered by the interaction of tumor necrosis factor α with its receptor [24]. Necroptosis is characterized by the expansion of organelles, rupture of the plasma membrane, cellular breakdown, and release of intracellular contents [41]. Pyroptosis, a form of programmed necrosis, is initiated by the activation of inflammasomes [42, 43]. Inflammasomes, acting as intracellular sensors, can be triggered by extracellular DAMPs, like HMGB1 [22, 44]. Pyroptosis is defined by the gasdermin protein family's role in causing membrane perforation, leading to cell rupture, and the subsequent release of inflammatory factors such as IL-1 β and IL-18 [43]. Our lab was able to show that pyroptosis is activated in neonatal kidneys following UUO [45].

2.3.3 Interstitial fibrosis

Progressive renal disease is typified by renal fibrosis, marked by both glomerular sclerosis and interstitial fibrosis [12]. The development of interstitial fibrosis is viewed as an inadequate response to tissue injury. UUO performed in 2-day old neonatal mice leads to renal interstitial fibrosis [3, 12]. This is due to an imbalance between collagen synthesizing and degrading, reparative and destructive processes. It involves the proliferation of interstitial fibroblasts, their transition into myofibroblasts, and the accumulation of ECM components [46]. Following UUO, activated myofibroblasts, which major morphological characteristics is α -smooth muscle actin expression, are the main producers of ECM [47, 48]. The initial activation of myofibroblasts occurs via profibrotic cytokines such as TGF- β , which is secreted by damaged tubular epithelial cells and infiltrating macrophages [49]. Matrix metalloproteinase-2 is one of many factors that stimulate ECM production and accelerates the development

of renal fibrosis [50]. Many signaling pathways are associated with interstitial fibrosis. Wnt/ β -catenin signaling is of importance in wound healing and its sustained activation leads to fibrogenesis [51, 52]. Our lab was able to highlight the role of RAGE and its pathway, which through increased autophagy contributes to renal fibrosis [3]. As fibrosis advances, the intricate renal microarchitecture deteriorates. The gap between tubules and peritubular capillaries expands progressively as collagen accumulates. Prolonged diffusion pathways result in insufficient blood supply to the tubules. The hypoxia-induced tubular atrophy ultimately leads to irreversible loss of kidney function [47, 53].

2.4 Interleukin-10

Interleukin-10 (IL-10) is a cytokine with immune-inhibitory properties. Originally identified as a cytokine produced by T helper 2 cells, it is now known to be generated by a variety of cell types [54]. IL-10 is known to be produced mainly by Th-cells, monocytes, macrophages, and dendritic cells [55]. IL-10 helps to regulate both natural and acquired immune responses, shielding the organism from damage to tissues caused by immune activity by primarily suppressing inflammatory signaling [56-58]. Although IL-10 is primarily recognized for its anti-inflammatory properties, it can also exhibit pro-inflammatory functions under certain conditions [59]. Notably, IL-10 can induce pro-inflammatory effects, such as induction of cytotoxic proteins, or stimulating interferon- γ production by cytotoxic T lymphocytes [60]. Moreover, administering potent doses of IL-10 to individuals with inflammatory conditions may lead to unintended pro-inflammatory effects [61, 62]. Additionally, IL-10 is associated with ureteral obstructions. Elevated concentrations of IL-10 were observed in urinary samples of human fetuses diagnosed with urethral valves [63]. In UUO experiments with adult mice it has been shown that a deficiency in IL-10 results in heightened infiltration of both T lymphocytes and macrophages into the renal tissue, consequently intensifying the inflammatory reaction [64]. Therefore, IL-10 appears to alleviate immune reactions and decrease the infiltration of white blood cells into the kidney. In the UUO model in 7-8 week old adult mice, IL-10 has been demonstrated to mitigate regulated cell death by modulating ER stress, as evidenced by the increased expression of GRP78, a known ER marker [40]. Ultimately, IL-10 has been demonstrated to hinder tissue fibrosis in different experimental settings, including UUO studies involving adult mice [40, 64-66]. In the context of UUO, the stimulation of fibroblasts and the release of

additional extracellular matrix proteins contribute to the progression of renal tubulointerstitial fibrosis, a process that is mitigated by IL-10.[40, 64]. All this evidence for a beneficial function of IL-10 following UUO, makes it a fitting candidate to evaluate its function in the neonatal model of UUO.

2.5 Toll-like receptor 2

Toll-like receptor (TLR) 2 is a member of the TLR family, a group of conserved pattern recognition receptors found on leukocytes, myofibroblasts, and renal cells. They have the ability to detect pathogen motifs, triggering both innate and adaptive immune responses [67]. Additionally, TLR2 can be activated by DAMPs and thus generate a sterile inflammation response [68]. During acute inflammation following UUO, TLRs frequently act as major contributors of pro-inflammatory cytokines and chemokines [69, 70]. TLRs have been associated with various renal diseases. In ischemia-reperfusion injury (IRI), it is believed that internal ligands for TLR2 and TLR4 are emitted from the renal epithelium [71, 72]. Following UUO in adult mice the expression of TLR2 markedly increases [67]. Additionally, TLR2 has been shown to influence renal fibrosis, a characteristic feature of UUO [68]. TLR2 might play a role in the progression of renal fibrosis by promoting a shift towards a TH2/M2-biased phenotype [73]. In the case of a bacterial disease, TLR2 triggers through MyD88 the apoptotic cell death pathway [74]. TLR2 was shown to activate apoptosis in adult mice following UUO [67]. Additionally, HMGB1, an activator of pyroptosis, has been shown to interact with TLR2 under certain conditions [75]. The involvement of TLR2 in inflammatory cell death and renal fibrosis following UUO is currently subject to debate. Nevertheless, it is an interesting candidate for detailed analysis in the neonatal model of UUO.

2.6 The importance of neonatal UUO research

The chapters discussed above present an overview of the pathophysiology and consequences of obstructive uropathies. Congenital obstructive uropathy, along with renal hypoplasia and dysplasia, is a major factor in renal failure and contributes to nearly half of all chronic kidney disease cases in infants and children [1]. Currently, 30-40% of patients require surgical correction. Infants with UPJO are incorrectly stratified conservatively in about 20-30% of cases [76]. For functional assessment of obstructive uropathies like UPJO, repeated nuclear renal scans in infants and toddlers are essential [77, 78]. Ultrasound and nuclear scan determine the need for

surgical removal of UPJO. Yet, these nuclear scans involve radiation exposure, requiring careful consideration in young patients. This problem underlines the importance for the search for suitable biomarkers for the severity of UPJO and renal injury in order to reduce nuclear scans and radiation in infants. In most cases, UPJO will resolve without intervention [77]. Hence, the decision to wait and further observe or to proceed with surgery must be carefully weighed. Urinary biomarkers could help to better identify patients with UPJO at risk. In the search for prognostic markers for obstructive uropathies, numerous components of fetal urine have been investigated, including electrolytes, IGF-1, creatinine, EGF, CA 19-9, NGAL, TGF- β , MCP-1. Also mass spectrometric analysis of urine proteomes appears promising [1, 79-83]. It has been shown that conservatively treated patients with UPJO, in contrast to patients who had undergone surgery, showed a pathologic urine proteome pattern after 5 years, which indicates persistent pathological remodeling processes in the kidney [84]. Newest metabolome analyses can predict the need for surgery in UPJO infants even before the age of 4 months. 26 operated UPJO infants already showed a different urine metabolome in the first 4 months of life compared to the infants with spontaneously regressed hydronephrosis [85]. It is important to find possibilities to reduce or even inhibit the irreversible injury done to the kidney, to improve diagnostics and identify UPJO-kidneys at risk that would profit from early intervention (surgery). Numerous signaling pathways are activated following ureteral obstruction, with numerous target proteins for research, like in the case of IL-10 and TLR2. In human fetuses diagnosed with urethral valves, a severe condition causing lower urinary tract obstruction, elevated levels of IL-10 in the urine were observed, suggesting its potential as a biomarker for obstructive nephropathies [63]. TLRs have been associated with several renal diseases and could provide insights into the severity of kidney injury [68, 69, 72, 86]. Uncovering the exact impact IL-10 and TLR2 have on neonatal UJO-kidneys may help in understanding of the highly diverse and severe pathophysiology of obstructive uropathies. Thought out and well executed research on such target proteins and biomarkers is key. It may help to determine if a surgery is needed and when it would be best to conduct it. Only if the search and research continue it will be possible to reduce renal failure in children significantly.

3. Paper



OPEN

Interleukin-10 enhances recruitment of immune cells in the neonatal mouse model of obstructive nephropathy

Maja Wyczanska¹, Franziska Thalmeier¹, Ursula Keller¹, Richard Klaus¹, Hamsa Narasimhan², Xingqi Ji², Barbara U. Schraml², Lou M. Wackerbarth² & Bärbel Lange-Sperandio¹✉

Urinary tract obstruction during renal development leads to inflammation, leukocyte infiltration, tubular cell death, and interstitial fibrosis. Interleukin-10 (IL-10) is an anti-inflammatory cytokine, produced mainly by monocytes/macrophages and regulatory T-cells. IL-10 inhibits innate and adaptive immune responses. IL-10 has a protective role in the adult model of obstructive uropathy. However, its role in neonatal obstructive uropathy is still unclear which led us to study the role of IL-10 in neonatal mice with unilateral ureteral obstruction (UO). UO serves as a model for congenital obstructive nephropathies, a leading cause of kidney failure in children. Newborn *Il-10*^{-/-} and C57BL/6 wildtype-mice (WT) were subjected to complete UO or sham-operation on the 2nd day of life. Neonatal kidneys were harvested at day 3, 7, and 14 of life and analyzed for different leukocyte subpopulations by FACS, for cytokines and chemokines by Luminex assay and ELISA, and for inflammation, programmed cell death, and fibrosis by immunohistochemistry and western blot. Compared to WT mice, *Il-10*^{-/-} mice showed reduced infiltration of neutrophils, CD11b^{hi} cells, conventional type 1 dendritic cells, and T-cells following UO. *Il-10*^{-/-} mice with UO also showed a reduction in pro-inflammatory cytokine and chemokine release compared to WT with UO, mainly of IP-10, IL-1 α , MIP-2 α and IL-17A. In addition, *Il-10*^{-/-} mice showed less necroptosis after UO while the rate of apoptosis was not different. Finally, α -SMA and collagen abundance as readout for fibrosis were similar in *Il-10*^{-/-} and WT with UO. Surprisingly and in contrast to adult *Il-10*^{-/-} mice undergoing UO, neonatal *Il-10*^{-/-} mice with UO showed a reduced inflammatory response compared to respective WT control mice with UO. Notably, long term changes such as renal fibrosis were not different between neonatal *Il-10*^{-/-} and neonatal WT mice with UO suggesting that IL-10 signaling is different in neonates and adults with UO.

Congenital obstructive nephropathy is the main cause of kidney failure in infants and children, impairs fetal nephrogenesis and induces severe disruption of nephron maturation leading to nephron loss¹⁻⁵. Unilateral ureteral obstruction (UO) performed in neonatal mice serves as a model for congenital obstructive nephropathy. UO induces sterile inflammation, kidney injury, cell death, and renal fibrosis, leading to loss of nephron mass in the developing kidney with obstruction^{4,6,7}.

Interleukin-10 (IL-10) is an immunosuppressive cytokine, initially described as a T helper 2 derived cytokine and now known to be produced by various cell types^{8,9}. Major sources of IL-10 include T helper cells, monocytes, macrophages, and dendritic cells. IL-10 limits innate as well as adaptive immune responses and protects the host from immune-related tissue damage^{10,11}. IL-10 dampens immune responses mainly through blocking activation of inflammatory pathways^{12,13}. IL-10 is mostly known for its anti-inflammatory functions, but under certain circumstances it exhibits pro-inflammatory functions as well¹⁴⁻¹⁶. IL-10 has the capacity to elicit pro-inflammatory effects, including stimulation of granzyme B and interferon- γ production by CD8⁺ T cells¹⁷. Additionally, high-dose IL-10 treatment in patients with inflammatory disorders can be associated with undesired pro-inflammatory effects^{16,18}.

¹Department of Pediatrics, Dr. v. Hauner Children's Hospital, University Hospital, LMU Munich, Lindwurmstraße 4, 80337 Munich, Germany. ²Biomedical Center, Institute for Cardiovascular Physiology and Pathophysiology, Faculty of Medicine, LMU Munich, 82152 Planegg-Martinsried, Germany. ✉email: baerbel.lange-sperandio@med.uni-muenchen.de

IL-10 has been shown to play an important part in several renal diseases, one example being renal ischemia–reperfusion injury^{19,20}. An association between IL-10 polymorphisms and the risk of developing diabetic nephropathy has been shown²¹. In human fetuses with urethral valves, a severe form of lower urinary tract obstruction, increased urinary levels of IL-10 were measured²².

Recently it has been shown that IL-10 deficiency leads to an increase of macrophage and T-cell infiltration into kidneys following UUO in adult mice, thereby increasing the inflammatory response²³. Thus, IL-10 seems to reduce immune responses and leukocyte infiltration into the kidney. IL-10 suppresses inflammatory processes by inhibiting the secretion of a broad variety of pro-inflammatory chemokines and cytokines, like interperitoneally-10 (IP-10/CXCL10), macrophage inflammatory protein (MIP-2 α /CXCL2), and IL-1 α ^{24,25}. Additionally, cytokines released by macrophages, like IL-6 and IL-18 are also inhibited by IL-10^{26,27}. Vice versa the knock-out of IL-10 leads to an increased expression of T cell produced cytokines IL-17 and IL-22²⁸.

A central player in obstructive nephropathy is tumor necrosis factor- α (TNF- α), which mediates the inflammatory response by promoting the activation and recruitment of immune cells²⁹. The balance of TNF- α and IL-10 is important for the maintenance of immune homeostasis³⁰. To counteract exuberant production of TNF- α following injury, IL-10 is able to suppress TNF- α secretion through different mechanisms³¹.

One of the hallmarks of UUO is cell death in various forms. Apoptosis is increased in the neonatal obstructed kidney⁴. For IL-10, a blocking effect in inducing apoptosis has been reported in several disorders^{32–34}. Most importantly, in the adult model of UUO, IL-10 has been shown to attenuate apoptosis through regulating endoplasmic reticulum (ER) stress as demonstrated by the upregulation of ER markers including 78-kDa glucose-regulated protein (GRP78)²³. Besides apoptosis there are other forms of regulated cell death that play a role in neonatal UUO⁴. Necroptosis, a necrotic form of cell death, is mediated by the receptor interacting serine/threonine-protein-kinase-3 (RIPK3) and unlike apoptosis triggers inflammation³⁵. Until now, IL-10 has not been investigated in relation to necroptosis, but it has been shown that IL-10 can prevent necrosis in murine experimental acute pancreatitis implying a potential protective role of IL-10 in necroptosis³⁶.

Finally, IL-10 has been shown to inhibit organ fibrosis in several animal models including UUO in adult mice^{37–40}. In UUO, activation of fibroblasts and secretion of additional extracellular matrix components induce development of renal tubulointerstitial fibrosis⁴¹, a process which is attenuated in the presence of IL-10^{23,42}.

Because of striking differences in the pathogenesis of UUO in adults and neonates, we set out to investigate the role of IL-10 in the neonatal mouse model of congenital obstructive nephropathy. Our results surprisingly reveal a pro-inflammatory role of IL-10 inducing immune cell recruitment into the obstructed kidney in neonatal mice with UUO without altering the course of renal fibrosis development following UUO.

Materials and methods

Experimental protocol

Il-10^{-/-} mice and WT mice (C57BL/6J) were subjected to complete left ureteral obstruction or sham operation under general anesthesia with isoflurane (3–5% v/v) and oxygen (0.8 L/min) on the second day of life, as described before⁴³. The animals received carprofen (5 mg/kg) to alleviate possible pain after the surgery. The sex distribution was equal in both groups. All mice were raised in the same environmental condition, group-housed in the same room, under the same controlled temperature (20–22 °C) and photoperiods (12:12-h light–dark cycle) and fed with the same chow and water. After recovery, neonatal mice were returned to their mothers until sacrifice on day 3, 7 and 14 of life. The animals were sacrificed by cervical dislocation. The weight of the kidneys harvested was on average between 15 mg (d3) and 65 mg (d14). *Il-10*^{-/-} mice with a C57BL/6 background (B6.129P2-Il10tm1Cgn/J) were obtained from Charles River Laboratories (Sulzfeld, Germany). All experiments were performed according to national animal protection laws and the guidelines of animal experimentation established and approved by governmental committee (Regierungspräsidium von Oberbayern) (Az ROB-55.2-2532.Vet_02-19-109). This study is reported in accordance with ARRIVE guidelines.

IL-10 ELISA assay

WT mice were either subjected to UUO or not operated. At day 7 mice were sacrificed by decapitation to collect blood samples into serum-separating tubes; additionally, blood samples from adult mice were collected (neonatal UUO n = 4, neonatal mice non-operated n = 5, adult mice n = 3). The tubes were inverted 5 times, left standing for 30 min and centrifuged at 8000g for 90 s. The serum was collected and used for an IL-10 ELISA assay (R&D Systems M1000B-1, Minneapolis, MN) as per manufacturer's instructions.

Cell isolation

Kidneys were isolated from neonatal *Il-10*^{-/-} and WT mice without perfusion at day 3, 7, and 14 (n = 3 for each group) and cut into small pieces. The samples were processed as described previously⁴⁴. In brief, kidneys were digested in 2 ml of RPMI (Thermo Fisher Scientific, MA) with 200 U/ml collagenase IV (Worthington Biochemical, NJ) and 0.2 mg/ml DNase I (Roche, Switzerland) for 1 h at 37 °C while shaking (120 rpm). After digestion, cells were passed through a 70- μ m strainer and washed once with FACS buffer. Leukocytes were enriched using a 70%–37%–30% Percoll gradient by centrifugation (2000 rpm for 30 min at room temperature). Cells were collected at the 70%–37% interface. Percoll (100%) was prepared by adding nine parts of Percoll (GE Healthcare, IL) to one part of 10 \times concentrated PBS. After Percoll enrichment, cells were washed once and resuspended in FACS buffer (PBS with 1% FBS, 2.5 mM EDTA (Invitrogen, CA), 0.02% sodium azide (Sigma-Aldrich, MO)) for analysis.

Flow cytometry

For surface staining, cells were incubated with 50 μ l purified anti-mouse CD16/32/FcBlock for 10 min at 4 °C, as described previously⁴⁵. Additional antibodies were then added in FACS buffer to a final volume of 100 μ l at 4 °C for 20 min. After staining, cells were washed twice and resuspended in FACS buffer for analysis. Dead cells were excluded from analysis by fixable viability dye eFluor™ 780 (Thermo Fisher Scientific, MA). Flow cytometry was performed on an LSR Fortessa (BD Biosciences, NJ) with subsequent data analysis using FlowJo software (Tree Star). Cells were quantified by using CountBright Absolute Counting Beads (Thermo Fisher Scientific, MA). The following antibodies were purchased from Biolegend: anti-CD45.2-R-phycoerythrin-cyanine 7 (PECy7) (clone: 104), anti-MHCII I-A/I-E-AF700 (clone: M5/114.15.2), anti-CD11c-BV786 (clone: N418), anti-CD3e-PECy5 (clone: 145-2C11), anti-CD19-BV650 (clone: 6D5), anti-Ly6G-Peridinin-chlorophyll (PerCP)-Cy5.5 (clone: 1A8), anti-F4/80-AF647 (clone: BM8), anti-CD24-BUV395 (clone: M1/69), anti-CD64-PE (clone: X54-5/7.1), anti-Ly6C-BV605 (clone: HK1.5). The following antibodies were purchased from BD Biosciences: anti-CD11b-Brilliant UltraViolet (BUV) 737 (clone: M1/70).

Identification of infiltrating macrophages and T-lymphocytes

The abundance of infiltrating macrophages and T-lymphocytes in the neonatal kidney was examined by immunohistochemical staining. Formalin-fixed, paraffin-embedded kidney sections were subjected to antigen retrieval and incubated with either rat anti-mouse F4/80 antibody (Cell Signaling Technology #70076, MA, 1:200) or anti-human CD3 antibody (Serotec MCA 1477, Bio-Rad, UK) (n = 10 for each group). Specificity was assessed through simultaneous staining of control sections with an unspecific, species-controlled primary antibody. Biotinylated mouse anti-rabbit IgG (Santa Cruz Biotechnology sc2491, TX) and goat anti-rat IgG (Southern Biotech 3050-8, AL) were used as secondary antibodies. Sections were incubated with ABC reagent (Vectastain PK6100, Vector Laboratories, CA), detected with DAB (CD3: Dako, Agilent Technologies, CA, #K3468) (F4/80: Vectastain, Vector Laboratories, CA) and counterstained with methylene blue or hematoxylin. Images were taken using the LEICA DM1000 microscope and the digital camera (LEICA ICC50HD, Germany). Macrophages and CD3-positive lymphocytes in cortex and medulla were counted in twenty nonoverlapping high-power fields at 400 \times magnification and were analyzed in a blinded manner. Data were expressed as the mean score \pm SEM per 20 high-power fields.

Cytokine and chemokine protein expression

Kidneys of UUO and control mice were harvested on 3, 7 and 14 days of life (n = 3 in each group) as described previously⁴. In brief, kidneys were homogenized in protein lysis buffer (Tris 50 mM, Na₂VO₂ 1 mM, 2% SDS) containing protease inhibitor cocktail (Roche, Switzerland, #1836153). The protein content of the supernatants was measured using the BCA Protein Assay Kit (ThermoFisher, MA, Pierce #23225). The supernatants were diluted to contain the same protein concentration. Expression of 36 cytokines and chemokines (i.a. IP-10, MIP-2 α , IL-1 α , IL-17A, IL-4, eotaxin, ENA-78) was determined by Luminex multiplex assay (ThermoFisher, MA, cat. No. EPX360-26092-901) as per manufacturer's instructions.

Detection of apoptosis

Apoptotic cells were detected by the terminal deoxynucleotidyl transferase (TdT)-mediated dUTP-biotin nick end labeling (TUNEL) assay, as described before⁴. Briefly, 4% formalin-fixed tissue sections were deparaffinized and rehydrated in ethanol, followed by incubation with proteinase K. After quenching, equilibration buffer and working strength enzyme (ApopTag Peroxidase In Situ Apoptosis Detection Kit, Millipore, MA) were applied. If the nuclei were stained black and displayed typical apoptotic morphology cells were regarded as TUNEL-positive. Apoptosis in each kidney was calculated by counting the number of TUNEL-positive tubular and interstitial cells in 20 sequentially selected fields at 400 \times magnification and expressed as the mean number \pm SEM per 20 high-power fields using the LEICA DM1000 microscope and the digital camera (LEICA ICC50HD, Germany) (n = 10 for each group).

Measurement of interstitial fibrosis

Interstitial collagen deposition was measured in Masson's trichrome-stained sections as described before⁶. Digital images of the sections were superimposed on a grid, and the number of grid points overlapping interstitial blue-staining collagen was recorded for each field. In addition, formalin-fixed and paraffin embedded sections were subjected to antigen retrieval and incubated with mouse anti-mouse α -smooth muscle actin antibody (Sigma Aldrich, Germany, A2547, 1:400) as shown before⁶. Biotinylated horse anti-mouse IgG (Santa Cruz, Germany) was used as a secondary antibody. Sections were incubated with ABC reagent (Vectastain PK 6100, Vector Laboratories, CA), detected with AEC-Mix Romulin (Biocare 901-RAEC810-082117, CA) and counterstained with hematoxylin. Digital images of the sections (n = 10 in each group) were superimposed on a grid, and the number of grid points overlapping collagen I fibers or α -smooth muscle actin fibers was recorded for each field. Twenty non-overlapping high-power fields at 400 \times magnification were analyzed in a blinded fashion. Data were expressed as the mean score \pm SEM per 20 high power fields.

Western immunoblotting

Il-10^{-/-} and WT male and female neonatal mice underwent UUO surgery or sham operation at the second day of life for Western blot analysis. Kidneys were harvested on 3, 7 and 14 days of life (n = 3 in each group), homogenized in protein lysis buffer (Tris 50 mM, Na₂VO₂ 1 mM, 2% SDS) containing protease inhibitor cocktail (Roche, Switzerland, #1836153). The protein content of the supernatants was measured using the BCA Protein Assay Kit (ThermoFisher, MA, Pierce #23225). 20 μ g of protein were separated on polyacrylamide gels at 160 V

for 45 min and blotted onto nitrocellulose membranes (100 mA per gel, 120 min). After blocking antibody-specific for 2 h in Tris-buffered saline with Tween-20 containing 5% nonfat dry milk and/or BSA, blots were incubated with primary antibodies 2 h at room temperature or at 4 °C overnight. PARP antibody (Cell Signaling Technology #9542, MA, 1:500), RIPK3/RIP3 antibody (Novus Biologicals #77299, Germany, 1:2000), GRP78/BiP antibody (Cell Signaling Technology #3183, MA, 1:1000), α -SMA antibody (Sigma Aldrich A2547, Germany, 1:5000), β -catenin antibody (Upstate Biotechnology 05-665, Fisher Specific, NY, 1:200), and TGF- β antibody (Cell Signaling Technology #3711, MA, 1:2000) were used for western blot analysis. GAPDH (Bioss Meridian LifeScience H86540M, Memphis, TN, 1:40,000) was used as an internal loading control and to normalize samples. Blots were washed with Tris-buffered saline with Tween-20 and incubated with horseradish peroxidase-conjugated secondary antibody for 1 h at room temperature. Immune complexes were detected using enhanced chemiluminescence method. Blots were exposed to x-ray films (Kodak, Germany), the films were scanned, and protein bands were quantified using the densitometry program Image J. Each band represents one single neonatal mouse kidney.

Statistical analysis

Data are presented as x-fold increase after UO. For this the results obtained from analysis of UO kidneys are divided by the average of sham results. This form of presentation allows us to show the actual impact of UO with the sham-measurements as basis. Data are presented as mean \pm standard error. Comparisons between groups were made using one-way analysis of variance followed by the Student–Newman–Keuls test. Comparisons between left and right kidneys were performed using the Students *t*-test for paired data. Statistical significance was defined as $p < 0.05$.

Results

Neonatal UO induces upregulation of IL-10 serum concentrations in neonatal WT mice

We performed unilateral ureteral obstruction (UO) in neonatal mice at day 2 of life and measured concentrations of serum IL-10 at day 7 of life by ELISA. IL-10 concentrations in UO mice increased significantly in comparison to neonatal non-operated control mice (Fig. 1a) confirming earlier reports in adult mice with UO²³. We also measured IL-10 concentrations in serum of adult non-operated mice; notably, the IL-10 concentrations were too low to detect compared to IL-10 concentrations in neonatal mice.

Leukocyte infiltration into obstructed kidneys of neonatal mice is reduced in the absence of IL-10

Because IL-10 deficiency led to an increase in recruited leukocytes into kidneys from adult mice subjected to UO²³, we profiled leukocyte infiltration in neonatal *Il-10*^{-/-} and WT mouse kidneys with UO using FACS analysis. Surprisingly, neonatal *Il-10*^{-/-} mice showed less leukocyte infiltration in both sham-operated and UO-kidneys compared to respective WT mice (Fig. 1b–d). We also performed a steady state analysis; no differences were found between sham-operated and non-operated kidneys in both lines (Supplementary Material Fig. S1) indicating that there is no induction of leukocyte recruitment in sham-operated neonatal *Il-10*^{-/-} and WT mice. Next, we analyzed leukocyte subpopulations including Ly6G⁺ neutrophils, CD11b^{hi} cells, CD3⁺ T-cells, and type 1 and type 2 conventional dendritic cells, including CD11b^{hi}CD64⁺ DC like cell type and F4/80⁺ macrophages (here called cDCs). The gating strategy is shown in Supplementary Fig. S2, as recently reported⁴⁶. UO induced an increase in the infiltration of all leukocyte subtypes investigated (Fig. 2). This was true for the frequency, which is defined as the percentage of subtype number to total leukocyte number. We then studied the influence of IL-10 on the infiltration of leukocyte subsets. Compared to UO in neonatal WT mice, infiltration of neutrophils was most prominently reduced in d14 *Il-10*^{-/-} mice with UO (Fig. 2a). We also found some reduction in the infiltration of CD11b^{hi}, cDCs, and T-cells in neonatal *Il-10*^{-/-} compared to WT mice with UO (Fig. 2b–d). These findings on leukocyte subset infiltration were confirmed for CD3⁺ and F4/80⁺ cells by immunohistochemistry (Fig. 3), suggesting that loss of IL-10 attenuated leukocyte infiltration into obstructed kidneys of neonatal mice which is the opposite to findings in adult mice with UO²³. Results of these analyzes in sham-operated kidneys only are displayed in Supplementary Fig. S3.

Release of cytokines and chemokines after UO is reduced in neonatal *Il-10*^{-/-} mice

To assess released cytokines and chemokines in the kidney after neonatal UO in the presence and absence of IL-10, a Luminex analysis of 36 chemokines and cytokines was performed in *Il-10*^{-/-} and WT mice at day 7 and 14 of life (Fig. 4a–f). At day 7, UO provoked a marked increase in IP-10 release in both *Il-10*^{-/-} and WT mice, while we observed no substantial release of MIP-2 α , IL-1 α , IL-17A, eotaxin, and ENA-78 in *Il-10*^{-/-} and WT mice at day 7 of life (Fig. 4a–f). All here investigated cytokines were released at much higher quantities in WT mice with UO at day 14 of life compared to respective *Il-10*^{-/-} mice with UO at day 14 of life (Fig. 4a–f), suggesting a potential pro-inflammatory role of IL-10 in obstructed kidneys of neonatal mice. Expression of these chemokines and cytokines in sham-operated kidneys only are displayed in Supplementary Fig. S4. We also measured interleukin-4 (IL-4) in obstructed kidneys (Supplementary Fig. S5), however it did show neither a response to UO nor a difference between *Il-10*^{-/-} and WT kidneys.

Necroptosis but not apoptosis is reduced in neonatal *Il-10*^{-/-} mice following UO

Next, we assessed the rate of apoptosis and necroptosis in neonatal mice following UO. Tubular apoptosis in neonatal *Il-10*^{-/-} and WT sham-operated and UO kidneys was measured by TUNEL staining for apoptotic nuclei (Fig. 5a,b). The number of tubular apoptotic cells in neonatal kidneys following UO increased in a similar fashion in both *Il-10*^{-/-} and WT mice (Fig. 5a,b). Additionally, full length expression of PARP as a read

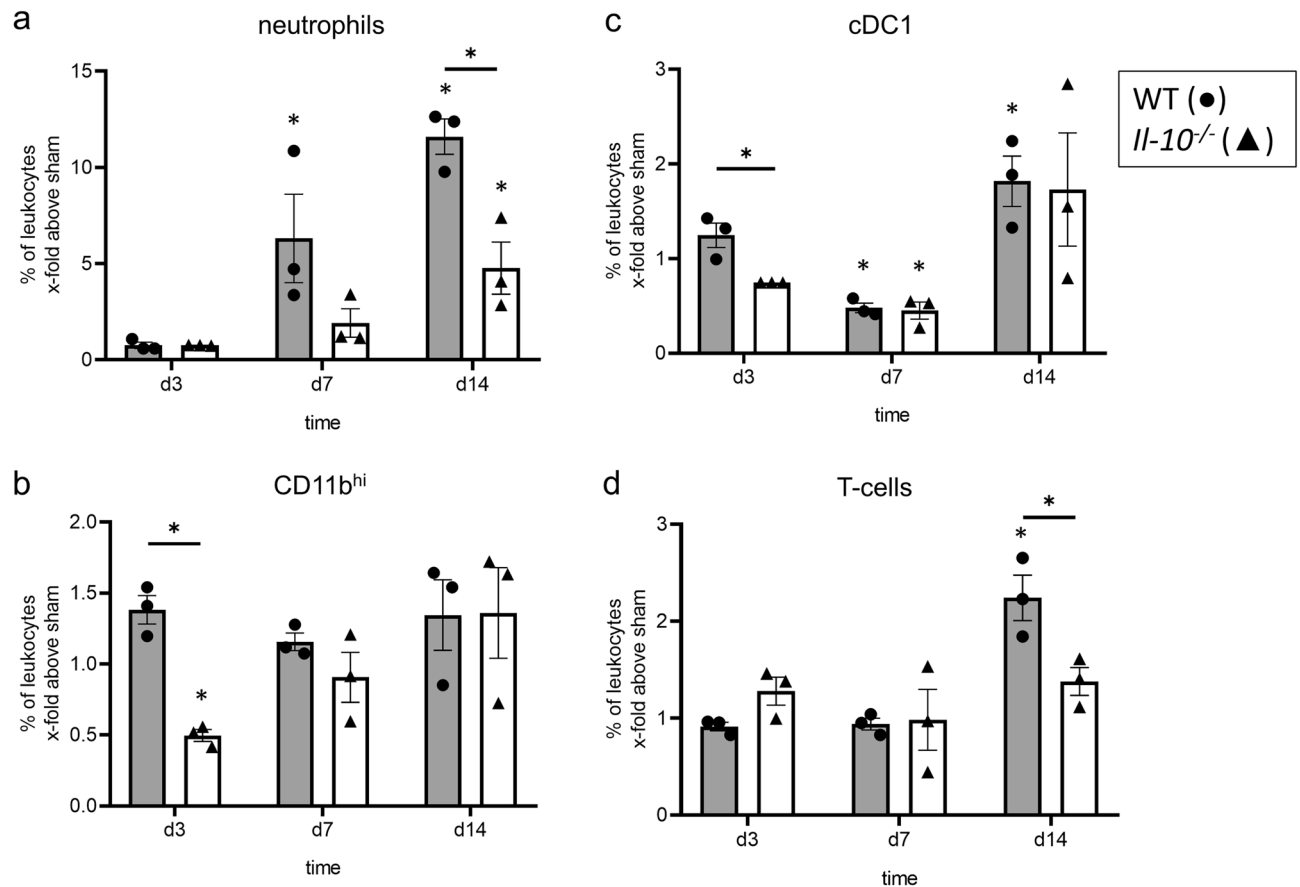


Figure 2. IL-10 induces the infiltration of neutrophils, macrophages, dendritic cells and T-cells after neonatal UUO. Neonatal mice were subjected to UUO or sham operation. Frequency of renal Ly6G⁺ neutrophils (**a**), CD11b^{hi} cells (**b**), cDC1 dendritic cells (**c**), and CD3⁺ T-cells (**d**) at the indicated ages are shown. Neutrophils infiltrated the obstructed kidney; the infiltration was lower in the *Il-10*^{-/-} than in the WT (**a**). UUO induced infiltration of CD11b^{hi} cells (**b**) and dendritic cells (**c**); the infiltration was lower in the *Il-10*^{-/-} compared to the WT on d3. T-cells infiltrated the kidney following UUO; T-cell infiltration was lower in the *Il-10*^{-/-} in comparison to WT on d14 (**d**). Results are indicated as x-fold increase above sham operated control; n = 3; *p < 0.05. Data are presented as individual points with mean ± SEM. Standalone * represents significant differences between Sham and UUO results.

significantly different only at day 7 of life (Fig. 6f) (uncropped western blot image: Supplementary Fig. S12). Expression of these fibrosis markers in sham-operated kidneys only is displayed in Supplementary Fig. S13. From these findings we conclude that IL-10 does not play a major role in the development of renal fibrosis in neonatal kidneys with UUO.

Discussion

Interleukin 10 is an anti-inflammatory and antifibrotic cytokine produced by a broad variety of cells^{11,18}. Hence, we investigated a potential anti-inflammatory role of IL-10 in neonatal kidneys with obstructive nephropathy. Obstructive nephropathies belong to the congenital anomalies of kidneys and urinary tract (CAKUT) and are one of the leading causes for kidney failure in children^{47,48}. Using *Il-10*^{-/-} mice, we demonstrate that IL-10 stimulates the recruitment of immune cells into the obstructed neonatal kidney. In addition, we show IL-10 dependent release of pro-inflammatory cytokines and chemokines within the obstructed neonatal kidney. This is in contrast to findings in adult mice with UUO where IL-10 was reported to exert anti-inflammatory effects in obstructed kidneys²³. However, our study has its limitations, as the usage of *Il-10*^{-/-} and WT littermates was not possible due to the low age required for the UUO surgery. This may lead to a potential bias.

We also found that IL-10 is upregulated after UUO in serum samples of neonatal WT mice, which provides additional support of a potential role of this cytokine in modulating immune responses in obstructive nephropathy. Immune cells are important mediators of the inflammatory response after UUO^{49–52}. Following obstruction, neonatal kidneys of *Il-10*^{-/-} mice displayed a reduced number of infiltrating leukocytes, especially neutrophils, CD11b^{hi} cells, F4/80⁺ cells, cDC1, and T-cells. By contrast, in adult mice with UUO the absence of IL-10 led to an increase in the number of infiltrated T-cells and F4/80⁺ cells in the obstructed kidneys²³. This differential regulation in neonatal and adult mice suggests that IL-10 may have an influence on the overall development and/or recruitment of immune cells in the neonatal period, thus inducing a different immune response to UUO

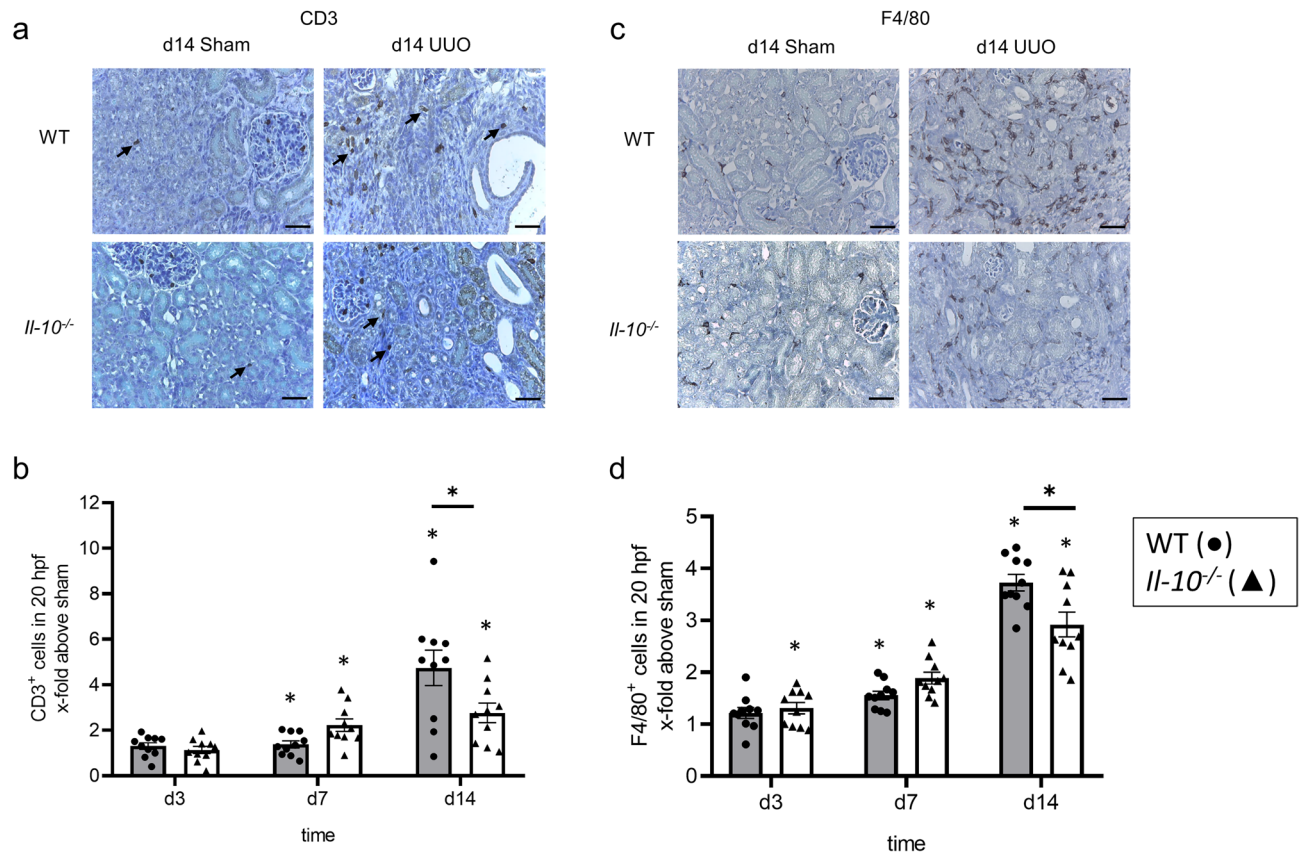


Figure 3. Immune cell infiltration of CD3⁺ and F4/80⁺ cells. Immunohistological staining for CD3 (positive cells marked with arrows), a marker for T-cells and F4/80, a macrophage and dendritic cells marker, of WT sham and UUO, and *Il-10*^{-/-} sham and UUO mice on d14 (a,c). Neonatal UUO induced infiltration of CD3⁺ T-cells in the kidney; the infiltration was lower for *Il-10*^{-/-} compared to WT on d14 (b). Following UUO F4/80⁺ cells infiltrated the kidney, with more cells infiltrating *Il-10*^{-/-} on d7 and fewer cells on d14 (d). The gating strategy for these leukocyte subpopulations can be found in Supplementary Fig. S2. Results are indicated as x-fold increase above sham operated control in 20 hpf (×400); n = 10; *p < 0.05. Data are presented as individual points with mean ± SEM. Bar = 100 μm. Standalone * represents significant differences between Sham and UUO results.

compared to adult mice. In *Il-10*^{-/-} mice cDC1 and CD11b^{hi} cells show a delayed infiltration into the obstructed kidney in comparison to WT, which emphasizes the possibility of a still unknown function of IL-10 in the development of the immune system during the neonatal period. In neonatal UUO, nephrogenesis is still ongoing with constant changes in gene regulation and composition of the immune system in the kidney^{46,53}. Even under basal conditions several of our markers already show diminished expression in *Il-10*^{-/-} mice compared to WT.

IL-10 is known as an anti-inflammatory cytokine that limits innate immune responses mainly by inhibition of pro-inflammatory cytokines¹¹. Since the markers we used to assess infiltration of leukocytes don't assess their degree of activation, we also analyzed the chemokine and cytokine profiles in the neonatal kidneys of *Il-10*^{-/-} and WT mice following UUO. Surprisingly, neonatal *Il-10*^{-/-} mice with UUO showed a reduction in pro-inflammatory cytokine and chemokine content in obstructed kidneys when compared to WT with UUO, mainly of IP-10, IL-1α, MIP-2α, IL-17A, eotaxin, and ENA-78. These results are congruent with the reduction of infiltrating leukocytes into the neonatal kidney and demonstrate again the differential regulation of immune responses by IL-10 in the neonatal versus adult organism. Under inflammatory conditions a variety of cells can express the chemokines IP-10 and MIP-2α, which attracts inflammatory cells in different renal diseases^{54–56}. Here, we show an increase in levels of IP-10 and MIP-2α following neonatal UUO, which was markedly reduced in neonatal *Il-10*^{-/-} mice in comparison to neonatal WT mice. Contrary to our findings, in the model of cisplatin nephrotoxicity IL-10 deficiency in adult mice has been shown to induce an increase of IP-10 levels in the kidney²⁴. Additionally, IL-10 has been shown to decrease MIP-2α after infection^{57,58}. In the adult UUO model, MIP-2α mRNA expression increased greatly in the obstructed kidney⁵⁹. Low concentration of MIP-2α after neonatal obstruction may be also due to low concentration of IL-17A, an activator of MIP-2α production. IL17A induces cytokine production in renal epithelial cells⁶⁰. Deficiency of IL-17A attenuated injury in a renal ischemia reperfusion model⁶¹. Following UUO in adult mice, IL-17A increased and induced renal fibrosis⁶². IL-10 has been shown to suppress IL-17A production in various models^{58,63}. In the neonatal setting, we observed a significant reduction in IL-17A levels in obstructed kidneys of neonatal *Il-10*^{-/-} mice compared to neonatal WT mice. This could be related to the fact that IL-17A is mostly produced by T-cells which are reduced in number in obstructed neonatal kidneys

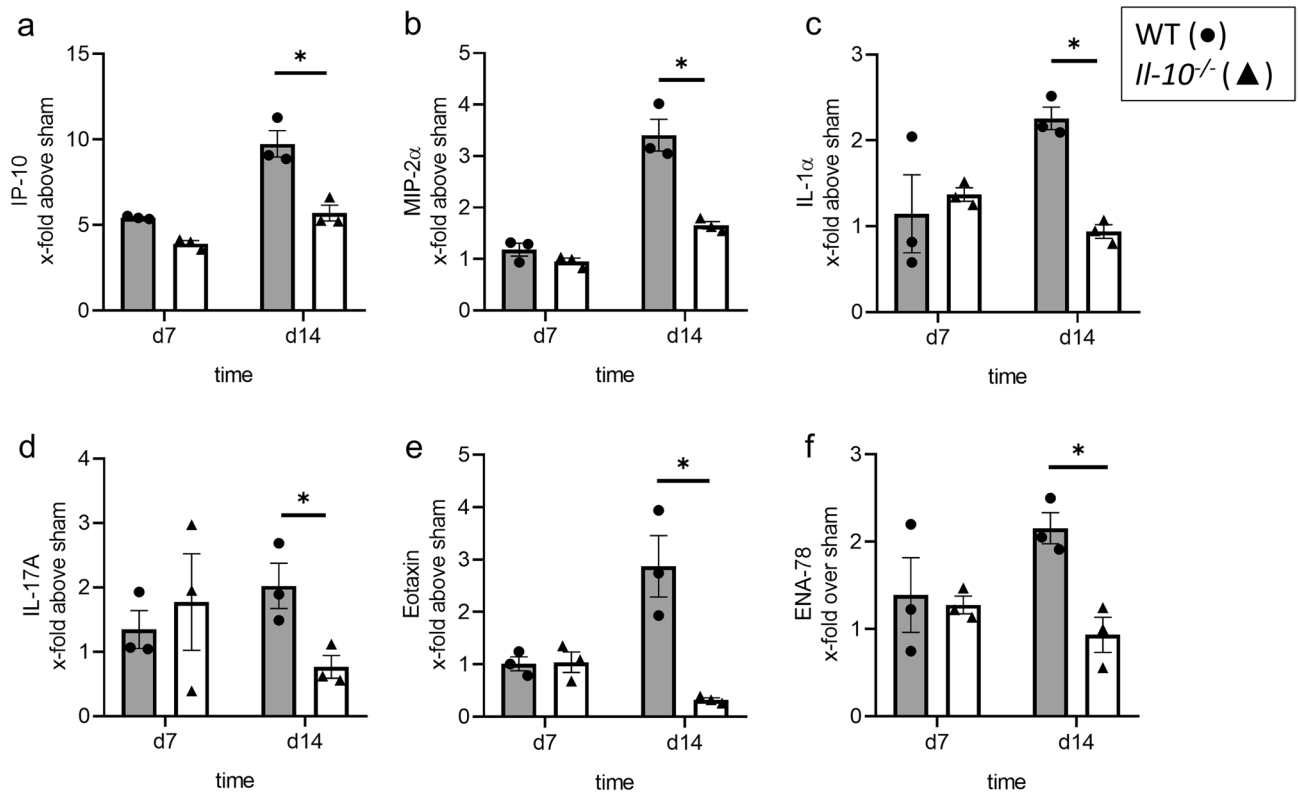


Figure 4. IL-10 influences cytokine and chemokine release after neonatal UUO. Whole sham-operated and UUO kidneys of neonatal mice were harvested and analyzed for cytokine and chemokine concentration. IP-10/CXCL10 concentration increased markedly after UUO, with a lower increase in *Il-10^{-/-}* kidneys compared to WT (a). UUO induced IL-1α release in WT kidneys, but not in *Il-10^{-/-}* on d14 (b). MIP-2α/CXCL2 increased following UUO, the increase was lower in the *Il-10^{-/-}* kidneys in comparison to WT (c). Neonatal UUO induced IL-17A release, the concentration of IL-17A was lower in *Il-10^{-/-}* compared to WT on d14 (d). Following UUO concentrations of the chemokines eotaxin/CCL11 (e) and ENA-78/CXCL5 (f) increased in WT mice, while no increase was observed in *Il-10^{-/-}* mice on d14. Concentration is indicated as x-fold increase above sham operated control; n = 3; *p < 0.05. Data are presented as individual points with mean ± SEM. Standalone * represents significant differences between Sham and UUO results.

of *Il-10^{-/-}* mice. We also investigated IL-1α, a cytokine which is a key mediator of sterile inflammation^{4,64,65}. Neonatal UUO induced IL-1α release in WT, but not in *Il-10^{-/-}* kidneys. The observed increase of IL-1α in neonatal WT UUO kidneys is in line with our previous findings⁴. However, IL-10 has been shown to suppress IL-1α production by resident peritoneal macrophages in vitro⁶⁶. This contrasts with our finding suggesting a differentially regulated interplay between IL-1α and IL-10 in neonatal and adult mice with UUO. The increased concentration of chemokines following UUO in WT in comparison to *Il-10^{-/-}* shows a possible mechanism driving the pro-inflammatory role of IL-10 in neonatal UUO. IP-10 is mostly known for its role in recruiting T cells⁶⁷. MIP-2α, MIP-1β, and GM-CSF play a role in macrophage recruitment^{68–70}. Eotaxin, although mostly associated with eosinophil recruitment, was shown to be critical in mammary gland development and also takes part in the inflammatory response in diabetic nephropathy^{71,72}. Overall, the cytokines and chemokines we investigated here are also involved in neutrophil recruitment, especially ENA-78 being the epithelial neutrophil-activating protein^{64,73–76}. The reduction of these chemokines in the obstructed kidneys of *Il-10^{-/-}* mice is in line with the observed reduction of the infiltration of neutrophils, macrophages, and T cells into the obstructed kidneys of neonatal *Il-10^{-/-}* mice. IL-10 promotes proliferation and activation of CD8⁺ T cells and thus release of cytokines and chemokines by these cells¹⁶. In a model of human endotoxemia an upregulation of interferon-γ and the chemokine IP-10 associated with it was observed after administration of recombinant human IL-10⁷⁷. This may indicate that IL-10 is regulated differently in neonatal and adult mice with a pro-inflammatory function in the neonatal kidney via recruitment of immune cells through increased secretion of chemokines.

Our findings propose a differential regulation of IL-10 in the neonatal period. In fact, the neonatal immune system differs significantly from the adult one with marked suppression of pro-inflammatory canonical NF-κB signaling and activation of anti-inflammatory non canonical NF-κB signaling, as recently demonstrated⁷⁷. This shifted balance reflects a fine-tuned adaption during the transition from fetal life in a protected environment to postnatal life with the sudden exposition of the neonate to a microbial-rich outside world⁷⁸. Interestingly, in a sepsis model it has been shown that infants have a diminished response to IL-10 and the expression of the IL-10 receptor is strongly reduced in neonatal T-cells^{79,80}. Recently it has been shown that IL-4 enhances IL-10 production, and the lack of its receptor inhibits IL-10 production in Th1 cells⁸¹. The concentration of IL-4 we measured

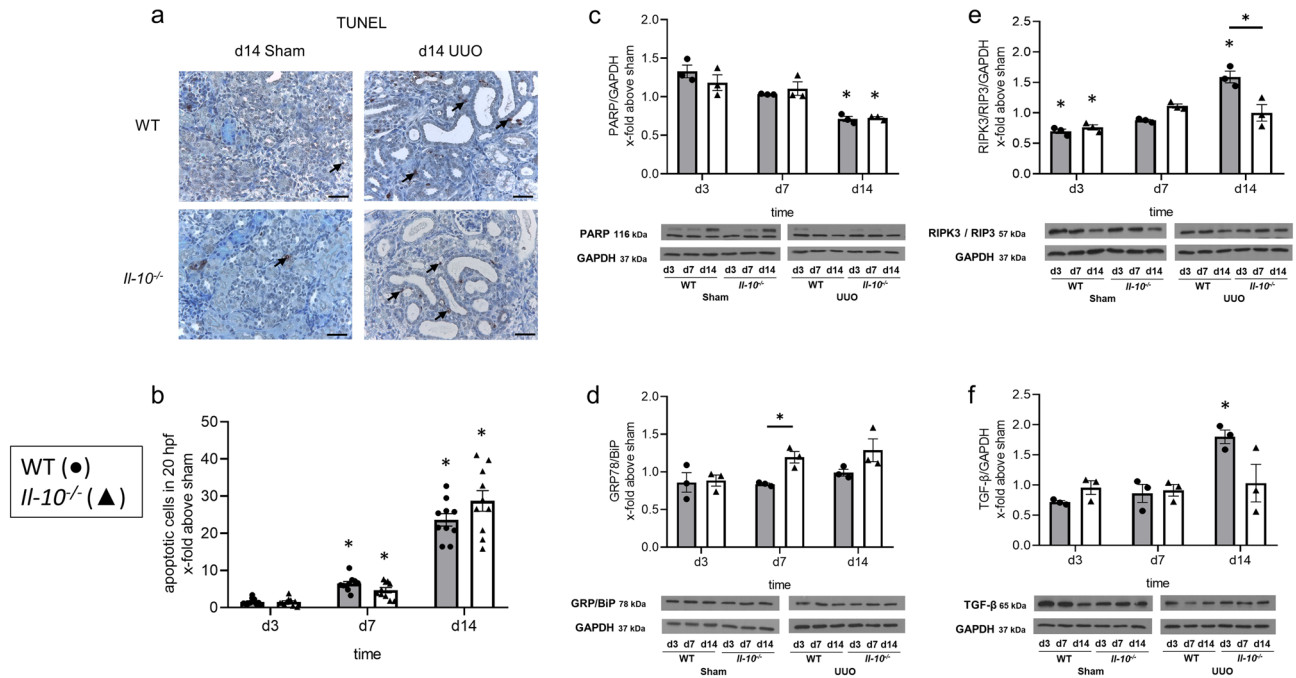


Figure 5. Cell death in neonatal *Il-10*^{-/-} mice in comparison to the WT. Apoptotic cells in sham-operated and UUO kidneys were detected by TUNEL staining in sections. TUNEL-positive cells (marked with arrow) in WT sham and UUO, and in *Il-10*^{-/-} sham and UUO appeared in distal tubules (a). Number of tubular apoptotic nuclei increased following UUO, without significant differences between neonatal *Il-10*^{-/-} and WT kidneys (b). Whole kidneys were processed for western blot analysis at day 3, 7 and 14. Expression of PARP, a marker for apoptosis, which is cleaved in the process of cell death, decreased following UUO, but was not significantly different between *Il-10*^{-/-} and WT mice (c). ER stress, measured by the expression of GRP78/BiP, increased following UUO and was increased in *Il-10*^{-/-} kidneys on d7 compared to WT (d). Expression of RIPK3, a marker for necroptosis, increased after UUO, but with a weaker increase in the *Il-10*^{-/-} compared to WT (e). UUO induced TGF-β expression with a decreasing trend for *Il-10*^{-/-} in comparison to WT (f). The shown western blot images are cropped, for uncropped western blots see Supplementary Figs. S4–S7 online. Expression is indicated as x-fold increase above sham operated control; n = 3 for western blot analysis and n = 10 for immunohistochemical staining; *p < 0.05. Data are presented as individual points with mean ± SEM. Bar = 100 μm. Standalone * represents significant differences between Sham and UUO results.

in neonatal obstructed kidneys did show neither a response to UUO nor a difference between *Il-10*^{-/-} and WT. IL-4 is also a product of the IL-10 pathway, the fact that it's not upregulated after UUO in our model indicates that the mechanism of IL-10 production and its effects in response to injury are differentially regulated in neonates and adults. Future studies are warranted to uncover the molecular mechanisms of IL-10 driven pro-inflammatory response to injury in neonatal development.

Cell death is an important hallmark of UUO. UUO induces apoptosis in the developing kidney with obstruction. However, we did not observe a difference in full length PARP expression following UUO in both neonatal *Il-10*^{-/-} and WT kidneys indicating that IL-10 has no impact on the induction of apoptosis in neonatal UUO. TUNEL staining of tubular apoptotic nuclei further confirmed our findings regarding apoptosis. Recently it has been shown that ER stress induced by UUO in adult mice is a major source for apoptosis in this model and IL-10 protects the kidney by suppressing ER stress in adult mice⁴². In our study we show that neonatal UUO induces ER stress in the kidney through GRP78/BiP expression and we also observed for one time point (day 7) more ER stress in *Il-10*^{-/-} in comparison to WT. However, for the other time points we found no differences suggesting that IL-10 has no impact on ER stress in neonatal UUO. Apoptosis is highly upregulated during nephrogenesis⁸², given this slight differences between the transgenic lines may not be detectable in our model.

Besides apoptosis we also measured necroptosis, a pro-inflammatory form of regulated necrosis, in which RIPK3 is involved^{83,84}. Following UUO, the protein expression of RIPK3 increased in neonatal WT kidneys. However, *Il-10*^{-/-} did not show this increase which then also became significant at day 14. Whether TGF-β is involved here is not clear at the moment. TGF-β has been described to activate RIPK3-dependent cell death pathways leading to necroptosis⁸⁵. Our results did not find a significant difference, but a decreasing trend in TGF-β expression in obstructed kidneys of *Il-10*^{-/-} versus WT mice.

End-stage outcome of the UUO model is severe interstitial fibrosis in the obstructed kidney. The basis for fibrotic diseases consists of expansion of connective tissue and abnormal deposition of fibrotic collagen fibers. The main source of extracellular matrix in renal fibrosis are myofibroblasts⁸⁶. We measured the quantity of fibrotic collagen fibers, as well as evaluated myofibroblasts in neonatal *Il-10*^{-/-} and WT kidneys. The results show an overall increase in fibrotic fibers and α-SMA expression (a myofibroblast marker after UUO) with no significant

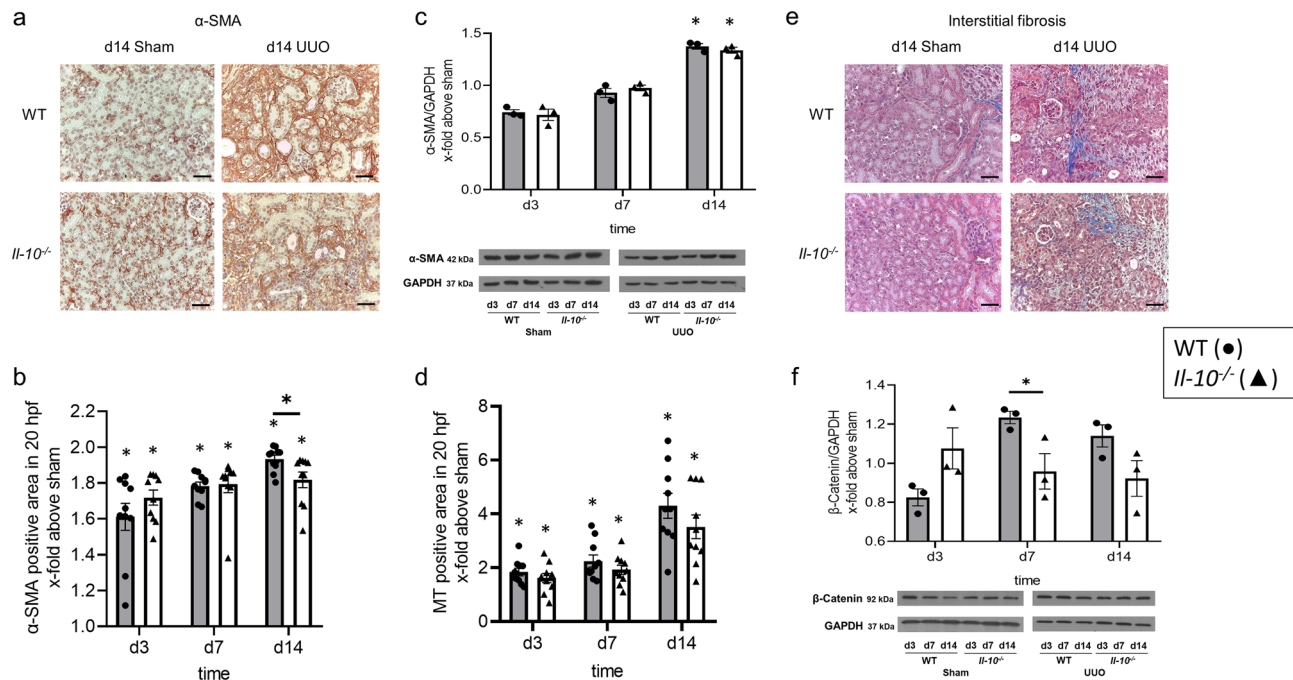


Figure 6. Interstitial fibrosis in neonatal UUO kidneys. Renal sections of UUO- and sham-operated neonatal kidneys were stained for α -SMA and Masson's Trichrome (MT). UUO induced α -SMA expression in neonatal kidneys in WT and *Il-10*^{-/-} (a). α -SMA positive area was slightly reduced in *Il-10*^{-/-} on d14 (b). α -SMA protein expression, measured via western blot, also increased following UUO, but without significant differences between WT and *Il-10*^{-/-} (c). UUO induced collagen deposition in WT and *Il-10*^{-/-} kidneys (d,e). MT positive did not differ significantly between WT and *Il-10*^{-/-} (d,e). β -Catenin expression increased after UUO, *Il-10*^{-/-} showed less fibrosis on d7 than WT (f). The shown western blot images are cropped, for uncropped western blots see Supplementary Figs. S8, S9 online. Expression is indicated as x-fold increase above sham operated control; n = 3 for western blot analysis and n = 10 for immunohistochemical staining; *p < 0.05. Data are presented as individual points with mean \pm SEM. Bar = 100 μ m. Standalone * represents significant differences between Sham and UUO results.

differences between *Il-10*^{-/-} and WT mice. β -catenin, which is highly involved in nephrogenesis and kidney fibrosis, was reduced at one point in *Il-10*^{-/-} mice, suggesting an amelioration, however the significant difference vanished over time⁸⁷. Deletion of IL-10 in adult UUO mice had promoted α -SMA accumulation, as well as collagen deposition in the adult mouse kidney after obstruction⁴². Overall, we did not find considerable differences in renal fibrosis development between obstructed kidneys in neonatal *Il-10*^{-/-} versus WT mice suggesting that IL-10 does not play a major role in modulating renal fibrosis in neonatal obstruction, which is contrasting the functional role of IL-10 in adult mice with UUO. Renal fibrosis following ureteral obstruction is more severe in neonatal compared to adult mice^{6,88,89}. The amount of extracellular matrix deposition in the neonatal kidneys may be too strong to detect slight differences coming from a differentially regulated immune response by the loss of IL-10. In addition, the effect of the IL-10 deletion with less immune cell infiltration in the kidney could be only transient and overall too weak to reduce interstitial fibrosis in neonatal UUO.

Conclusion

We show that IL-10 plays a critical role in the recruitment of immune cells and concomitant cytokine release in obstructed neonatal kidneys. However, and in contrast to adult mice with obstruction, deficiency of IL-10 seems to have an anti-inflammatory and recruitment inhibitory effect in neonatal kidneys after obstruction accompanied with diminished release of pro-inflammatory cytokines. Notably, IL-10 does not have a substantial effect on cell death and interstitial fibrosis in the neonatal UUO model highlighting the differential and in part opposing role IL-10 plays in obstructed kidneys of neonatal and adult mice. Further investigations are now warranted to clarify the functional role of IL-10 and the mechanism behind its pro-inflammatory function in neonatal versus adult UUO and beyond.

Data availability

The datasets generated during and/or analyzed during the current study are available from the corresponding author on reasonable request.

Received: 1 September 2023; Accepted: 23 February 2024

Published online: 06 March 2024

References

- Klein, J. *et al.* Congenital ureteropelvic junction obstruction: Human disease and animal models. *Int. J. Exp. Pathol.* **92**(3), 168–192 (2011).
- Truong, L. D., Gaber, L. & Eknoyan, G. Obstructive uropathy. *Contrib. Nephrol.* **169**, 311–326 (2011).
- Lange-Sperandio, B. Pediatric Obstructive Uropathy. In *Pediatric Nephrology* 1369–1398 (Springer, 2022).
- Popper, B. *et al.* Neonatal obstructive nephropathy induces necroptosis and necroinflammation. *Sci. Rep.* **9**(1), 18600 (2019).
- Thornhill, B. A. & Chevalier, R. L. Variable partial unilateral ureteral obstruction and its release in the neonatal and adult mouse. *Methods Mol. Biol.* **886**, 381–392 (2012).
- Gasparitsch, M. *et al.* Tyrphostin AG490 reduces inflammation and fibrosis in neonatal obstructive nephropathy. *PLoS One* **14**(12), e0226675 (2019).
- Chevalier, R. L. *et al.* Mechanisms of renal injury and progression of renal disease in congenital obstructive nephropathy. *Pediatr. Nephrol.* **25**(4), 687–697 (2010).
- de Waal Malefyt, R. *et al.* Interleukin-10. *Curr. Opin. Immunol.* **4**(3), 314–320 (1992).
- Saraiva, M. & O'Garra, A. The regulation of IL-10 production by immune cells. *Nat. Rev. Immunol.* **10**(3), 170–181 (2010).
- Asadullah, K., Sterry, W. & Volk, H. D. Interleukin-10 therapy—Review of a new approach. *Pharmacol. Rev.* **55**(2), 241–269 (2003).
- Couper, K. N., Blount, D. G. & Riley, E. M. IL-10: The master regulator of immunity to infection. *J. Immunol.* **180**(9), 5771–5777 (2008).
- Ding, L. & Shevach, E. M. IL-10 inhibits mitogen-induced T cell proliferation by selectively inhibiting macrophage costimulatory function. *J. Immunol.* **148**(10), 3133–3139 (1992).
- de Waal Malefyt, R. *et al.* Interleukin 10 (IL-10) and viral IL-10 strongly reduce antigen-specific human T cell proliferation by diminishing the antigen-presenting capacity of monocytes via downregulation of class II major histocompatibility complex expression. *J. Exp. Med.* **174**(4), 915–924 (1991).
- Sinuani, I. *et al.* Role of IL-10 in the progression of kidney disease. *World J. Transplant.* **3**(4), 91–98 (2013).
- Wilke, C. M. *et al.* Dual biological effects of the cytokines interleukin-10 and interferon-gamma. *Cancer Immunol. Immunother.* **60**(11), 1529–1541 (2011).
- Lauw, F. N. *et al.* Proinflammatory effects of IL-10 during human endotoxemia. *J. Immunol.* **165**(5), 2783–2789 (2000).
- Saxton, R. A. *et al.* Structure-based decoupling of the pro- and anti-inflammatory functions of interleukin-10. *Science* **371**, 6535 (2021).
- Ng, T. H. *et al.* Regulation of adaptive immunity; the role of interleukin-10. *Front. Immunol.* **4**, 129 (2013).
- Wei, W. *et al.* The role of IL-10 in kidney disease. *Int. Immunopharmacol.* **108**, 108917 (2022).
- Sakai, K. *et al.* Protective effect and mechanism of IL-10 on renal ischemia-reperfusion injury. *Lab. Invest.* **99**(5), 671–683 (2019).
- Naing, C. *et al.* An association between IL-10 promoter polymorphisms and diabetic nephropathy: A meta-analysis of case-control studies. *J. Diabetes Metab. Disord.* **17**(2), 333–343 (2018).
- Vieira, E. L. M. *et al.* Posterior urethral valve in fetuses: Evidence for the role of inflammatory molecules. *Pediatr. Nephrol.* **32**(8), 1391–1400 (2017).
- Jin, Y. *et al.* Interleukin-10 deficiency aggravates kidney inflammation and fibrosis in the unilateral ureteral obstruction mouse model. *Lab. Invest.* **93**(7), 801–811 (2013).
- Tadagavadi, R. K. & Reeves, W. B. Endogenous IL-10 attenuates cisplatin nephrotoxicity: Role of dendritic cells. *J. Immunol.* **185**(8), 4904–4911 (2010).
- de Waal Malefyt, R. *et al.* Interleukin 10(IL-10) inhibits cytokine synthesis by human monocytes: An autoregulatory role of IL-10 produced by monocytes. *J. Exp. Med.* **174**(5), 1209–1220 (1991).
- Shibata, Y. *et al.* Immunoregulatory roles of IL-10 in innate immunity: IL-10 inhibits macrophage production of IFN-gamma-inducing factors but enhances NK cell production of IFN-gamma. *J. Immunol.* **161**(8), 4283–4288 (1998).
- Fiorentino, D. F. *et al.* IL-10 inhibits cytokine production by activated macrophages. *J. Immunol.* **147**(11), 3815–3822 (1991).
- Gu, Y. *et al.* Interleukin 10 suppresses Th17 cytokines secreted by macrophages and T cells. *Eur. J. Immunol.* **38**(7), 1807–1813 (2008).
- Lousa, I. *et al.* The signaling pathway of TNF receptors: Linking animal models of renal disease to human CKD. *Int. J. Mol. Sci.* **23**(6), 3284 (2022).
- Shmarina, G. V. *et al.* Tumor necrosis factor-alpha/interleukin-10 balance in normal and cystic fibrosis children. *Mediat. Inflamm.* **10**(4), 191–197 (2001).
- Shin, D. I. *et al.* Interleukin 10 inhibits TNF-alpha production in human monocytes independently of interleukin 12 and interleukin 1 beta. *Immunol. Investig.* **28**(2–3), 165–175 (1999).
- Zhong, J. *et al.* Lipopolysaccharide-induced liver apoptosis is increased in interleukin-10 knockout mice. *Biochim. Biophys. Acta* **1762**(4), 468–477 (2006).
- Cohen, S. B. *et al.* Interleukin-10 rescues T cells from apoptotic cell death: Association with an upregulation of Bcl-2. *Immunology* **92**(1), 1–5 (1997).
- Boyd, Z. S. *et al.* Interleukin-10 receptor signaling through STAT-3 regulates the apoptosis of retinal ganglion cells in response to stress. *Investig. Ophthalmol. Vis. Sci.* **44**(12), 5206–5211 (2003).
- Morgan, M. J. & Kim, Y. S. Roles of RIPK3 in necroptosis, cell signaling, and disease. *Exp. Mol. Med.* **54**(10), 1695–1704 (2022).
- Van Laethem, J. L. *et al.* Interleukin 10 prevents necrosis in murine experimental acute pancreatitis. *Gastroenterology* **108**(6), 1917–1922 (1995).
- Chou, W. Y. *et al.* Electroporative interleukin-10 gene transfer ameliorates carbon tetrachloride-induced murine liver fibrosis by MMP and TIMP modulation. *Acta Pharmacol. Sin.* **27**(4), 469–476 (2006).
- Arai, T. *et al.* Introduction of the interleukin-10 gene into mice inhibited bleomycin-induced lung injury in vivo. *Am. J. Physiol. Lung Cell Mol. Physiol.* **278**(5), L914–L922 (2000).
- Demols, A. *et al.* Endogenous interleukin-10 modulates fibrosis and regeneration in experimental chronic pancreatitis. *Am. J. Physiol. Gastrointest. Liver Physiol.* **282**(6), G1105–G1112 (2002).
- Nonaka-Sarukawa, M. *et al.* Adeno-associated virus vector-mediated systemic interleukin-10 expression ameliorates hypertensive organ damage in Dahl salt-sensitive rats. *J. Gene Med.* **10**(4), 368–374 (2008).
- Chevalier, R. L., Forbes, M. S. & Thornhill, B. A. Ureteral obstruction as a model of renal interstitial fibrosis and obstructive nephropathy. *Kidney Int.* **75**(11), 1145–1152 (2009).
- Jung, K. *et al.* Interleukin-10 protects against ureteral obstruction-induced kidney fibrosis by suppressing endoplasmic reticulum stress and apoptosis. *Int. J. Mol. Sci.* **23**(18), 10702 (2022).
- Lange-Sperandio, B. *et al.* Distinct roles of Mac-1 and its counter-receptors in neonatal obstructive nephropathy. *Kidney Int.* **69**(1), 81–88 (2006).
- Probst, H. C. *et al.* Guidelines for DC preparation and flow cytometry analysis of mouse nonlymphoid tissues. *Eur. J. Immunol.* **53**, e2249819 (2023).
- Bayerl, F. *et al.* Guidelines for visualization and analysis of DC in tissues using multiparameter fluorescence microscopy imaging methods. *Eur. J. Immunol.* **53**, e2249923 (2023).

46. Salei, N. *et al.* The kidney contains ontogenetically distinct dendritic cell and macrophage subtypes throughout development that differ in their inflammatory properties. *J. Am. Soc. Nephrol.* **31**(2), 257–278 (2020).
47. Wuhl, E. *et al.* Timing and outcome of renal replacement therapy in patients with congenital malformations of the kidney and urinary tract. *Clin. J. Am. Soc. Nephrol.* **8**(1), 67–74 (2013).
48. Calderon-Margalit, R., Skorecki, K. & Vivante, A. History of childhood kidney disease and risk of adult end-stage renal disease. *N. Engl. J. Med.* **378**(18), 1751–1752 (2018).
49. Wang, H. *et al.* MMP-9-positive neutrophils are essential for establishing profibrotic microenvironment in the obstructed kidney of UUO mice. *Acta Physiol. (Oxf)* **227**(2), e13317 (2019).
50. Tapmeier, T. T. *et al.* Pivotal role of CD4+ T cells in renal fibrosis following ureteric obstruction. *Kidney Int.* **78**(4), 351–362 (2010).
51. Snelgrove, S. L. *et al.* Renal dendritic cells adopt a pro-inflammatory phenotype in obstructive uropathy to activate T cells but do not directly contribute to fibrosis. *Am. J. Pathol.* **180**(1), 91–103 (2012).
52. Vernon, M. A., Mylonas, K. J. & Hughes, J. Macrophages and renal fibrosis. *Semin. Nephrol.* **30**(3), 302–317 (2010).
53. Kubik, M. J. *et al.* Renal developmental genes are differentially regulated after unilateral ureteral obstruction in neonatal and adult mice. *Sci. Rep.* **10**(1), 19302 (2020).
54. Gao, J. *et al.* Role of chemokine (C-X-C motif) ligand 10 (CXCL10) in renal diseases. *Mediat. Inflamm.* **2020**, 6194864 (2020).
55. Rouault, C. *et al.* Roles of chemokine ligand-2 (CXCL2) and neutrophils in influencing endothelial cell function and inflammation of human adipose tissue. *Endocrinology* **154**(3), 1069–1079 (2013).
56. Chung, A. C. & Lan, H. Y. Chemokines in renal injury. *J. Am. Soc. Nephrol.* **22**(5), 802–809 (2011).
57. Kasama, T. *et al.* Regulation of neutrophil-derived chemokine expression by IL-10. *J. Immunol.* **152**(7), 3559–3569 (1994).
58. Darling, A. R. *et al.* IL-10 suppresses IL-17-mediated dermal inflammation and reduces the systemic burden of Vaccinia virus in a mouse model of eczema vaccinatum. *Clin. Immunol.* **150**(2), 153–160 (2014).
59. Elbjairami, W. M. *et al.* Early differential expression of oncostatin M in obstructive nephropathy. *J. Interferon Cytokine Res.* **30**(7), 513–523 (2010).
60. Iyoda, M. *et al.* IL-17A and IL-17F stimulate chemokines via MAPK pathways (ERK1/2 and p38 but not JNK) in mouse cultured mesangial cells: Synergy with TNF-alpha and IL-1beta. *Am. J. Physiol. Renal Physiol.* **298**(3), F779–F787 (2010).
61. Li, L. *et al.* IL-17 produced by neutrophils regulates IFN-gamma-mediated neutrophil migration in mouse kidney ischemia-reperfusion injury. *J. Clin. Investig.* **120**(1), 331–342 (2010).
62. Weng, C. H. *et al.* Interleukin-17A induces renal fibrosis through the ERK and Smad signaling pathways. *Biomed. Pharmacother.* **123**, 109741 (2020).
63. Piepke, M. *et al.* Interleukin-10 improves stroke outcome by controlling the detrimental Interleukin-17A response. *J. Neuroinflamm.* **18**(1), 265 (2021).
64. Kono, H., Onda, A. & Yanagida, T. Molecular determinants of sterile inflammation. *Curr. Opin. Immunol.* **26**, 147–156 (2014).
65. Wyczanska, M. & Lange-Sperandio, B. DAMPs in unilateral ureteral obstruction. *Front. Immunol.* **11**, 581300 (2020).
66. Sasaki, H. *et al.* IL-10, but not IL-4, suppresses infection-stimulated bone resorption in vivo. *J. Immunol.* **165**(7), 3626–3630 (2000).
67. Dufour, J. H. *et al.* IFN-gamma-inducible protein 10 (IP-10; CXCL10)-deficient mice reveal a role for IP-10 in effector T cell generation and trafficking. *J. Immunol.* **168**(7), 3195–3204 (2002).
68. Tumpey, T. M. *et al.* Role for macrophage inflammatory protein 2 (MIP-2), MIP-1alpha, and interleukin-1alpha in the delayed-type hypersensitivity response to viral antigen. *J. Virol.* **76**(16), 8050–8057 (2002).
69. Menten, P., Wuyts, A. & Van Damme, J. Macrophage inflammatory protein-1. *Cytokine Growth Factor Rev.* **13**(6), 455–481 (2002).
70. Ushach, I. & Zlotnik, A. Biological role of granulocyte macrophage colony-stimulating factor (GM-CSF) and macrophage colony-stimulating factor (M-CSF) on cells of the myeloid lineage. *J. Leukoc. Biol.* **100**(3), 481–489 (2016).
71. Araujo, L. S. *et al.* Renal expression of cytokines and chemokines in diabetic nephropathy. *BMC Nephrol.* **21**(1), 308 (2020).
72. Gouon-Evans, V., Rothenberg, M. E. & Pollard, J. W. Postnatal mammary gland development requires macrophages and eosinophils. *Development* **127**(11), 2269–2282 (2000).
73. McDonald, B. & Kubes, P. Cellular and molecular choreography of neutrophil recruitment to sites of sterile inflammation. *J. Mol. Med. (Berl.)* **89**(11), 1079–1088 (2011).
74. Ichikawa, A. *et al.* CXCL10-CXCR3 enhances the development of neutrophil-mediated fulminant lung injury of viral and nonviral origin. *Am. J. Respir. Crit. Care Med.* **187**(1), 65–77 (2013).
75. Flannigan, K. L. *et al.* IL-17A-mediated neutrophil recruitment limits expansion of segmented filamentous bacteria. *Mucosal Immunol.* **10**(3), 673–684 (2017).
76. Walz, A. *et al.* Regulation and function of the CXC chemokine ENA-78 in monocytes and its role in disease. *J. Leukoc. Biol.* **62**(5), 604–611 (1997).
77. Rohwedder, I. *et al.* A20 and the noncanonical NF-kappaB pathway are key regulators of neutrophil recruitment during fetal ontogeny. *JCI Insight* **8**(4), e155968 (2023).
78. Henneke, P. *et al.* Perinatal development of innate immune topology. *Elife* **10**, e67793 (2021).
79. Schultz, C. *et al.* Immature anti-inflammatory response in neonates. *Clin. Exp. Immunol.* **135**(1), 130–136 (2004).
80. Schultz, C. *et al.* Reduced IL-10 production and -receptor expression in neonatal T lymphocytes. *Acta Paediatr.* **96**(8), 1122–1125 (2007).
81. Mitchell, R. E. *et al.* IL-4 enhances IL-10 production in Th1 cells: Implications for Th1 and Th2 regulation. *Sci. Rep.* **7**(1), 11315 (2017).
82. Ho, J. The regulation of apoptosis in kidney development: Implications for nephron number and pattern?. *Front. Pediatr.* **2**, 128 (2014).
83. Linkermann, A. & Green, D. R. Necroptosis. *N. Engl. J. Med.* **370**(5), 455–465 (2014).
84. Rodriguez, D. A. *et al.* Characterization of RIPK3-mediated phosphorylation of the activation loop of MLKL during necroptosis. *Cell Death Differ.* **23**(1), 76–88 (2016).
85. Shi, Y. *et al.* RIPK3: A new player in renal fibrosis. *Front. Cell Dev. Biol.* **8**, 502 (2020).
86. Meran, S. & Steadman, R. Fibroblasts and myofibroblasts in renal fibrosis. *Int. J. Exp. Pathol.* **92**(3), 158–167 (2011).
87. Deacon, P. *et al.* Beta-catenin regulates the formation of multiple nephron segments in the mouse kidney. *Sci. Rep.* **9**(1), 15915 (2019).
88. Martinez-Klimova, E. *et al.* Unilateral ureteral obstruction as a model to investigate fibrosis-attenuating treatments. *Biomolecules* **9**(4), 141 (2019).
89. Gasparitsch, M. *et al.* RAGE-mediated interstitial fibrosis in neonatal obstructive nephropathy is independent of NF-kappaB activation. *Kidney Int.* **84**(5), 911–919 (2013).

Author contributions

B.L.-S. and B.S. contributed to conception and design of the study. M.W., F.T., U.K., R.K., L.W., X.J. and H.N. performed the experiments. M.W., F.T. and U.K. analysed the data and performed statistical analysis. M.W. and B.L.-S. wrote the manuscript. All authors contributed to manuscript revision, read and approved the submitted version.

Funding

Open Access funding enabled and organized by Projekt DEAL. Bärbel Lange-Sperandio is supported by the German Research Foundation (DFG LA 1257/5-1). BS is supported by the ERC (STG-715182) and DFG (Emmy Noether Schr 1444/1-1; 322359157-FOR2599-A03; 360372040-SFB 1335-P08; TRR 359-P05-491676693).

Competing interests

The authors declare no competing interests.

Additional information

Supplementary Information The online version contains supplementary material available at <https://doi.org/10.1038/s41598-024-55469-9>.

Correspondence and requests for materials should be addressed to B.L.-S.

Reprints and permissions information is available at www.nature.com/reprints.

Publisher's note Springer Nature remains neutral with regard to jurisdictional claims in published maps and institutional affiliations.



Open Access This article is licensed under a Creative Commons Attribution 4.0 International License, which permits use, sharing, adaptation, distribution and reproduction in any medium or format, as long as you give appropriate credit to the original author(s) and the source, provide a link to the Creative Commons licence, and indicate if changes were made. The images or other third party material in this article are included in the article's Creative Commons licence, unless indicated otherwise in a credit line to the material. If material is not included in the article's Creative Commons licence and your intended use is not permitted by statutory regulation or exceeds the permitted use, you will need to obtain permission directly from the copyright holder. To view a copy of this licence, visit <http://creativecommons.org/licenses/by/4.0/>.

© The Author(s) 2024


4. Paper II

RESEARCH ARTICLE

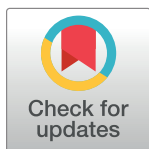
TLR2 mediates renal apoptosis in neonatal mice subjected experimentally to obstructive nephropathy

Maja Wyczanska¹ , Jana Rohling¹ , Ursula Keller¹, Marcus R. Benz², Carsten Kirschning³, Bärbel Lange-Sperandio^{1*} 

1 Department of Pediatrics, Dr. v. Hauner Children's Hospital, University Hospital, LMU Munich, Munich, Germany, **2** Pediatric Nephrology Dachau, Dachau, Germany, **3** Institute of Medical Microbiology, University of Essen, Essen, Germany

 These authors contributed equally to this work.

* baerbel.lange-sperandio@med.uni-muenchen.de



Abstract

Urinary tract obstruction during renal development leads to inflammation, tubular apoptosis, and interstitial fibrosis. Toll like receptors (TLRs) expressed on leukocytes, myofibroblasts and renal cells play a central role in acute inflammation. TLR2 is activated by endogenous danger signals in the kidney; its contribution to renal injury in early life is still a controversial topic. We analyzed TLR2 for a potential role in the neonatal mouse model of congenital obstructive nephropathy. Inborn obstructive nephropathies are a leading cause of end-stage kidney disease in children. Thus, newborn *Tlr2*^{-/-} and wild type (WT) C57BL/6 mice were subjected to complete unilateral ureteral obstruction (UUO) or sham-operation on the 2nd day of life. The neonatal kidneys were harvested and analyzed at days 7 and 14 of life. Relative expression levels of TLR2, caspase-8, Bcl-2, Bax, GSDMD, GSDME, HMGB1, TNF, galectin-3, α -SMA, MMP-2, and TGF- β proteins were quantified semi-quantitatively by immunoblot analyses. Tubular apoptosis, proliferation, macrophage- and T-cell infiltration, tubular atrophy, and interstitial fibrosis were analyzed immunohistochemically. Neonatal *Tlr2*^{-/-} mice kidneys exhibited less tubular and interstitial apoptosis as compared to those of WT C57BL/6 mice after UUO. UUO induced neonatally did trigger pyroptosis in kidneys, however to similar degrees in *Tlr2*^{-/-} and WT mice. Also, tubular atrophy, interstitial fibrosis, tubular proliferation, as well as macrophage and T-cell infiltration were unremarkable. We conclude that while TLR2 mediates apoptosis in the kidneys of neonatal mice subjected to UUO, leukocyte recruitment, interstitial fibrosis, and consequent neonatal obstructive nephropathy might lack a TLR2 involvement.

 OPEN ACCESS

Citation: Wyczanska M, Rohling J, Keller U, Benz MR, Kirschning C, Lange-Sperandio B (2023) TLR2 mediates renal apoptosis in neonatal mice subjected experimentally to obstructive nephropathy. PLoS ONE 18(11): e0294142. <https://doi.org/10.1371/journal.pone.0294142>

Editor: Franziska Theilig, Anatomy, SWITZERLAND

Received: April 21, 2023

Accepted: October 25, 2023

Published: November 28, 2023

Peer Review History: PLOS recognizes the benefits of transparency in the peer review process; therefore, we enable the publication of all of the content of peer review and author responses alongside final, published articles. The editorial history of this article is available here: <https://doi.org/10.1371/journal.pone.0294142>

Copyright: © 2023 Wyczanska et al. This is an open access article distributed under the terms of the [Creative Commons Attribution License](https://creativecommons.org/licenses/by/4.0/), which permits unrestricted use, distribution, and reproduction in any medium, provided the original author and source are credited.

Data Availability Statement: The data from this study is available in a public repository (Zenodo) under this DOI: [10.5281/zenodo.8060419](https://doi.org/10.5281/zenodo.8060419).

Introduction

Congenital obstructive nephropathy is a frequent cause of chronic kidney disease in infants and children [1, 2]. Inborn obstruction of the urinary tract impairs renal growth and development and leads to reduced nephron numbers. The reduction of nephrons corresponds with a

Funding: The author(s) received specific funding for this work. Deutsche Forschungsgemeinschaft (DFG) 1257/5-1, Prof. Dr. Bärbel Lange-Sperandio.

Competing interests: The authors have declared that no competing interests exist.

lifelong risk of end stage kidney disease [3]. Unilateral ureteral obstruction (UO) in neonatal mice at the second day of life serves as a model for congenital obstructive nephropathy. It studies the effects of urinary tract obstruction on renal development, as nephrogenesis in mice finishes postnatally 2–3 weeks after birth [4]. Contrary, in humans nephrogenesis finishes in utero at 34–36 weeks of gestation. Neonatal UO elicits tubular apoptosis, renal inflammation, and interstitial fibrosis, which contribute to a loss of nephron mass in the kidney [5]. Inflammatory macrophages, which produce pro-inflammatory cytokines like tumor necrosis factor (TNF), are key players in this process [6]. Toll like receptors (TLRs) are a family of innate pattern recognition receptors. E.g. TLR2 and TLR4 are expressed on leukocytes, myofibroblasts and renal cells which often play a central role in acute inflammation as major sources of pro-inflammatory chemokines and cytokines [7–9]. Besides being implicated as cellular pathogen-associated molecular pattern sensors, TLR might also bind danger-associated molecular patterns (DAMPs) released upon sterile damage of tissue and thus being of endogenous origin [10]. Cognate ligand activated TLRs initiate intracellular signaling cascades such as through myeloid differentiation primary response gene (MyD88)-dependent phosphorylation of MAPK towards activation of nuclear factors such as activating protein-1 (AP-1) and NF- κ B [11]. TLRs have been implicated in various renal diseases, including ischemia-reperfusion injury (IRI), wherein endogenous TLR2 and TLR4 ligands are thought to be released from the renal epithelium [8, 12]. For instance, adult *Tlr2*^{-/-} mice displayed in the IRI model ameliorated kidney inflammation and injury [13]. TLR2 also influenced renal fibrosis, a hallmark of UO [14].

TLR2 forms heterodimers with TLR1 or TLR6, as well as a variety of further receptors for recognition of diverse ligands [15]. It plays a central role in the innate immune signaling in renal disease [8, 16–18]. During a bacterial infection, TLR2 signals for apoptosis through MyD88 via a pathway involving caspase-8 [19]. High mobility group box 1 (HMGB1) might carry DAMPs that might activate TLR2 [20]. HMGB1 is mostly associated with TLR4 [20, 21]. However, the release of HMGB1 into extracellular fluid also initiates immune responses through TLR2 [22]. Various reports implicate HMGB1 as an important role holder in the pathogenesis of kidney diseases by affecting renal epithelial cell apoptosis, kidney tissue fibrosis, and inflammation [22]. HMGB1 can also trigger pyroptosis, a regulated necrotic cell death, which involves inflammasome activities [23]. Inflammasomes can be activated by DAMPs towards cleavage of gasdermin (GSDM) D or E and consequent cell rupture and release of pro-inflammatory alarmins [23, 24]. The role of TLR2 in the UO model, inflammatory cell death and fibrosis is being discussed controversially. Renal function of adult *Tlr2*^{-/-} mice is enhanced as compared to WT controls while T_H2 cytokine production and renal fibrosis following UO are reduced [25]. Here, we comparatively analyzed *Tlr2*^{-/-} mice for the first time in a neonatal mouse model of congenital obstructive nephropathy.

Materials and methods

Experimental protocol

The *Tlr2*^{-/-} mouse strain used (and crossed with other Tlr ko strains) has been generated by Deltagen, Cal, USA, and provided to CK through Tularik (merged into Amgen in the aftermath) [26]. *Tlr2*^{-/-} mice and WT mice (C57BL/6) were subjected to complete left ureteral obstruction or sham operation under general anesthesia with isoflurane (3–5% v/v) and oxygen (0.8 L/min) on the second day of life, as described before [27]. The animals received carprofen to alleviate possible pain after the surgery. The sex distribution was equal in both groups. After recovery, neonatal mice were returned to their mothers until sacrifice on day 7 and 14 of life. The animals were sacrificed by cervical dislocation. All experiments were

performed according to national animal protection laws and the guidelines of animal experimentation established and approved by the Regierungspräsidium von Oberbayern (Az 55.2-1-54-2531-136-06).

Identification of infiltrating macrophages and T-lymphocytes

The abundance of infiltrating macrophages and T-lymphocytes in the neonatal kidney was examined by immunohistochemistry. Formalin-fixed, paraffin-embedded kidney sections were subjected to antigen retrieval and incubated with either rat anti-mouse MAC-2 (galectin-3) antibody against macrophages (Cedarlane Laboratories, Canada, CL8942AP, 1:500) or anti-CD3 antibody against T-lymphocytes (Bio-Rad AbD Serotec GmbH, Germany, MCA1477, 1:50). Specificity was assessed through simultaneous staining of control sections with an unspecific, species-controlled primary antibody. Biotinylated horse anti-mouse IgG (Vector Laboratories, CA) was used as secondary antibody. Sections were incubated with ABC reagent, detected with DAB (Vectastain, Vector Laboratories, CA) and counterstained with methylene blue or hematoxylin. Images were taken using the LEICA DM1000 microscope and the digital camera (LEICA ICC50HD, Germany). Macrophages and CD3-positive lymphocytes in cortex and medulla were counted in twenty non-overlapping high-power fields at x400 magnification and were analyzed in a blinded manner ($n = 8$ in each group). Data were expressed as the mean score \pm SEM per 20 high-power fields.

Detection of apoptosis and proliferation

Apoptotic cells were detected by the terminal deoxynucleotidyl transferase (TdT)-mediated dUTP-biotin nick end labeling (TUNEL) assay, as described before [5]. Briefly, 4% formalin-fixed tissue sections were deparaffinized and rehydrated in ethanol, followed by incubation with proteinase K. After quenching, equilibration buffer and working strength enzyme (Apop-Tag Peroxidase In Situ Apoptosis Detection Kit, Millipore, MA) were applied. Cells were regarded as TUNEL-positive if their nuclei were stained black and displayed typical apoptotic morphology. Apoptosis in each kidney was calculated by counting the number of TUNEL-positive tubular and interstitial cells in 20 sequentially selected fields at x400 magnification in a blinded fashion and expressed as the mean number \pm SEM per 20 high-power fields using the LEICA DM1000 microscope and the digital camera (LEICA ICC50HD, Germany). For detection of proliferation formalin-fixed, paraffin-embedded kidney sections were subjected to antigen retrieval and incubated with mouse anti-rat Ki67 antibody (Dako, # M7248, Agilent Technologies, CA) at 1:50. Sections were incubated with ABC reagent, detected with DAB (Vectastain, Vector Laboratories, CA) and counterstained with hematoxylin. Digital images of the sections ($n = 8$ in each group) were superimposed on a grid, and the number of dark brown Ki67 positive nuclei was recorded for each field. Proliferating tubular and interstitial cells in cortex and medulla were counted in twenty non-overlapping high-power fields at x400 magnification and were analyzed in a blinded manner using the LEICA DM1000 microscope and the digital camera (LEICA ICC50HD, Germany). Data were expressed as the mean score \pm SEM per 20 high-power fields.

Measurement of tubular atrophy

Kidney sections were stained with periodic acid Schiff for assessment of tubular basement membranes, and tubular atrophy was determined as described previously [5]. Atrophic tubules were identified by their thickened and sometimes duplicated or wrinkled basement membranes. Digital images of the sections ($n = 8$ in each group) were superimposed on a grid, and the number of atrophic tubules was recorded for each field. Twenty non-overlapping high-

power fields at x400 magnification were analyzed in a blinded fashion. Data were expressed as the mean score \pm SEM per 20 high power fields.

Measurement of interstitial fibrosis

Interstitial collagen deposition was measured in Masson's trichrome-stained sections. Digital images of the sections were superimposed on a grid, and the number of grid points overlapping interstitial blue-staining collagen was recorded for each field in a blinded manner. In addition, formalin-fixed and paraffin embedded sections were subjected to antigen retrieval and incubated with mouse anti-mouse α -smooth muscle actin antibody (Sigma Aldrich MO851, Germany, A2547, 1:5000) as shown before [28]. Biotinylated donkey anti goat IgG and horse anti-mouse IgG (Santa Cruz, Germany) were used as secondary antibodies. Sections were incubated with ABC reagent, detected with DAB (Vectastain, Vector Laboratories, CA) and counterstained with hematoxylin. Digital images of the sections ($n = 8$ in each group) were superimposed on a grid, and the number of grid points overlapping collagen I fibers or α -smooth muscle actin fibers was recorded for each field. Twenty non-overlapping high-power fields at x400 magnification were analyzed in a blinded fashion. Data were expressed as the mean score \pm SEM per 20 high power fields.

Western immunoblotting

Kidneys of UO and control mice were harvested on 7 and 14 days of life ($n = 3$ in each group) as described previously [5]. Neonatal kidneys were homogenized in protein lysis buffer (Tris 50 mM, Na₄P₂O₃ 1 mM, 2% SDS) containing protease inhibitor cocktail (Roche, Switzerland, #1836153). The protein content of the supernatants was measured using the BCA Protein Assay Kit (Pierce Biotechnology, MA, #23225). 20 μ g of protein were separated on polyacrylamide gels at 160 V for 45 min and blotted onto nitrocellulose membranes (0,1 A per gel, 120 min). After blocking antibody-specific for 2 h in Tris-buffered saline with Tween-20 containing 5% nonfat dry milk and/or BSA, blots were incubated with primary antibodies 2 h at room temperature or at 4°C overnight. TLR2 antibody (ThermoFisher Scientific, MA, #MA5-32787, 1:1000), Caspase-8 antibody (Cell Signaling Technology, MA, #4927, 1:1000), Bcl-2 antibody (Santa Cruz, Germany, sc7382, 1:200), Bax antibody (Cell Signaling Technology, MA, #27725, 1:1000), GSDMD antibody (Cell Signaling Technology, MA, #39754, 1:1000), GSDME antibody (Abcam, UK, ab215191, 1:500), HMGB1 antibody (Abcam, UK, ab18256, 1:1000), TNF antibody (Cell Signaling Technology, MA, #3707, 1:500), Galectin-3 antibody (Santa Cruz, Germany, sc19283, 1:500), α -SMA antibody (Sigma Aldrich, Germany, A2547, 1:5000), MMP-2 antibody (Santa Cruz, Germany, sc10736, 1:1000), TGF- β (Cell Signaling Technology, MA, #3711, 1:1000) were used for western blot analysis. GAPDH (DUNN Labortechnik, Germany, H86540M, 1:40000) was used as an internal loading control and to normalize samples. Blots were washed with Tris-buffered saline with Tween-20 and incubated with horseradish peroxidase-conjugated secondary antibody for 1 h at room temperature. Immune complexes were detected using enhanced chemiluminescence method. Blots were exposed to x-ray films (Kodak, Germany), the films were scanned, and protein bands were quantified using the densitometry program Image J. Each band represents one single neonatal mouse kidney. The uncropped gel images can be found in [S1 Raw](#) images.

Statistical analysis

Data are presented as mean \pm standard error. Comparisons between groups were made using one-way analysis of variance followed by the Student-Newman-Keuls test. Comparisons between left and right kidneys were performed using the Students t-test for paired data. Statistical significance was defined as $p < 0.05$.

Results

Neonatal UUO induces protein expression of TLR2

To measure the protein expression of TLR2 after UUO, we performed a western blot analysis of UUO and sham-operated kidneys of neonatal WT mice. Following UUO renal TLR2 protein expression increased significantly on day 14 of life in comparison to sham-operated controls (Fig 1A). We observed that as a response to the injury, TLR2 expression levels in neonatal

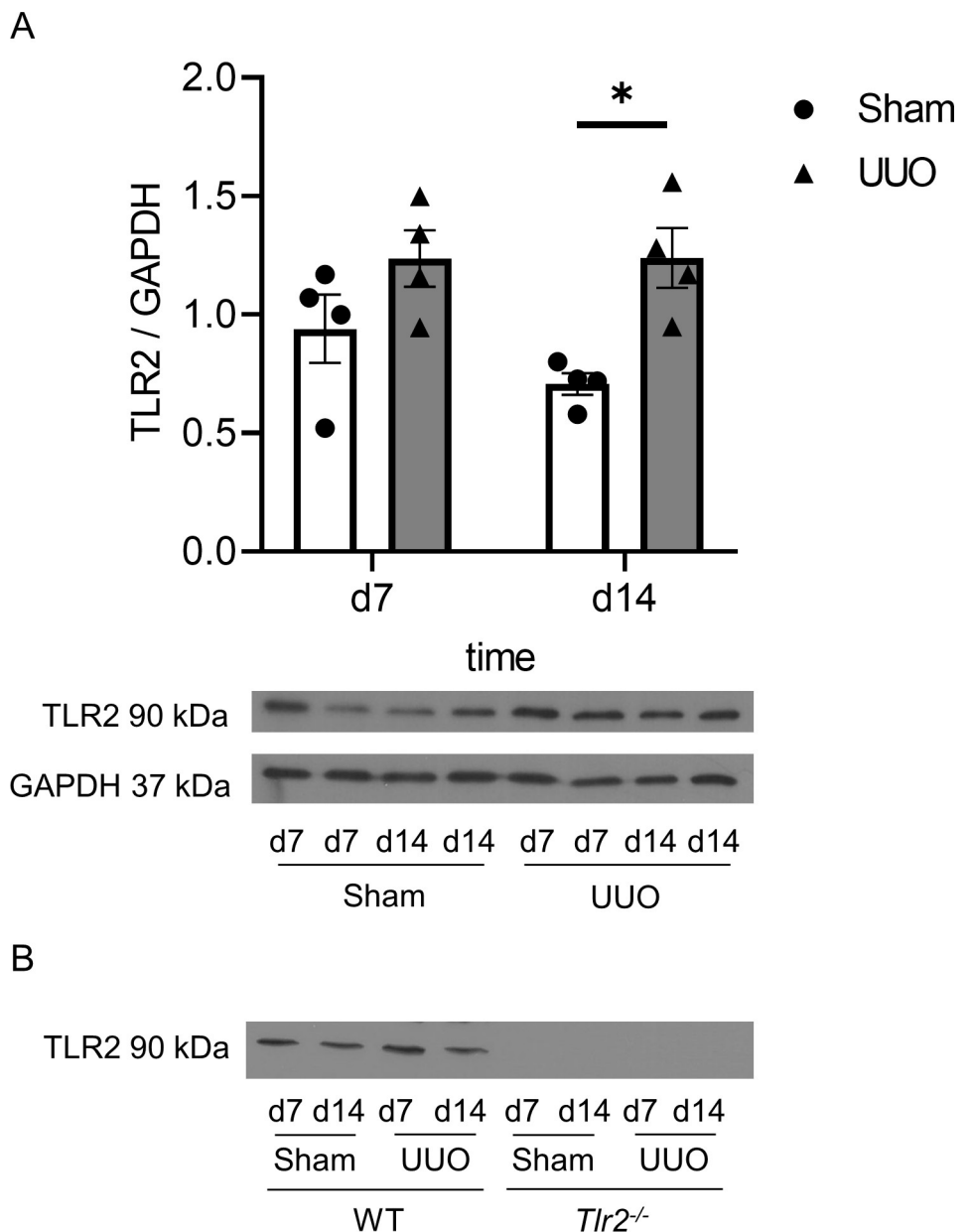


Fig 1. Neonatal unilateral ureteral obstruction induces the expression of TLR2. Neonatal WT mice were subjected to UUO or sham operation and their kidneys were harvested on d7 and d14. Lysates of whole kidneys were applied to SDS PAGE and consequent western blot analyses. The TLR2 expression level was significantly higher in UUO kidneys as compared to sham-operated controls on d14 (A). *Tlr2*^{-/-} mice did not express TLR2 (B). n = 4; *p<0,05. Data are presented as mean +/- SEM.

<https://doi.org/10.1371/journal.pone.0294142.g001>

WT-kidneys were increased. This analysis was also used to confirm that *Tlr2*^{-/-} mice indeed did not express TLR2 (Fig 1B).

TLR2 mediates tubular and interstitial apoptosis in neonatal kidneys with UUO

We next investigated tubular and interstitial apoptosis in neonatal kidneys from *Tlr2*^{-/-} and WT mice having undergone UUO using TUNEL staining. Tubular apoptosis increased significantly in the obstructed kidneys at day 7 and 14 of life (Fig 2A–2C). TUNEL positive cells were mainly present in dilated distal tubules of the neonatal kidney. *Tlr2*^{-/-} mice showed less tubular apoptosis compared to WT (Fig 2A–2C). Tubular apoptosis in *Tlr2*^{-/-} mice was reduced on day 7 and day 14 of life by 41% and 30%, respectively (Fig 2C). Interstitial apoptosis increased following UUO and *Tlr2*^{-/-} mice showed less interstitial apoptosis compared to WT (Fig 2D). Interstitial apoptosis in *Tlr2*^{-/-} kidneys after UUO was reduced on day 7 and day 14 by 41%

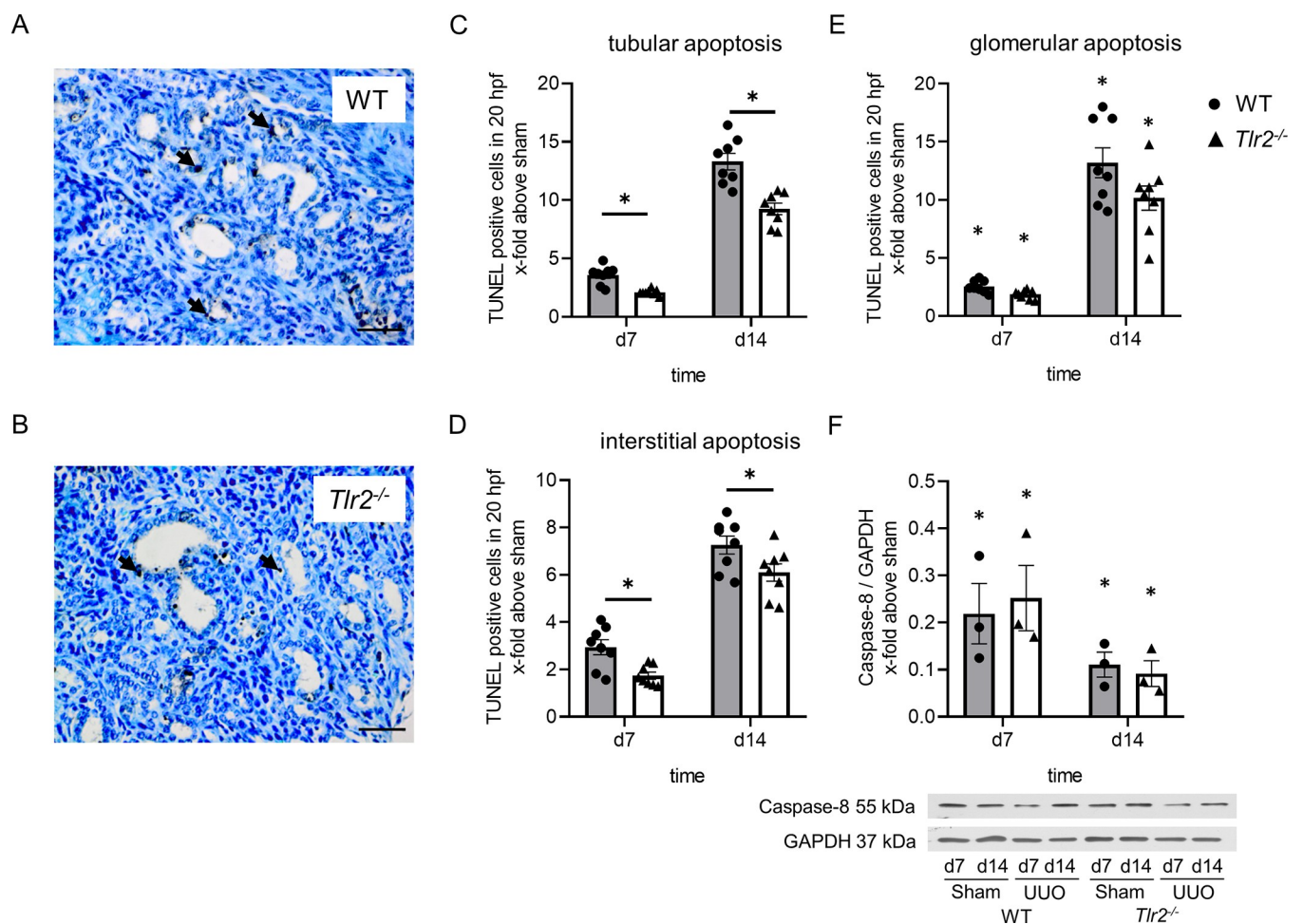


Fig 2. Tubular and interstitial apoptosis in *Tlr2*^{-/-} mice with UUO. UUO was performed on the second day of life. Apoptotic cells were detected by TUNEL staining in sections. TUNEL-positive cells in WT (A) and *Tlr2*^{-/-} (B) neonatal mouse kidneys appeared predominantly in distal tubules and in the interstitium. Arrows indicate tubular apoptotic cells. Quantification indicates significant decreases of numbers of TUNEL-positive tubular (C) and interstitial (D) cells in *Tlr2*^{-/-} as compared to WT UUO kidneys. The number of apoptotic nuclei in glomeruli did not differ between *Tlr2*^{-/-} and WT specimen (E); n = 8. Whole kidneys were lysed for western blot analyses (F). Caspase-8 expression was reduced in UUO-kidneys indicating apoptosis following ureteral obstruction. Significant differences between WT and *Tlr2*^{-/-} were not observed (F). Results are indicated as x-fold relative to sham-operated controls. n = 3 (Western Blot); *p<0,05. Data are presented as mean +/- SEM. Bar = 100µm. Standalone * represents significant differences between Sham and UUO results.

<https://doi.org/10.1371/journal.pone.0294142.g002>

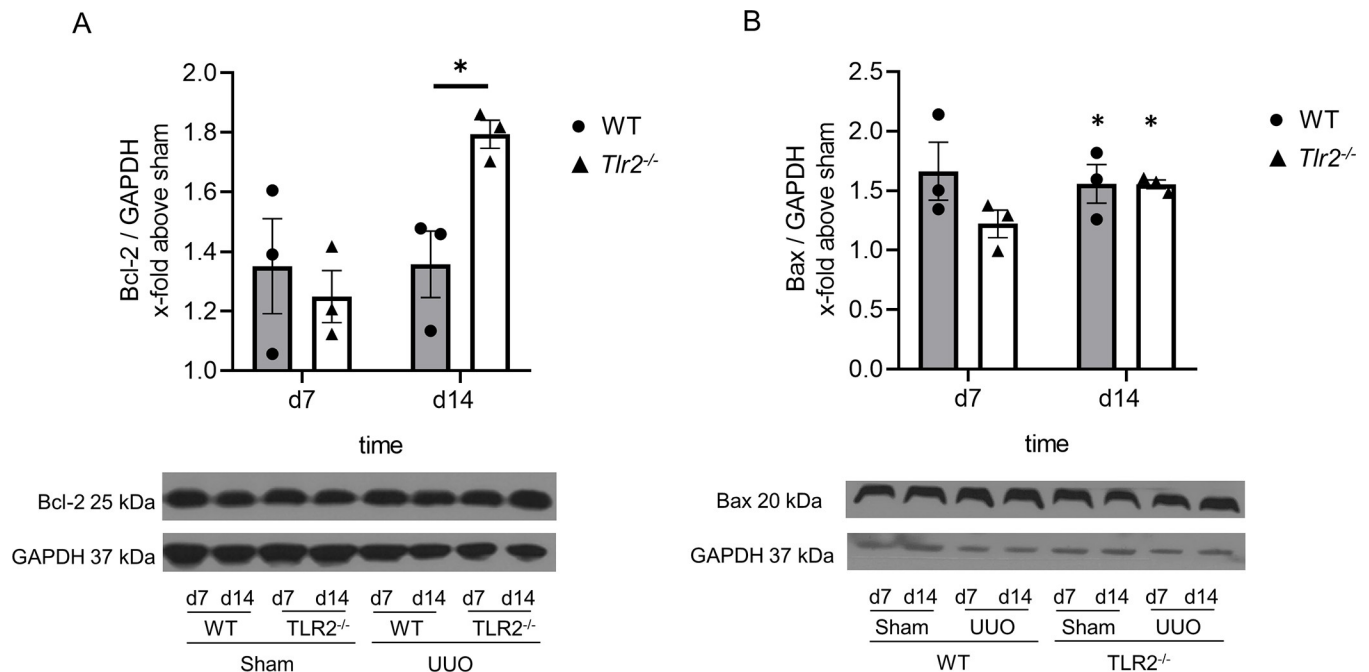


Fig 3. *Tlr2*^{-/-} mice show increased renal Bcl-2 expression in comparison to WT following UUO. Neonatal mice were subjected to UUO or sham operation. Western blot analysis was performed at day 7 and 14 of life. UUO induced the expression of Bcl-2 in *Tlr2*^{-/-}, but not in WT kidneys at day 14 (A). UUO induced expression of Bax in the neonatal kidney without significant differences between WT and *Tlr2*^{-/-} (B). Results are indicated as x-fold relative to sham-operated controls. n = 3; *p < 0.05. Data are presented as mean ± SEM. Standalone * represents significant differences between Sham and UUO results.

<https://doi.org/10.1371/journal.pone.0294142.g003>

and 16%, respectively (Fig 2D). Glomerular apoptosis increased following UUO, but without significant differences between *Tlr2*^{-/-} and WT kidneys (Fig 2E). Apoptosis was also measured by caspase-8 protein expression using western blot (Fig 2F). Cleavage of caspase-8 indicates apoptotic cell death after UUO (Fig 2F). However, caspase-8 expression was not significantly different between WT and *Tlr2*^{-/-} mice (Fig 2F), which may be explained by the lack of compartment-specific analysis of the neonatal kidney. For further analysis of cell death in our model we analyzed the anti-apoptotic marker Bcl-2 and the pro-apoptotic marker Bax using western blot (Fig 3). Neonatal *Tlr2*^{-/-} mice showed a higher expression of Bcl-2 at day 14 in comparison to WT (Fig 3A), confirming that TLR2 mediates apoptosis in the neonatal model of obstructive nephropathy. Bax expression increased following UUO at day 14, without significant differences between *Tlr2*^{-/-} and WT kidneys.

Pyroptosis generally increased after neonatal UUO, yet its grades in WT are indistinguishable from those of *Tlr2*^{-/-} murine specimen

To measure the potential impact of TLR2 expression on pyroptosis upon UUO versus samples from sham-operated mice, abundance of cleaved GSDMD and full-length GSDME expression in respective kidneys at day 7 and 14 of life were measured by immunoblotting (Fig 4A and 4B). While the abundance of cleaved GSDMD increased due to the obstruction in samples of both phenotypes at d14 (Fig 4A), that of full-length GSDME decreased after UUO (Fig 4B) as if pyroptosis became operative upon UUO. However, WT and *Tlr2*^{-/-} mice borne specimen were undistinguishable in this regard (Fig 4A and 4B). Thus, TLR2 is not involved in pyroptosis after ureteral obstruction in the neonatal kidney. Additionally, we analyzed the expression of the pyroptosis markers HMGB1 and TNF in UUO- and sham-operated neonatal kidneys at

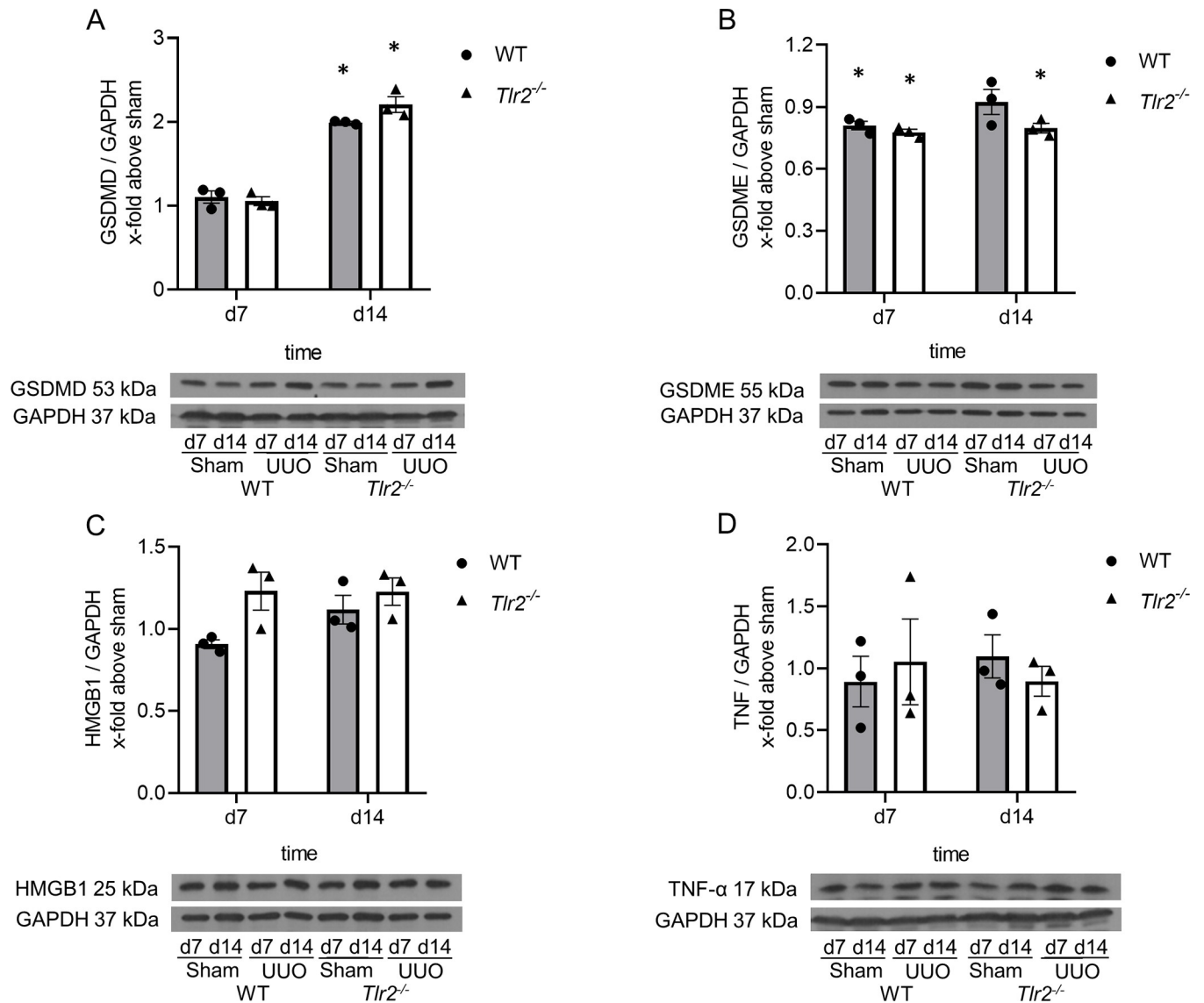


Fig 4. Pyroptosis increases after UUO. Neonatal mice were subjected to UUO or sham operation. Whole kidneys were processed for western blot analysis at day 7 and 14 of life. UUO induced cleaved GSDMD expression (A) and full-length GSDME cleavage (B), but with no significant differences between WT and *Tlr2*^{-/-}. Pyroptosis markers HMGB1 (C) and TNF- α (D) did not show significant differences between WT and *Tlr2*^{-/-}. Results are indicated as x-fold relative to sham-operated controls. n = 3; *p < 0.05. Data are presented as mean \pm SEM. Standalone * represents significant differences between Sham and UUO results.

<https://doi.org/10.1371/journal.pone.0294142.g004>

day 7 and 14 of life (Fig 4C and 4D). Expression levels of both proteins remained constant throughout the analysis period and were indistinguishable in specimen of both genotypes (Fig 4C and 4D). We conclude that TLR2 has no impact on pyroptosis, HMGB1 and TNF expression in the neonatal kidney having been subjected to UUO.

Proliferation decreased and tubular atrophy increased in neonatal kidneys after UUO, without significant differences between *Tlr2*^{-/-} and WT mice

Proliferation in neonatal *Tlr2*^{-/-} and WT mouse kidneys was measured using Ki67 staining in obstructed and sham-operated kidneys at day 7 and 14 of life (Fig 5A–5C). Following obstruction, proliferation decreased significantly, but without a significant difference between WT

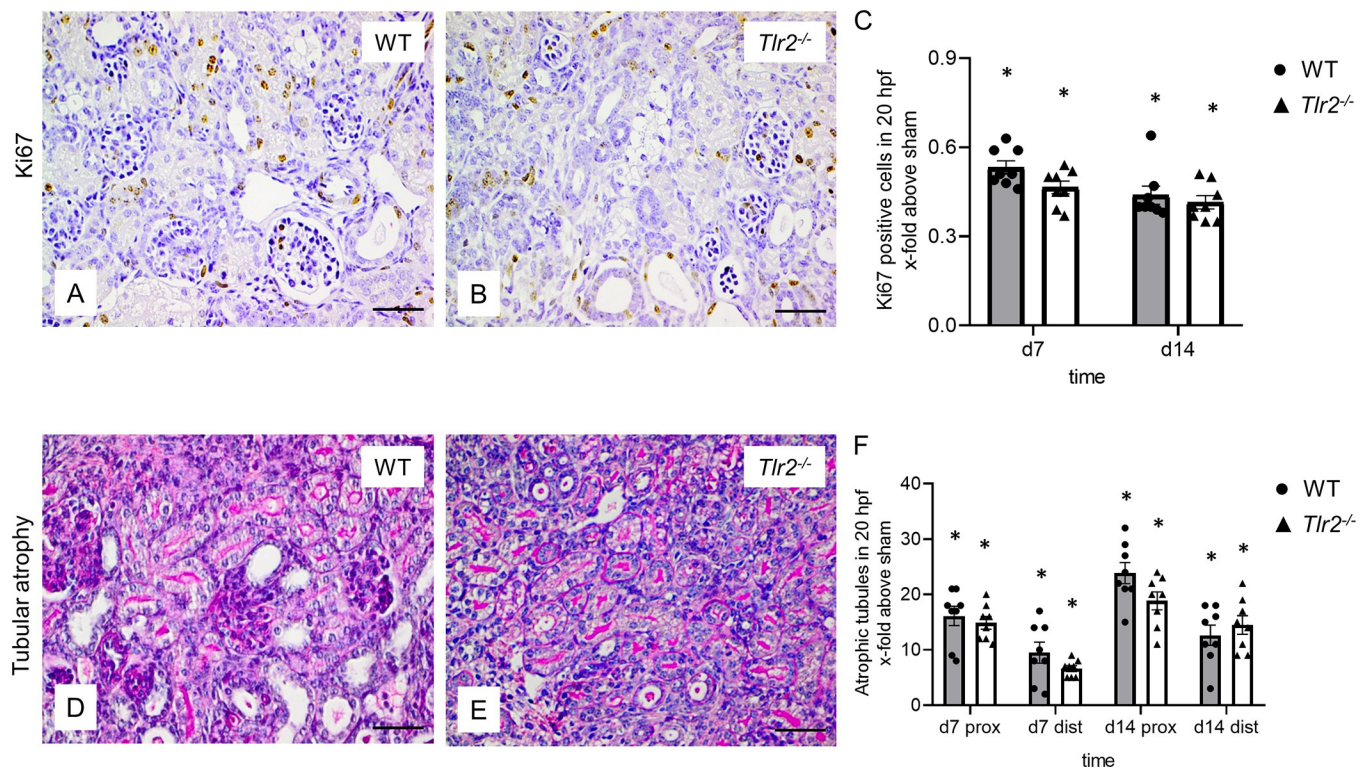


Fig 5. Analysis of tubular proliferation and atrophy in neonatal mice following UUO. Immunohistochemical staining of Ki67 (A and B) and proximal (prox) and distal (dist) atrophic tubules (D and E) in neonatal UUO WT (A and D) and *Tlr2*^{-/-} (B and E) mice at day 7. Quantification of Ki67-positive tubular cells in UUO-kidneys (C) shows a decrease following UUO without significant differences between WT and *Tlr2*^{-/-}. Quantitative analysis of tubular atrophy in UUO-kidneys on day 7 and day 14 (F) shows an increase of tubular atrophy in proximal and distal tubules following UUO, but no significant differences between WT and *Tlr2*^{-/-} mice in neither compartment. Results are indicated as x-fold increase above sham operated control in 20 hpfs; n = 8. Data are presented as mean +/- SEM. Bar = 100µm. Standalone * represents significant differences between Sham and UUO results.

<https://doi.org/10.1371/journal.pone.0294142.g005>

and *Tlr2*^{-/-} mice (Fig 5C). To measure tubular atrophy, a Periodic Acid Schiff (PAS) staining of neonatal WT and *Tlr2*^{-/-} kidneys was performed after UUO at day 7 and 14 of life (Fig 5D–5F). Tubular atrophy increased at d7 and d14 in UUO kidneys and was more prominent in proximal than distal tubules following UUO. Between WT and *Tlr2*^{-/-} mice no significant differences in tubular atrophy could be observed (Fig 5F). We conclude that TLR2 does not influence proliferation or tubular atrophy in the neonatal kidney with UUO.

M2 macrophage infiltration, T-lymphocyte infiltration and fibrosis increased after UUO but were not different between *Tlr2*^{-/-} and WT mice

Influence of TLR2 on M2 macrophage infiltration in neonatal *Tlr2*^{-/-} and WT mouse kidneys with UUO was measured using galectin-3 staining (Fig 6A–6C) and galectin-3 protein expression using western blot (Fig 7A). Increased expression of interstitial galectin-3 is a feature of the regenerative anti-inflammatory alternative (M2) macrophage phenotype. UUO induced a vast M2 macrophage infiltration in the interstitium of neonatal *Tlr2*^{-/-} and WT kidneys, 10-fold at d14, but without significant differences between the two lines (Fig 6A–6C). UUO induced a marked galectin-3 expression in the neonatal kidneys but was not different between *Tlr2*^{-/-} and WT mice (Fig 7A). T-lymphocyte infiltration was assessed by CD3 staining (Fig 6D–6F). UUO induced CD3 positive T-cell-infiltration in neonatal kidneys of WT and *Tlr2*^{-/-} mice, at d7 and d14 (Fig 6D–6F). No significant differences between WT and *Tlr2*^{-/-} kidneys

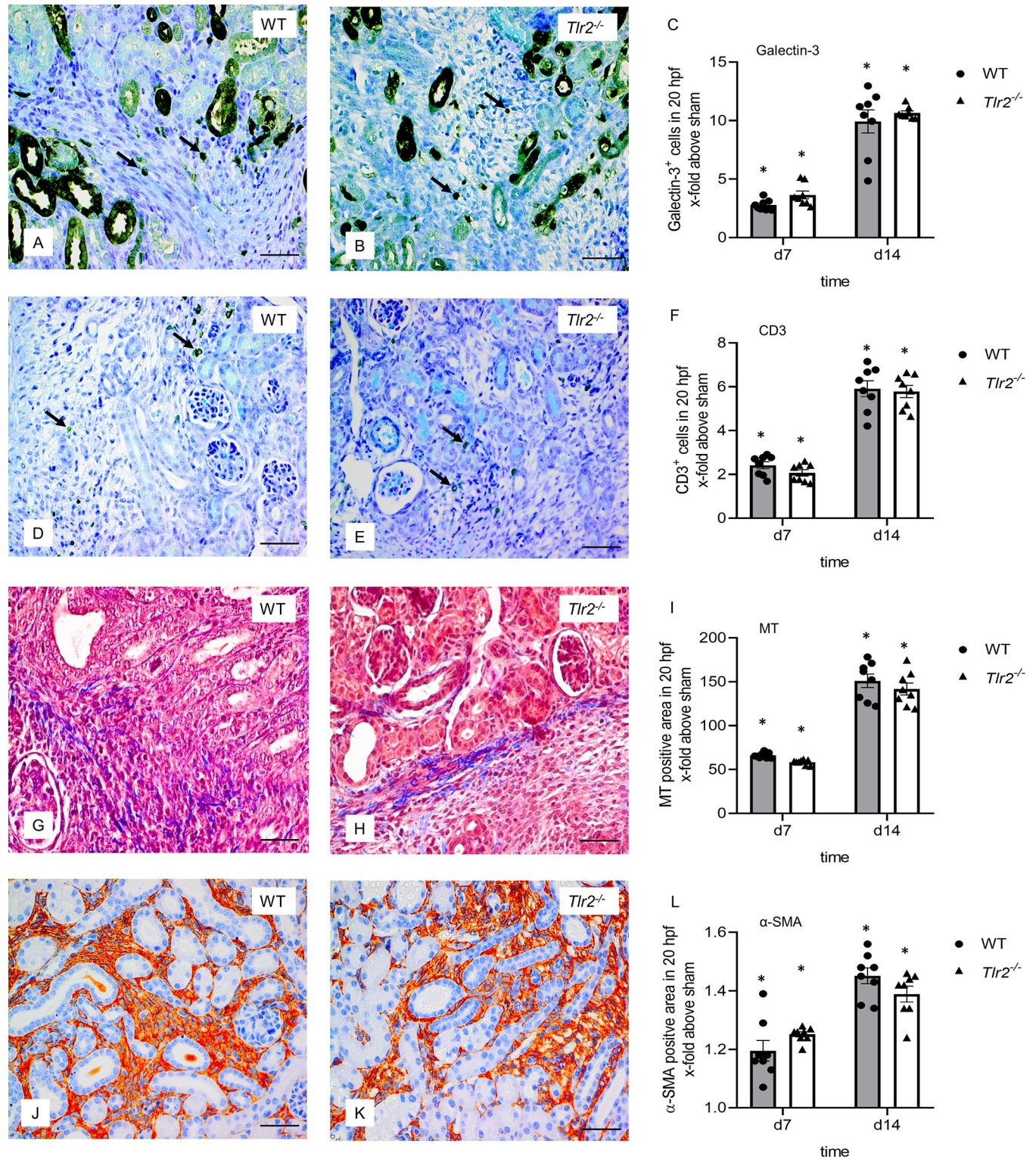


Fig 6. Immune cell infiltration and fibrosis in neonatal UUO kidneys. Immunohistological staining for galectin-3, a M2 macrophage marker, of WT (A) and *Tlr2*^{-/-} (B) mice on day 14. Quantitative analysis shows that UUO induced interstitial galectin-3 positive macrophage infiltration (arrow) in neonatal kidneys (C), but without significant differences between WT and *Tlr2*^{-/-} mice. Immunohistological staining for CD3 (arrow), a T-lymphocyte marker, of WT (D) and *Tlr2*^{-/-} (E) mice on day 14. Quantitative analysis shows CD3 positive T-cell infiltration in neonatal kidneys following UUO (F) without significant differences between WT and *Tlr2*^{-/-} mice. Renal sections of UUO- and sham-operated were stained for Masson's Trichrome (MT) at 7 and 14 days of life. UUO induced collagen deposition in neonatal kidneys of WT (G) and *Tlr2*^{-/-} mice (H) on day 14. Renal sections of UUO- and sham-operated mice were stained for alpha-SMA at

7 and 14 days of life. UUO induced α -SMA expression in neonatal kidneys of WT (J) and *Tlr2*^{-/-} mice (K) on day 14. Analysis of α -SMA positive myofibroblasts in UUO-kidneys on day 7 and 14 (L) showed no significant differences between the two groups. Results are indicated as x-fold increase above sham operated control in 20 hpfs (x400); n = 8. Data are presented as mean +/- SEM. Bar = 100 μ m. Standalone * represents significant differences between Sham and UUO results.

<https://doi.org/10.1371/journal.pone.0294142.g006>

could be observed (Fig 6F). We conclude that TLR2 does not have an impact on the M2 macrophage and T-lymphocyte infiltration in the neonatal kidney with UUO. To study interstitial fibrosis in WT and *Tlr2*^{-/-} mice after neonatal UUO, Masson's Trichrome and α -smooth muscle actin (α -SMA) staining of kidney sections were performed (Fig 6G–6L). Additionally, protein expression of α -SMA, matrix metalloproteinase-2 (MMP-2), and transforming growth factor (TGF)- β was measured by western blot (Fig 7B–7D). Interstitial collagen deposition

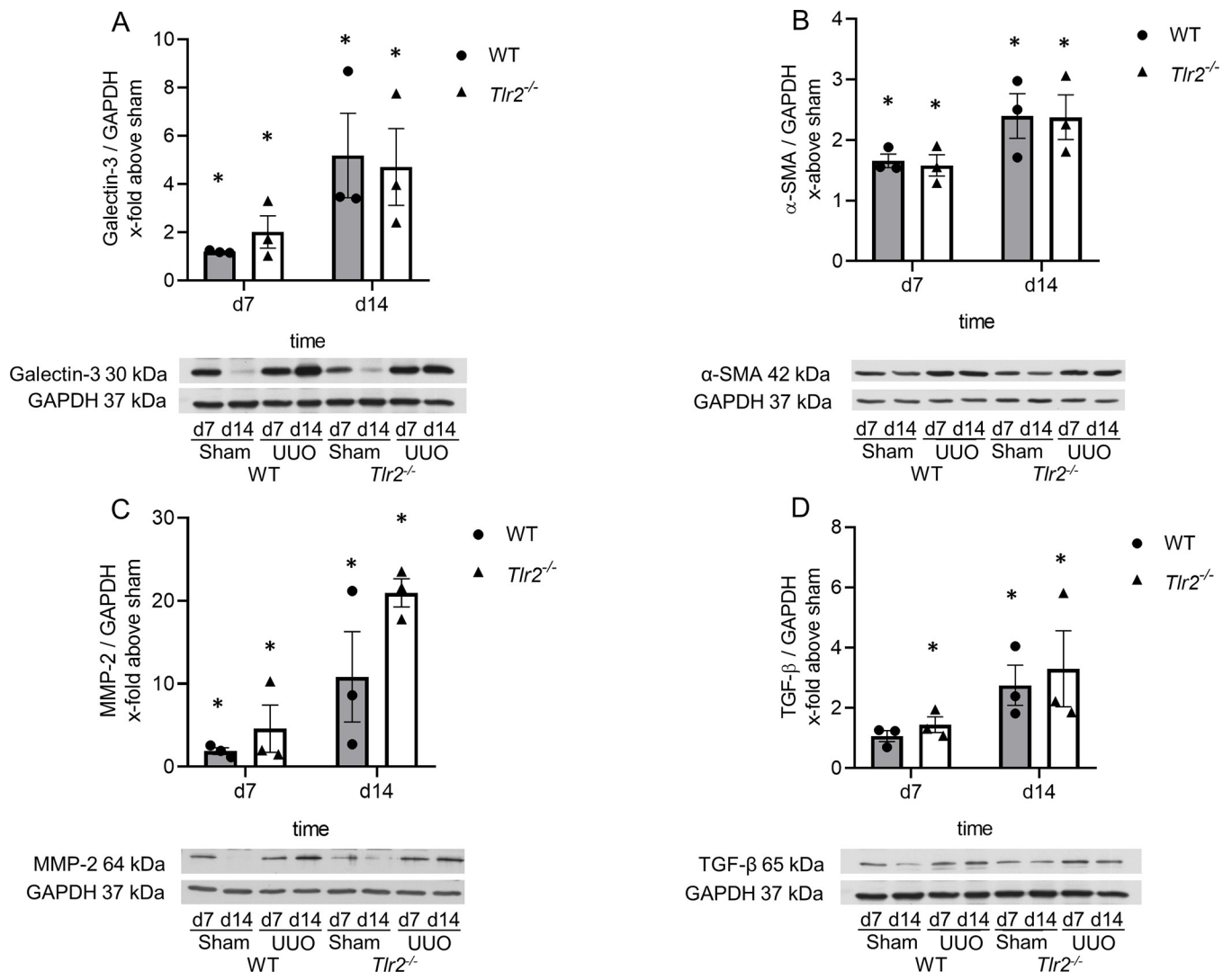


Fig 7. Protein expression of macrophage and fibrosis markers after UUO. Neonatal mice were subjected to UUO or sham operation. Whole kidneys were processed for western blot analysis at day 7 and 14. UUO induced galectin-3 expression in neonatal UUO kidneys, without significant differences between WT and *Tlr2*^{-/-} kidneys (A). UUO induced the expression of the fibrotic markers α -SMA (B), MMP-2 (C) and TGF- β (D), but without significant differences between *Tlr2*^{-/-} and WT mice at day 7 and 14 of life. Expression is indicated as x-fold increase above sham operated control, n = 3. Data are presented as mean +/- SEM. Standalone * represents significant differences between Sham and UUO results.

<https://doi.org/10.1371/journal.pone.0294142.g007>

measured by the Masson's Trichrome staining, increased after UUO in both WT and *Tlr2*^{-/-} mice (Fig 6G–6I). The abundance of α -SMA increased at d7 and d14 after UUO but was not different in *Tlr2*^{-/-} mice in comparison to WT mice (Fig 6J–6L). Following neonatal UUO, α -SMA expression increased significantly at d7 and d14 (Fig 7B), but without significant differences between WT and *Tlr2*^{-/-} kidneys. MMP-2 expression increased significantly after ureteral obstruction at d7 and d14 in WT and *Tlr2*^{-/-} mice (Fig 7D), with a slightly increasing trend for *Tlr2*^{-/-} kidneys, but without significant differences between the two lines. UUO induced increased TGF- β -expression (Fig 7D) in the neonatal kidneys, but *Tlr2*^{-/-} mice were not significantly different from WT mice. We therefore conclude that TLR2 does not attenuate renal fibrosis in the neonatal kidney with UUO.

Discussion

Our study indicates involvement of TLR2 in the mediation of apoptosis in the early life developing murine kidney suffering from ureteral obstruction. This result is of potential relevance because the pattern recognition receptor TLR2 is an element of innate immunity, which drives various kidney diseases elicited experimentally in animal models [8, 30]. Exemplarily, TLR2 induces inflammation and renal injury in the adult model of ischemia/reperfusion injury and in streptozotocin-induced diabetic mice [13, 17, 31].

Here, we investigated a potential pro-apoptotic role of TLR2 using neonatal *Tlr2*^{-/-} mice we subjected to UUO. Firstly, we show that TLR2 expression is upregulated after UUO in neonatal mouse kidneys, which indicates a potential role of this receptor in obstructive nephropathy. This is in line with studies in adult mice, where TLR2 expression is markedly upregulated after UUO [32].

Secondly, by using neonatal *Tlr2*^{-/-} mice we demonstrate that TLR2 mediates tubular and interstitial apoptosis in the obstructed neonatal kidney. Following UUO, neonatal kidneys of *Tlr2*^{-/-} mice displayed markedly reduced abundance of tubular apoptotic nuclei, measured by a TUNEL assay. These apoptotic nuclei were predominantly present in distal tubular cells, which is in line with our published data on programmed cell death in the neonatal kidney [5]. In addition, interstitial apoptosis was also markedly reduced in neonatal *Tlr2*^{-/-} mouse kidneys, suggesting their carriage of either less apoptotic infiltrating leukocytes or less apoptotic myofibroblasts and fibroblasts as compared to controls. In contrast, glomerular apoptosis did not differ between *Tlr2*^{-/-} and WT kidneys. To potentially reinforce differences in tubular and interstitial apoptosis in WT and *Tlr2*^{-/-} mice borne kidneys, caspase 8 expression was measured, but showed no difference between the lines in the neonatal kidneys of newborn mice undergoing UUO. Caspase-8 expression has limitations as an apoptotic marker, as it is a marker of the early phase of apoptosis [33]. In contrast, TUNEL staining has been designed to detect apoptotic cells that undergo extensive DNA degradation during the late stages of apoptosis [34]. Therefore, the differences between *Tlr2*^{-/-} and WT kidneys may not be detectable during the initiation phase of apoptosis but become apparent in the late apoptotic stages of DNA degradation. In addition, as caspase-8 protein expression is measured for all compartments of the kidney by using whole neonatal kidney lysates for western blot analysis, a compartment-restricted expression of caspase 8 might have indicated differences we missed by our global approach. As our results were conflicting, we decided to include Bcl-2 as an anti-apoptotic marker [35, 36]. The increase of Bcl-2 expression in *Tlr2*^{-/-} kidneys further confirms our findings that TLR2 mediates apoptosis in neonatal UUO. Our result “apoptosis reduction in *Tlr2*^{-/-} mice” is in line with Leemans et al., who showed that TLR2 activates the apoptotic pathway in UUO-kidneys of adult mice [32]. The authors measured apoptosis through staining of active caspase-3 in cells, which was significantly reduced in *Tlr2*^{-/-} mice after 7 days of ureteral

obstruction. Unfortunately, we were not able to measure caspase-3 in neonatal kidneys most certainly as the abundance of this antigen was below the detection limit. In the neonatal model of unilateral ureteral obstruction, it is currently unknown how this *Tlr2*^{-/-} associated apoptotic pathway is activated, caspase-3 might not be involved at all. TLR2, as a part of the innate immune system is activated by bacterial lipoproteins and signals for apoptosis through MyD88 via a pathway involving Fas-associated death domain protein and caspase-8 [37, 38]. Inflammation following UO is not mediated by bacteria. UO induces sterile inflammation, which is mediated by DAMPs, of which a variety might be able to activate the TLR2 mediated apoptotic pathway [23, 39]. High levels of apoptosis are associated with nephron loss in the developing kidney and thus the loss of renal function [40].

Besides apoptosis, necrosis and regulated necrosis are cell death mechanisms that are operative during UO [41]. Previously we demonstrated necroptosis, a form of regulated necrosis, to be increased in the neonatal kidney undergoing UO [5]. Here we demonstrate for the first time, that pyroptosis is also upregulated in the neonatal kidney with UO. Pyroptosis is a gasdermin-mediated programmed cell death that involves the activation of inflammasomes by DAMPs [42]. Pyroptosis plays an important role in the progression of kidney disease and is involved in various kidney disease models [43]. Here we analyzed pyroptosis in neonatal *Tlr2*^{-/-} and WT mice with UO by the analyzing cleaved GSDMD and full-length GSDME abundances. The cleavage of GSDMD, or alternatively GSDME is a crucial step in the initiation of pyroptosis and pore formation [24]. In our study we show that UO in neonatal kidneys induces. This observation is in accordance with findings in adult mice and rats subjected to UO [44, 45]. However, pyroptosis was not different in *Tlr2*^{-/-} mice as compared to WT controls suggesting that TLR2 is not involved in pyroptotic cell death following neonatal UO.

TLR2 borne intracellular signal transduction is induced by sterile insult and triggers inflammation [46]. Inflammation is a major driver of UO pathology associated with release of DAMPs and pro-inflammatory cytokines initiating it [23, 39]. It is currently unknown what DAMP induces apoptosis through TLR2. Numerous DAMPs are putative ligands of TLR2 [23, 47]. HMGB1 is involved in inflammasome activation as well as regulation of apoptosis [48, 49]. To investigate if HMGB1 mediates sterile inflammation in neonatal kidneys after UO, we measured kidney borne HMGB1 expression levels. We show here for the first time that HMGB1 expression in neonatal kidneys did not increase after UO. This contrasts with findings in kidneys of adult mice, where UO caused a marked upregulation of kidney inherent HMGB1 [50] and may be explainable by differential expression in the course of kidney development. Nephrogenesis in mice starts at embryonic day 8 and is completed 2–3 weeks after birth. In contrast to adult UO, neonatal UO impairs kidney development and reduces nephron mass, as nephrogenesis is still going on. Thus, HMGB1 signaling may be differentially regulated in neonatal and adult mice with UO. TNF, a pro-inflammatory cytokine, is another mediator of sterile inflammation following UO. The activation of TLR2 principally leads to production of TNF [13, 51]. TNF is highly upregulated in kidneys of adult mice with UO [52]. Contrary to our expectations, *Tlr2*^{-/-} and WT mice did not upregulate TNF expression after UO. Additionally, there were no differences between kidneys of the genotypes. Thus, sterile inflammation in neonatal kidneys after UO seems to be mediated by neither HMGB1 nor TNF. Identification of DAMPs and mediators eliciting apoptosis in neonatal kidneys through TLR2 still is to be investigated.

In order to examine if TLR2 has an influence on proliferation in the neonatal UO model, we analyzed relative abundances of KI67 positive tubular cells. We show that the number of proliferating tubules decreased following UO. Whereas in adult UO a decrease of proliferation was observed in *Tlr2*^{-/-} kidneys in comparison to WT [32], in neonatal UO lacked such

dichotomy. Since neonatal kidney cells highly proliferate in general, slight differences between the two lines could have been overshadowed by the impact UO has on nephrogenesis.

Morphological alterations in the tubular compartment play an important role in the pathogenesis of neonatal obstructive uropathy. Tubular atrophy is mainly a concern in proximal tubules, which is in line with previous results [5]. We were not able to observe differences between *Tlr2*^{-/-} and WT neonatal kidneys regarding tubular atrophy. TLR2 does not influence tubular atrophy after neonatal UO.

Renal interstitial fibrosis develops parallel to renal injury and sterile inflammation after neonatal UO. Fibroblast density increases due to local proliferation of resident fibroblasts, the recruitment of fibrocytes and possibly epithelial-mesenchymal transition (EMT) [53]. T-lymphocytes and M2 macrophages are crucial in the development of renal fibrosis [54, 55]. It has been shown that in the adult UO model M2 macrophages facilitate renal fibrosis [56]. Several studies have shown that depletion of T-cells after UO in adult mice results in a reduction of renal fibrosis [57, 58]. Here, we observed a marked infiltration of M2-macrophages and T-cells after neonatal UO. However, for all measured parameters there were no significant differences between *Tlr2*^{-/-} and WT neonatal mice. This is in line with published data showing that a TLR2 knockout does not influence macrophage infiltration in adult UO [32]. Expansion of fibrous connective tissue and abnormal deposition of extracellular matrix produced by myofibroblasts build the basis for fibrotic diseases. We measured the quantity of fibrotic collagen fibers in neonatal UO kidneys, evaluated myofibroblasts by α -SMA staining and protein expression, and investigated the fibrotic marker TGF- β . The results show a significant increase of renal fibrosis in neonatal kidneys after UO. We were not able to observe differences between *Tlr2*^{-/-} and WT mice. Matrix metalloproteinases are involved in EMT following UO. MMP-2 aggravates the expression of EMT-associated molecules and renal fibrosis in adult UO [59]. In our study, MMP-2 increased noticeably after neonatal UO, but without differences between *Tlr2*^{-/-} and WT mice. By contrast, adult UO kidneys showed a diminished expression of MMP-2 in *Tlr2*^{-/-} mice. Thus, expression of MMP-2 after UO may be differently regulated in neonatal and adult kidneys. Overall, TLR2 does not influence interstitial fibrosis in neonatal mouse kidneys with UO.

Numerous studies showed involvement of TLR2 in acute kidney injury [13, 60]. Inhibition of TLR2 reduced the recruitment of NK cells, as well as neutrophil infiltration and renal damage to the kidney after IRI [60, 61]. TLR2 and its endogenous stress ligands are markedly upregulated in obstructed kidneys in adult mice [32, 62]. Our results demonstrate that TLR2 does play an essential role neither in kidney inflammation nor in the development of renal fibrosis following neonatal UO. Recently, it has been shown that inhibition of both RAS and TLR2 has an additive ameliorative effect on UO injury of the kidney [63]. Given this information it may be more effective to target additional pathways besides TLR2 in the obstructed kidney to ameliorate inflammation and fibrosis.

Conclusion

TLR2 plays an important role in mediating tubular and interstitial apoptosis in the neonatal kidney with obstruction. Inhibition of TLR2 in obstructive nephropathy could prevent apoptosis and save nephron mass, which would be otherwise irreversibly lost. Blocking TLR2 may be beneficial in the developing kidney with obstruction until the obstruction resolves or a surgical correction is performed. However, TLR2 does not influence inflammatory responses or development of renal fibrosis after UO. Thus, a combination with other inhibitors may be of advantage.

Supporting information

S1 Raw images. Western blot raw images. Uncropped western blot gel images for TLR2 and GAPDH in neonatal WT kidneys (on day 7 and 14 of life). * marks the section used in Fig 1. TLR2 and GAPDH were visualized separately, but they represent the same gel. Uncropped western blot gel images for TLR2 and GAPDH in neonatal WT kidneys (on day 7 and 14 of life). * marks the section used in Fig 1. For Bax Gel 2 was used. Uncropped western blot gel images for Caspase-8 and GAPDH in neonatal WT and TLR2^{-/-} kidneys (on day 7 and 14 of life). * marks the section used in Fig 2. Caspase-8 and GAPDH were visualized separately, but they represent the same gel. Uncropped western blot gel images for GSDMD and GAPDH in neonatal WT and TLR2^{-/-} kidneys (on day 7 and 14 of life). * marks the section used in Fig 3. GSDMD and GAPDH were visualized separately, but they represent the same gel. Uncropped western blot gel images for GSDME and GAPDH in neonatal WT and TLR2^{-/-} kidneys (on day 7 and 14 of life). * marks the section used in Fig 3. GSDME and GAPDH were visualized separately, but they represent the same gel. Uncropped western blot gel images for HMGB1 and GAPDH in neonatal WT and TLR2^{-/-} kidneys (on day 7 and 14 of life). * marks the section used in Fig 3. Uncropped western blot gel images for TNF- α and GAPDH in neonatal WT and TLR2^{-/-} kidneys (on day 7 and 14 of life). * marks the section used in Fig 3. TNF- α and GAPDH were visualized separately (different exposer times), but they represent the same gel. Uncropped western blot gel images for Galectin-3, TGF- β , and GAPDH in neonatal WT and TLR2^{-/-} kidneys (on day 7 and 14 of life). * marks the section used in Fig 6. Uncropped western blot gel images for α -SMA and GAPDH in neonatal WT and TLR2^{-/-} kidneys (on day 7 and 14 of life). * marks the section used in Fig 6. Uncropped western blot gel images for MMP-2 and GAPDH in neonatal WT and TLR2^{-/-} kidneys (on day 7 and 14 of life). * marks the section used in Fig 6. MMP-2 and GAPDH were visualized separately, but they represent the same gel.
(PDF)

Author Contributions

Conceptualization: Carsten Kirschning.

Data curation: Maja Wyczanska.

Formal analysis: Maja Wyczanska, Jana Rohling.

Investigation: Ursula Keller.

Methodology: Maja Wyczanska, Jana Rohling, Marcus R. Benz.

Project administration: Bärbel Lange-Sperandio.

Resources: Bärbel Lange-Sperandio.

Supervision: Bärbel Lange-Sperandio.

Validation: Bärbel Lange-Sperandio.

Writing – original draft: Maja Wyczanska, Bärbel Lange-Sperandio.

Writing – review & editing: Maja Wyczanska, Bärbel Lange-Sperandio.

References

1. van der Ven AT, Connaughton DM, Ityel H, Mann N, Nakayama M, Chen J, et al. Whole-Exome Sequencing Identifies Causative Mutations in Families with Congenital Anomalies of the Kidney and

- Urinary Tract. *J Am Soc Nephrol*. 2018; 29(9):2348–61. Epub 2018/08/26. <https://doi.org/10.1681/ASN.2017121265> PMID: 30143558; PubMed Central PMCID: PMC6115658.
2. Babu R, Vittalraj P, Sundaram S, Shalini S. Pathological changes in ureterovesical and ureteropelvic junction obstruction explained by fetal ureter histology. *J Pediatr Urol*. 2019; 15(3):240 e1–e7. Epub 20190211. <https://doi.org/10.1016/j.jpuro.2019.02.001> PMID: 30850354.
 3. Luyckx VA, Brenner BM. Clinical consequences of developmental programming of low nephron number. *Anat Rec (Hoboken)*. 2020; 303(10):2613–31. Epub 20191006. <https://doi.org/10.1002/ar.24270> PMID: 31587509.
 4. Lange-Sperandio B. Pediatric Obstructive Uropathy. *Pediatric Nephrology*. Berlin Heidelberg: Springer-Verlag; 2022. p. 1369–98.
 5. Popper B, Rammer MT, Gasparitsch M, Singer T, Keller U, Doring Y, et al. Neonatal obstructive nephropathy induces necroptosis and necroinflammation. *Sci Rep*. 2019; 9(1):18600. Epub 2019/12/11. <https://doi.org/10.1038/s41598-019-55079-w> PMID: 31819111; PubMed Central PMCID: PMC6901532.
 6. Meng XM, Mak TS, Lan HY. Macrophages in Renal Fibrosis. *Adv Exp Med Biol*. 2019; 1165:285–303. https://doi.org/10.1007/978-981-13-8871-2_13 PMID: 31399970.
 7. Liu M, Zen K. Toll-Like Receptors Regulate the Development and Progression of Renal Diseases. *Kidney Dis (Basel)*. 2021; 7(1):14–23. Epub 2021/02/23. <https://doi.org/10.1159/000511947> PMID: 33614730; PubMed Central PMCID: PMC7879300.
 8. Sepe V, Libetta C, Gregorini M, Rampino T. The innate immune system in human kidney inflammaging. *J Nephrol*. 2022; 35(2):381–95. Epub 2021/11/27. <https://doi.org/10.1007/s40620-021-01153-4> PMID: 34826123; PubMed Central PMCID: PMC8617550.
 9. Fitzgerald KA, Kagan JC. Toll-like Receptors and the Control of Immunity. *Cell*. 2020; 180(6):1044–66. Epub 20200311. <https://doi.org/10.1016/j.cell.2020.02.041> PMID: 32164908; PubMed Central PMCID: PMC9358771.
 10. Feldman N, Rotter-Maskowitz A, Okun E. DAMPs as mediators of sterile inflammation in aging-related pathologies. *Ageing Res Rev*. 2015; 24(Pt A):29–39. Epub 20150129. <https://doi.org/10.1016/j.arr.2015.01.003> PMID: 25641058.
 11. Gay NJ, Symmons MF, Gangloff M, Bryant CE. Assembly and localization of Toll-like receptor signalling complexes. *Nat Rev Immunol*. 2014; 14(8):546–58. <https://doi.org/10.1038/nri3713> PMID: 25060580.
 12. Lin Z, Lin H, Li W, Huang Y, Dai H. Complement Component C3 Promotes Cerebral Ischemia/Reperfusion Injury Mediated by TLR2/NFkappaB Activation in Diabetic Mice. *Neurochem Res*. 2018; 43(8):1599–607. Epub 20180613. <https://doi.org/10.1007/s11064-018-2574-z> PMID: 29948726.
 13. Mohamed ME, Kandeel M, Abd El-Lateef HM, El-Beltagi HS, Younis NS. The Protective Effect of Anethole against Renal Ischemia/Reperfusion: The Role of the TLR2,4/MYD88/NFkappaB Pathway. *Antioxidants (Basel)*. 2022; 11(3). Epub 20220311. <https://doi.org/10.3390/antiox11030535> PMID: 35326185; PubMed Central PMCID: PMC8944622.
 14. Yiu WH, Lin M, Tang SC. Toll-like receptor activation: from renal inflammation to fibrosis. *Kidney Int Suppl (2011)*. 2014; 4(1):20–5. <https://doi.org/10.1038/kisup.2014.5> PMID: 26312146; PubMed Central PMCID: PMC4536963.
 15. van Bergenhenegouwen J, Plantinga TS, Joosten LA, Netea MG, Folkerts G, Kraneveld AD, et al. TLR2 & Co: a critical analysis of the complex interactions between TLR2 and coreceptors. *J Leukoc Biol*. 2013; 94(5):885–902. Epub 20130829. <https://doi.org/10.1189/jlb.0113003> PMID: 23990624.
 16. Habib R. Multifaceted roles of Toll-like receptors in acute kidney injury. *Heliyon*. 2021; 7(3):e06441. Epub 20210308. <https://doi.org/10.1016/j.heliyon.2021.e06441> PMID: 33732942; PubMed Central PMCID: PMC7944035.
 17. Ma J, Wu H, Zhao CY, Panchapakesan U, Pollock C, Chadban SJ. Requirement for TLR2 in the development of albuminuria, inflammation and fibrosis in experimental diabetic nephropathy. *Int J Clin Exp Pathol*. 2014; 7(2):481–95. Epub 2014/02/20. PMID: 24551269; PubMed Central PMCID: PMC3925893.
 18. Liu C, Shen Y, Huang L, Wang J. TLR2/caspase-5/Panx1 pathway mediates necrosis-induced NLRP3 inflammasome activation in macrophages during acute kidney injury. *Cell Death Discov*. 2022; 8(1):232. Epub 20220426. <https://doi.org/10.1038/s41420-022-01032-2> PMID: 35473933; PubMed Central PMCID: PMC9042857.
 19. Paveljssek D, Ivicak-Kocjan K, Treven P, Bencina M, Jerala R, Rogelj I. Distinctive probiotic features share common TLR2-dependent signalling in intestinal epithelial cells. *Cell Microbiol*. 2021; 23(1):e13264. Epub 20201001. <https://doi.org/10.1111/cmi.13264> PMID: 32945079; PubMed Central PMCID: PMC7757178.

20. Yang H, Wang H, Andersson U. Targeting Inflammation Driven by HMGB1. *Front Immunol.* 2020; 11:484. Epub 20200320. <https://doi.org/10.3389/fimmu.2020.00484> PMID: 32265930; PubMed Central PMCID: PMC7099994.
21. He M, Bianchi ME, Coleman TR, Tracey KJ, Al-Abed Y. Exploring the biological functional mechanism of the HMGB1/TLR4/MD-2 complex by surface plasmon resonance. *Mol Med.* 2018; 24(1):21. Epub 20180510. <https://doi.org/10.1186/s10020-018-0023-8> PMID: 30134799; PubMed Central PMCID: PMC6085627.
22. Chen Q, Guan X, Zuo X, Wang J, Yin W. The role of high mobility group box 1 (HMGB1) in the pathogenesis of kidney diseases. *Acta Pharm Sin B.* 2016; 6(3):183–8. Epub 2016/05/14. <https://doi.org/10.1016/j.apsb.2016.02.004> PMID: 27175328; PubMed Central PMCID: PMC4856949.
23. Wyczanska M, Lange-Sperandio B. DAMPs in Unilateral Ureteral Obstruction. *Front Immunol.* 2020; 11:581300. Epub 20201007. <https://doi.org/10.3389/fimmu.2020.581300> PMID: 33117389; PubMed Central PMCID: PMC7575708.
24. Liu P, Zhang Z, Li Y. Relevance of the Pyroptosis-Related Inflammasome Pathway in the Pathogenesis of Diabetic Kidney Disease. *Front Immunol.* 2021; 12:603416. Epub 2021/03/12. <https://doi.org/10.3389/fimmu.2021.603416> PMID: 33692782; PubMed Central PMCID: PMC7937695.
25. Braga TT, Correa-Costa M, Guise YF, Castoldi A, de Oliveira CD, Hyane MI, et al. MyD88 signaling pathway is involved in renal fibrosis by favoring a TH2 immune response and activating alternative M2 macrophages. *Mol Med.* 2012; 18:1231–9. Epub 2012/07/11. <https://doi.org/10.2119/molmed.2012.00131> PMID: 22777483; PubMed Central PMCID: PMC3510298.
26. Spiller S, Dreher S, Meng G, Grabiec A, Thomas W, Hartung T, et al. Cellular recognition of trimyristoylated peptide or enterobacterial lipopolysaccharide via both TLR2 and TLR4. *J Biol Chem.* 2007; 282(18):13190–8. Epub 20070312. <https://doi.org/10.1074/jbc.M610340200> PMID: 17353199.
27. Lange-Sperandio B, Schimpgen K, Rodenbeck B, Chavakis T, Bierhaus A, Nawroth P, et al. Distinct roles of Mac-1 and its counter-receptors in neonatal obstructive nephropathy. *Kidney Int.* 2006; 69(1):81–8. Epub 2005/12/24. <https://doi.org/10.1038/sj.ki.5000017> PMID: 16374427.
28. Gasparitsch M, Schieber A, Schaubeck T, Keller U, Cattaruzza M, Lange-Sperandio B. Tyrphostin AG490 reduces inflammation and fibrosis in neonatal obstructive nephropathy. *PLoS One.* 2019; 14(12):e0226675. Epub 2019/12/18. <https://doi.org/10.1371/journal.pone.0226675> PMID: 31846485; PubMed Central PMCID: PMC6917291.
29. Orning P, Lien E. Multiple roles of caspase-8 in cell death, inflammation, and innate immunity. *J Leukoc Biol.* 2021; 109(1):121–41. Epub 2020/06/13. <https://doi.org/10.1002/JLB.3MR0420-305R> PMID: 32531842; PubMed Central PMCID: PMC8664275.
30. Krivan S, Kapelouzou A, Vagios S, Tsilimigras DI, Katsimpoulas M, Moris D, et al. Increased expression of Toll-like receptors 2, 3, 4 and 7 mRNA in the kidney and intestine of a septic mouse model. *Sci Rep.* 2019; 9(1):4010. Epub 20190308. <https://doi.org/10.1038/s41598-019-40537-2> PMID: 30850654; PubMed Central PMCID: PMC6408498.
31. Yuan Y, Liu Y, Sun M, Ye H, Feng Y, Liu Z, et al. Aggravated renal fibrosis is positively associated with the activation of HMGB1-TLR2/4 signaling in STZ-induced diabetic mice. *Open Life Sci.* 2022; 17(1):1451–61. Epub 2022/12/01. <https://doi.org/10.1515/biol-2022-0506> PMID: 36448056; PubMed Central PMCID: PMC9658007.
32. Leemans JC, Butter LM, Pulskens WP, Teske GJ, Claessen N, van der Poll T, et al. The role of Toll-like receptor 2 in inflammation and fibrosis during progressive renal injury. *PLoS One.* 2009; 4(5):e5704. Epub 2009/05/30. <https://doi.org/10.1371/journal.pone.0005704> PMID: 19479087; PubMed Central PMCID: PMC2682651.
33. Elmore S. Apoptosis: a review of programmed cell death. *Toxicol Pathol.* 2007; 35(4):495–516. Epub 2007/06/15. <https://doi.org/10.1080/01926230701320337> PMID: 17562483; PubMed Central PMCID: PMC2117903.
34. Kyrylkova K, Kyryachenko S, Leid M, Kiousi C. Detection of apoptosis by TUNEL assay. *Methods Mol Biol.* 2012; 887:41–7. Epub 2012/05/09. https://doi.org/10.1007/978-1-61779-860-3_5 PMID: 22566045.
35. Chipuk JE, Moldoveanu T, Llambi F, Parsons MJ, Green DR. The BCL-2 family reunion. *Mol Cell.* 2010; 37(3):299–310. <https://doi.org/10.1016/j.molcel.2010.01.025> PMID: 20159550; PubMed Central PMCID: PMC3222298.
36. Zhang G, Oldroyd SD, Huang LH, Yang B, Li Y, Ye R, et al. Role of apoptosis and Bcl-2/Bax in the development of tubulointerstitial fibrosis during experimental obstructive nephropathy. *Exp Nephrol.* 2001; 9(2):71–80. <https://doi.org/10.1159/000052597> PMID: 11150855.
37. Aliprantis AO, Yang RB, Weiss DS, Godowski P, Zychlinsky A. The apoptotic signaling pathway activated by Toll-like receptor-2. *EMBO J.* 2000; 19(13):3325–36. Epub 2000/07/06. <https://doi.org/10.1093/emboj/19.13.3325> PMID: 10880445; PubMed Central PMCID: PMC313930.

38. Nguyen TNY, Padungros P, Wongsrisupphakul P, Sa-Ard-lam N, Mahanonda R, Matangkasombut O, et al. Cell wall mannan of *Candida krusei* mediates dendritic cell apoptosis and orchestrates Th17 polarization via TLR-2/MyD88-dependent pathway. *Sci Rep*. 2018; 8(1):17123. Epub 20181120. <https://doi.org/10.1038/s41598-018-35101-3> PMID: 30459422; PubMed Central PMCID: PMC6244250.
39. Gong T, Liu L, Jiang W, Zhou R. DAMP-sensing receptors in sterile inflammation and inflammatory diseases. *Nat Rev Immunol*. 2020; 20(2):95–112. Epub 20190926. <https://doi.org/10.1038/s41577-019-0215-7> PMID: 31558839.
40. Priante G, Gianesello L, Ceol M, Del Prete D, Anglani F. Cell Death in the Kidney. *Int J Mol Sci*. 2019; 20(14). Epub 20190723. <https://doi.org/10.3390/ijms20143598> PMID: 31340541; PubMed Central PMCID: PMC6679187.
41. Xiao X, Du C, Yan Z, Shi Y, Duan H, Ren Y. Inhibition of Necroptosis Attenuates Kidney Inflammation and Interstitial Fibrosis Induced By Unilateral Ureteral Obstruction. *Am J Nephrol*. 2017; 46(2):131–8. Epub 20170720. <https://doi.org/10.1159/000478746> PMID: 28723681.
42. Sarhan M, von Massenhausen A, Hugo C, Oberbauer R, Linkermann A. Immunological consequences of kidney cell death. *Cell Death Dis*. 2018; 9(2):114. Epub 2018/01/27. <https://doi.org/10.1038/s41419-017-0057-9> PMID: 29371597; PubMed Central PMCID: PMC5833784.
43. Zhang KJ, Wu Q, Jiang SM, Ding L, Liu CX, Xu M, et al. Pyroptosis: A New Frontier in Kidney Diseases. *Oxid Med Cell Longev*. 2021; 2021:6686617. Epub 2021/05/20. <https://doi.org/10.1155/2021/6686617> PMID: 34007404; PubMed Central PMCID: PMC8102120.
44. Zhang Y, Zhang R, Han X. Disulfiram inhibits inflammation and fibrosis in a rat unilateral ureteral obstruction model by inhibiting gasdermin D cleavage and pyroptosis. *Inflamm Res*. 2021; 70(5):543–52. Epub 2021/04/15. <https://doi.org/10.1007/s00011-021-01457-y> PMID: 33851234.
45. Wu M, Xia W, Jin Q, Zhou A, Wang Q, Li S, et al. Gasdermin E Deletion Attenuates Ureteral Obstruction- and 5/6 Nephrectomy-Induced Renal Fibrosis and Kidney Dysfunction. *Front Cell Dev Biol*. 2021; 9:754134. Epub 2021/11/09. <https://doi.org/10.3389/fcell.2021.754134> PMID: 34746148; PubMed Central PMCID: PMC8567074.
46. Shen H, Kreisel D, Goldstein DR. Processes of sterile inflammation. *J Immunol*. 2013; 191(6):2857–63. Epub 2013/09/10. <https://doi.org/10.4049/jimmunol.1301539> PMID: 24014880; PubMed Central PMCID: PMC3787118.
47. Schattner M. Sleep like a bear. *Science*. 2023; 380(6641):133–4. Epub 20230413. <https://doi.org/10.1126/science.adh3276> PMID: 37053327.
48. Yang H, Wang H, Chavan SS, Andersson U. High Mobility Group Box Protein 1 (HMGB1): The Prototypical Endogenous Danger Molecule. *Mol Med*. 2015; 21 Suppl 1:S6–S12. Epub 2015/11/26. <https://doi.org/10.2119/molmed.2015.00087> PMID: 26605648; PubMed Central PMCID: PMC4661054.
49. Foglio E, Pellegrini L, Germani A, Russo MA, Limana F. HMGB1-mediated apoptosis and autophagy in ischemic heart diseases. *Vasc Biol*. 2019; 1(1):H89–H96. Epub 20190812. <https://doi.org/10.1530/VB-19-0013> PMID: 32923959; PubMed Central PMCID: PMC7439920.
50. Tian S, Zhang L, Tang J, Guo X, Dong K, Chen SY. HMGB1 exacerbates renal tubulointerstitial fibrosis through facilitating M1 macrophage phenotype at the early stage of obstructive injury. *Am J Physiol Renal Physiol*. 2015; 308(1):F69–75. Epub 2014/11/08. <https://doi.org/10.1152/ajprenal.00484.2014> PMID: 25377911; PubMed Central PMCID: PMC4281691.
51. Papadopoulos G, Weinberg EO, Massari P, Gibson FC 3rd, Wetzler LM, Morgan EF, et al. Macrophage-specific TLR2 signaling mediates pathogen-induced TNF-dependent inflammatory oral bone loss. *J Immunol*. 2013; 190(3):1148–57. Epub 2012/12/25. <https://doi.org/10.4049/jimmunol.1202511> PMID: 23264656; PubMed Central PMCID: PMC3549226.
52. Al-Lamki RS, Mayadas TN. TNF receptors: signaling pathways and contribution to renal dysfunction. *Kidney Int*. 2015; 87(2):281–96. Epub 20140820. <https://doi.org/10.1038/ki.2014.285> PMID: 25140911.
53. Zhou J, Jiang H, Jiang H, Fan Y, Zhang J, Ma X, et al. The ILE1/LIFR complex induces EMT via the Akt and ERK pathways in renal interstitial fibrosis. *J Transl Med*. 2022; 20(1):54. Epub 20220129. <https://doi.org/10.1186/s12967-022-03265-2> PMID: 35093095; PubMed Central PMCID: PMC8800269.
54. Braga TT, Agudelo JS, Camara NO. Macrophages During the Fibrotic Process: M2 as Friend and Foe. *Front Immunol*. 2015; 6:602. Epub 2015/12/05. <https://doi.org/10.3389/fimmu.2015.00602> PMID: 26635814; PubMed Central PMCID: PMC4658431.
55. Tang PM, Nikolic-Paterson DJ, Lan HY. Macrophages: versatile players in renal inflammation and fibrosis. *Nat Rev Nephrol*. 2019; 15(3):144–58. Epub 20190128. <https://doi.org/10.1038/s41581-019-0110-2> PMID: 30692665.
56. Pan B, Liu G, Jiang Z, Zheng D. Regulation of renal fibrosis by macrophage polarization. *Cell Physiol Biochem*. 2015; 35(3):1062–9. Epub 2015/02/11. <https://doi.org/10.1159/000373932> PMID: 25662173.

57. Tapmeier TT, Fearn A, Brown K, Chowdhury P, Sacks SH, Sheerin NS, et al. Pivotal role of CD4+ T cells in renal fibrosis following ureteric obstruction. *Kidney Int.* 2010; 78(4):351–62. Epub 2010/06/18. <https://doi.org/10.1038/ki.2010.177> PMID: 20555323.
58. Liu L, Kou P, Zeng Q, Pei G, Li Y, Liang H, et al. CD4+ T Lymphocytes, especially Th2 cells, contribute to the progress of renal fibrosis. *Am J Nephrol.* 2012; 36(4):386–96. Epub 2012/10/12. <https://doi.org/10.1159/000343283> PMID: 23052013.
59. Du X, Shimizu A, Masuda Y, Kuwahara N, Arai T, Kataoka M, et al. Involvement of matrix metalloproteinase-2 in the development of renal interstitial fibrosis in mouse obstructive nephropathy. *Lab Invest.* 2012; 92(8):1149–60. Epub 2012/05/23. <https://doi.org/10.1038/labinvest.2012.68> PMID: 22614125.
60. Kim HJ, Park SJ, Koo S, Cha HJ, Lee JS, Kwon B, et al. Inhibition of kidney ischemia-reperfusion injury through local infusion of a TLR2 blocker. *J Immunol Methods.* 2014; 407:146–50. Epub 2014/04/01. <https://doi.org/10.1016/j.jim.2014.03.014> PMID: 24681240.
61. Kim HJ, Lee JS, Kim A, Koo S, Cha HJ, Han JA, et al. TLR2 signaling in tubular epithelial cells regulates NK cell recruitment in kidney ischemia-reperfusion injury. *J Immunol.* 2013; 191(5):2657–64. Epub 2013/08/02. <https://doi.org/10.4049/jimmunol.1300358> PMID: 23904170.
62. Skuginna V, Lech M, Allam R, Ryu M, Clauss S, Susanti HE, et al. Toll-like receptor signaling and SIGIRR in renal fibrosis upon unilateral ureteral obstruction. *PLoS One.* 2011; 6(4):e19204. Epub 2011/05/06. <https://doi.org/10.1371/journal.pone.0019204> PMID: 21544241; PubMed Central PMCID: PMC3081345.
63. Chung S, Jeong JY, Chang YK, Choi DE, Na KR, Lim BJ, et al. Concomitant inhibition of renin angiotensin system and Toll-like receptor 2 attenuates renal injury in unilateral ureteral obstructed mice. *Korean J Intern Med.* 2016; 31(2):323–34. Epub 2016/03/05. <https://doi.org/10.3904/kjim.2015.004> PMID: 26932402; PubMed Central PMCID: PMC4773720.

References

- [1] B. Lange-Sperandio, "Pediatric Obstructive Uropathy," in *Pediatric Nephrology*. Berlin Heidelberg: Springer-Verlag, 2022, ch. 57, pp. 1369-1398.
- [2] R. L. Chevalier, B. A. Thornhill, M. S. Forbes, and S. C. Kiley, "Mechanisms of renal injury and progression of renal disease in congenital obstructive nephropathy," *Pediatr Nephrol*, vol. 25, no. 4, pp. 687-97, Apr 2010, doi: 10.1007/s00467-009-1316-5.
- [3] M. Gasparitsch *et al.*, "RAGE-mediated interstitial fibrosis in neonatal obstructive nephropathy is independent of NF-kappaB activation," *Kidney Int*, vol. 84, no. 5, pp. 911-9, Nov 2013, doi: 10.1038/ki.2013.171.
- [4] B. A. Warady and V. Chadha, "Chronic kidney disease in children: the global perspective," *Pediatr Nephrol*, vol. 22, no. 12, pp. 1999-2009, Dec 2007, doi: 10.1007/s00467-006-0410-1.
- [5] B. Lange-Sperandio, H. Anders, M. Stehr, R. L. Chevalier, and R. Klaus, "Congenital Anomalies of the Kidney and Urinary Tract: A Continuum of Care," *Seminars in Nephrology*, vol. 43, no. 4, 2023, doi: <https://doi.org/10.1016/j.semnephrol.2023.151433>.
- [6] B. A. Thornhill and R. L. Chevalier, "Variable partial unilateral ureteral obstruction and its release in the neonatal and adult mouse," *Methods Mol Biol*, vol. 886, pp. 381-92, 2012, doi: 10.1007/978-1-61779-851-1_33.
- [7] M. M. Rodriguez, "Congenital Anomalies of the Kidney and the Urinary Tract (CAKUT)," *Fetal Pediatr Pathol*, vol. 33, no. 5-6, pp. 293-320, Oct-Dec 2014, doi: 10.3109/15513815.2014.959678.
- [8] A. Wiesel, A. Queisser-Luft, M. Clementi, S. Bianca, C. Stoll, and E. S. Group, "Prenatal detection of congenital renal malformations by fetal ultrasonographic examination: an analysis of 709,030 births in 12 European countries," *Eur J Med Genet*, vol. 48, no. 2, pp. 131-44, Apr-Jun 2005, doi: 10.1016/j.ejmg.2005.02.003.
- [9] C. P. Chang *et al.*, "Calcineurin is required in urinary tract mesenchyme for the development of the pyeloureteral peristaltic machinery," *J Clin Invest*, vol. 113, no. 7, pp. 1051-8, Apr 2004, doi: 10.1172/JCI20049.
- [10] J. Klein *et al.*, "Congenital ureteropelvic junction obstruction: human disease and animal models," *Int J Exp Pathol*, vol. 92, no. 3, pp. 168-92, Jun 2011, doi: 10.1111/j.1365-2613.2010.00727.x.
- [11] A. Avanoğlu and S. Tiryaki, "Embryology and Morphological (Mal)Development of UPJ," *Front Pediatr*, vol. 8, p. 137, 2020, doi: 10.3389/fped.2020.00137.
- [12] R. L. Chevalier, M. S. Forbes, and B. A. Thornhill, "Ureteral obstruction as a model of renal interstitial fibrosis and obstructive nephropathy," *Kidney Int*, vol. 75, no. 11, pp. 1145-1152, Jun 2009, doi: 10.1038/ki.2009.86.
- [13] A. C. Ucero *et al.*, "Unilateral ureteral obstruction: beyond obstruction," *Int Urol Nephrol*, vol. 46, no. 4, pp. 765-76, Apr 2014, doi: 10.1007/s11255-013-0520-1.
- [14] K. H. Yoo, B. A. Thornhill, M. S. Forbes, and R. L. Chevalier, "Inducible nitric oxide synthase modulates hydronephrosis following partial or complete unilateral ureteral obstruction in the neonatal mouse," *Am J Physiol Renal Physiol*, vol. 298, no. 1, pp. F62-71, Jan 2010, doi: 10.1152/ajprenal.00234.2009.
- [15] R. L. Chevalier, B. A. Thornhill, and A. Y. Chang, "Unilateral ureteral obstruction in neonatal rats leads to renal insufficiency in adulthood," *Kidney Int*, vol. 58, no. 5, pp. 1987-95, Nov 2000, doi: 10.1111/j.1523-1755.2000.00371.x.

- [16] R. Song and I. V. Yosypiv, "Genetics of congenital anomalies of the kidney and urinary tract," *Pediatr Nephrol*, vol. 26, no. 3, pp. 353-64, Mar 2011, doi: 10.1007/s00467-010-1629-4.
- [17] L. D. Truong, L. Gaber, and G. Eknoyan, "Obstructive uropathy," *Contrib Nephrol*, vol. 169, pp. 311-326, 2011, doi: 10.1159/000314578.
- [18] M. J. Kubik *et al.*, "Renal developmental genes are differentially regulated after unilateral ureteral obstruction in neonatal and adult mice," *Sci Rep*, vol. 10, no. 1, p. 19302, Nov 9 2020, doi: 10.1038/s41598-020-76328-3.
- [19] W. Y. Huang *et al.*, "Renal biopsy in congenital ureteropelvic junction obstruction: evidence for parenchymal maldevelopment," *Kidney Int*, vol. 69, no. 1, pp. 137-43, Jan 2006, doi: 10.1038/sj.ki.5000004.
- [20] M. J. Hiatt, L. Ivanova, P. Trnka, M. Solomon, and D. G. Matsell, "Urinary tract obstruction in the mouse: the kinetics of distal nephron injury," *Lab Invest*, vol. 93, no. 9, pp. 1012-23, Sep 2013, doi: 10.1038/labinvest.2013.90.
- [21] R. Norregaard, H. A. M. Mutsaers, J. Frokiaer, and T. H. Kwon, "Obstructive nephropathy and molecular pathophysiology of renal interstitial fibrosis," *Physiol Rev*, vol. 103, no. 4, pp. 2827-2872, Oct 1 2023, doi: 10.1152/physrev.00027.2022.
- [22] M. Wyczanska and B. Lange-Sperandio, "DAMPs in Unilateral Ureteral Obstruction," *Front Immunol*, vol. 11, p. 581300, 2020, doi: 10.3389/fimmu.2020.581300.
- [23] M. T. Grande, F. Perez-Barriocanal, and J. M. Lopez-Novoa, "Role of inflammation in tubulo-interstitial damage associated to obstructive nephropathy," *J Inflamm (Lond)*, vol. 7, p. 19, Apr 22 2010, doi: 10.1186/1476-9255-7-19.
- [24] B. Popper *et al.*, "Neonatal obstructive nephropathy induces necroptosis and necroinflammation," *Sci Rep*, vol. 9, no. 1, p. 18600, Dec 9 2019, doi: 10.1038/s41598-019-55079-w.
- [25] R. L. Chevalier, M. S. Forbes, C. I. Galarreta, and B. A. Thornhill, "Responses of proximal tubular cells to injury in congenital renal disease: fight or flight," *Pediatr Nephrol*, vol. 29, no. 4, pp. 537-41, Apr 2014, doi: 10.1007/s00467-013-2590-9.
- [26] M. S. Forbes, B. A. Thornhill, and R. L. Chevalier, "Proximal tubular injury and rapid formation of atubular glomeruli in mice with unilateral ureteral obstruction: a new look at an old model," *Am J Physiol Renal Physiol*, vol. 301, no. 1, pp. F110-7, Jul 2011, doi: 10.1152/ajprenal.00022.2011.
- [27] J. Gao, L. Wu, S. Wang, and X. Chen, "Role of Chemokine (C-X-C Motif) Ligand 10 (CXCL10) in Renal Diseases," *Mediators Inflamm*, vol. 2020, p. 6194864, 2020, doi: 10.1155/2020/6194864.
- [28] T. M. Tumpey, R. Fenton, S. Molesworth-Kenyon, J. E. Oakes, and R. N. Lausch, "Role for macrophage inflammatory protein 2 (MIP-2), MIP-1alpha, and interleukin-1alpha in the delayed-type hypersensitivity response to viral antigen," *J Virol*, vol. 76, no. 16, pp. 8050-7, Aug 2002, doi: 10.1128/jvi.76.16.8050-8057.2002.
- [29] M. Gasparitsch, A. Schieber, T. Schaubeck, U. Keller, M. Cattaruzza, and B. Lange-Sperandio, "Tyrphostin AG490 reduces inflammation and fibrosis in neonatal obstructive nephropathy," *PLoS One*, vol. 14, no. 12, p. e0226675, 2019, doi: 10.1371/journal.pone.0226675.

- [30] C. H. Weng *et al.*, "Interleukin-17A induces renal fibrosis through the ERK and Smad signaling pathways," *Biomed Pharmacother*, vol. 123, p. 109741, Mar 2020, doi: 10.1016/j.biopha.2019.109741.
- [31] R. S. Al-Lamki and T. N. Mayadas, "TNF receptors: signaling pathways and contribution to renal dysfunction," *Kidney Int*, vol. 87, no. 2, pp. 281-96, Feb 2015, doi: 10.1038/ki.2014.285.
- [32] P. M. Tang, D. J. Nikolic-Paterson, and H. Y. Lan, "Macrophages: versatile players in renal inflammation and fibrosis," *Nat Rev Nephrol*, vol. 15, no. 3, pp. 144-158, Mar 2019, doi: 10.1038/s41581-019-0110-2.
- [33] X. Wang, J. Chen, J. Xu, J. Xie, D. C. H. Harris, and G. Zheng, "The Role of Macrophages in Kidney Fibrosis," *Front Physiol*, vol. 12, p. 705838, 2021, doi: 10.3389/fphys.2021.705838.
- [34] R. L. Chevalier, K. H. Chung, C. D. Smith, M. Ficenc, and R. A. Gomez, "Renal apoptosis and clusterin following ureteral obstruction: the role of maturation," *J Urol*, vol. 156, no. 4, pp. 1474-9, Oct 1996. [Online]. Available: <https://www.ncbi.nlm.nih.gov/pubmed/8808911>.
- [35] E. Homsy, P. Janino, and J. B. de Faria, "Role of caspases on cell death, inflammation, and cell cycle in glycerol-induced acute renal failure," *Kidney Int*, vol. 69, no. 8, pp. 1385-92, Apr 2006, doi: 10.1038/sj.ki.5000315.
- [36] G. V. Chaitanya, A. J. Steven, and P. P. Babu, "PARP-1 cleavage fragments: signatures of cell-death proteases in neurodegeneration," *Cell Commun Signal*, vol. 8, p. 31, Dec 22 2010, doi: 10.1186/1478-811X-8-31.
- [37] G. Zhang *et al.*, "Role of apoptosis and Bcl-2/Bax in the development of tubulointerstitial fibrosis during experimental obstructive nephropathy," *Exp Nephrol*, vol. 9, no. 2, pp. 71-80, Mar-Apr 2001, doi: 10.1159/000052597.
- [38] E. Obeng, "Apoptosis (programmed cell death) and its signals - A review," *Braz J Biol*, vol. 81, no. 4, pp. 1133-1143, Oct-Dec 2021, doi: 10.1590/1519-6984.228437.
- [39] R. V. Rao *et al.*, "Coupling endoplasmic reticulum stress to the cell death program: role of the ER chaperone GRP78," *FEBS Lett*, vol. 514, no. 2-3, pp. 122-8, Mar 13 2002, doi: 10.1016/s0014-5793(02)02289-5.
- [40] K. Jung, T. Lee, J. Kim, E. Sung, and I. Song, "Interleukin-10 Protects against Ureteral Obstruction-Induced Kidney Fibrosis by Suppressing Endoplasmic Reticulum Stress and Apoptosis," *Int J Mol Sci*, vol. 23, no. 18, Sep 14 2022, doi: 10.3390/ijms231810702.
- [41] A. Linkermann and D. R. Green, "Necroptosis," *N Engl J Med*, vol. 370, no. 5, pp. 455-65, Jan 30 2014, doi: 10.1056/NEJMra1310050.
- [42] G. Priante, L. Ganesello, M. Ceol, D. Del Prete, and F. Anglani, "Cell Death in the Kidney," *Int J Mol Sci*, vol. 20, no. 14, Jul 23 2019, doi: 10.3390/ijms20143598.
- [43] K. J. Zhang *et al.*, "Pyroptosis: A New Frontier in Kidney Diseases," *Oxid Med Cell Longev*, vol. 2021, p. 6686617, 2021, doi: 10.1155/2021/6686617.
- [44] H. Yang, H. Wang, and U. Andersson, "Targeting Inflammation Driven by HMGB1," *Front Immunol*, vol. 11, p. 484, 2020, doi: 10.3389/fimmu.2020.00484.
- [45] M. Wyczanska, J. Rohling, U. Keller, M. R. Benz, C. Kirschning, and B. Lange-Sperandio, "TLR2 mediates renal apoptosis in neonatal mice subjected experimentally to obstructive nephropathy," *PLoS One*, vol. 18, no. 11, p. e0294142, 2023, doi: 10.1371/journal.pone.0294142.

- [46] Y. Liu, "Cellular and molecular mechanisms of renal fibrosis," *Nat Rev Nephrol*, vol. 7, no. 12, pp. 684-96, Oct 18 2011, doi: 10.1038/nrneph.2011.149.
- [47] R. Huang, P. Fu, and L. Ma, "Kidney fibrosis: from mechanisms to therapeutic medicines," *Signal Transduct Target Ther*, vol. 8, no. 1, p. 129, Mar 17 2023, doi: 10.1038/s41392-023-01379-7.
- [48] K. Ina, H. Kitamura, S. Tatsukawa, and Y. Fujikura, "Significance of alpha-SMA in myofibroblasts emerging in renal tubulointerstitial fibrosis," *Histol Histopathol*, vol. 26, no. 7, pp. 855-66, Jul 2011, doi: 10.14670/HH-26.855.
- [49] A. Sureshbabu, S. A. Muhsin, and M. E. Choi, "TGF-beta signaling in the kidney: profibrotic and protective effects," *Am J Physiol Renal Physiol*, vol. 310, no. 7, pp. F596-F606, Apr 1 2016, doi: 10.1152/ajprenal.00365.2015.
- [50] Z. Cheng, X. Zhang, Y. Zhang, L. Li, and P. Chen, "Role of MMP-2 and CD147 in kidney fibrosis," *Open Life Sci*, vol. 17, no. 1, pp. 1182-1190, 2022, doi: 10.1515/biol-2022-0482.
- [51] E. Deacon, A. Li, F. Boivin, A. Dvorkin-Gheva, J. Cunanan, and D. Bridgewater, "beta-Catenin in the kidney stroma modulates pathways and genes to regulate kidney development," *Dev Dyn*, vol. 252, no. 9, pp. 1224-1239, Sep 2023, doi: 10.1002/dvdy.603.
- [52] A. P. Lam and C. J. Gottardi, "beta-catenin signaling: a novel mediator of fibrosis and potential therapeutic target," *Curr Opin Rheumatol*, vol. 23, no. 6, pp. 562-7, Nov 2011, doi: 10.1097/BOR.0b013e32834b3309.
- [53] K. Wang, Q. Liao, and X. Chen, "Research progress on the mechanism of renal interstitial fibrosis in obstructive nephropathy," *Heliyon*, vol. 9, no. 8, p. e18723, Aug 2023, doi: 10.1016/j.heliyon.2023.e18723.
- [54] R. de Waal Malefyt, H. Yssel, M. G. Roncarolo, H. Spits, and J. E. de Vries, "Interleukin-10," *Curr Opin Immunol*, vol. 4, no. 3, pp. 314-20, Jun 1992, doi: 10.1016/0952-7915(92)90082-p.
- [55] M. Saraiva and A. O'Garra, "The regulation of IL-10 production by immune cells," *Nat Rev Immunol*, vol. 10, no. 3, pp. 170-81, Mar 2010, doi: 10.1038/nri2711.
- [56] L. Ding and E. M. Shevach, "IL-10 inhibits mitogen-induced T cell proliferation by selectively inhibiting macrophage costimulatory function," *J Immunol*, vol. 148, no. 10, pp. 3133-9, May 15 1992. [Online]. Available: <https://www.ncbi.nlm.nih.gov/pubmed/1578140>.
- [57] D. F. Fiorentino, A. Zlotnik, T. R. Mosmann, M. Howard, and A. O'Garra, "IL-10 inhibits cytokine production by activated macrophages," *J Immunol*, vol. 147, no. 11, pp. 3815-22, Dec 1 1991. [Online]. Available: <https://www.ncbi.nlm.nih.gov/pubmed/1940369>.
- [58] K. N. Couper, D. G. Blount, and E. M. Riley, "IL-10: the master regulator of immunity to infection," *J Immunol*, vol. 180, no. 9, pp. 5771-7, May 1 2008, doi: 10.4049/jimmunol.180.9.5771.
- [59] C. M. Wilke, S. Wei, L. Wang, I. Kryczek, J. Kao, and W. Zou, "Dual biological effects of the cytokines interleukin-10 and interferon-gamma," *Cancer Immunol Immunother*, vol. 60, no. 11, pp. 1529-41, Nov 2011, doi: 10.1007/s00262-011-1104-5.
- [60] R. A. Saxton *et al.*, "Structure-based decoupling of the pro- and anti-inflammatory functions of interleukin-10," *Science*, vol. 371, no. 6535, Mar 19 2021, doi: 10.1126/science.abc8433.

- [61] T. H. Ng, G. J. Britton, E. V. Hill, J. Verhagen, B. R. Burton, and D. C. Wraith, "Regulation of adaptive immunity; the role of interleukin-10," *Front Immunol*, vol. 4, p. 129, 2013, doi: 10.3389/fimmu.2013.00129.
- [62] F. N. Lauw, D. Pajkrt, C. E. Hack, M. Kurimoto, S. J. van Deventer, and T. van der Poll, "Proinflammatory effects of IL-10 during human endotoxemia," *J Immunol*, vol. 165, no. 5, pp. 2783-9, Sep 1 2000, doi: 10.4049/jimmunol.165.5.2783.
- [63] E. L. M. Vieira *et al.*, "Posterior urethral valve in fetuses: evidence for the role of inflammatory molecules," *Pediatr Nephrol*, vol. 32, no. 8, pp. 1391-1400, Aug 2017, doi: 10.1007/s00467-017-3614-7.
- [64] Y. Jin, R. Liu, J. Xie, H. Xiong, J. C. He, and N. Chen, "Interleukin-10 deficiency aggravates kidney inflammation and fibrosis in the unilateral ureteral obstruction mouse model," *Lab Invest*, vol. 93, no. 7, pp. 801-11, Jul 2013, doi: 10.1038/labinvest.2013.64.
- [65] W. Y. Chou *et al.*, "Electroporative interleukin-10 gene transfer ameliorates carbon tetrachloride-induced murine liver fibrosis by MMP and TIMP modulation," *Acta Pharmacol Sin*, vol. 27, no. 4, pp. 469-76, Apr 2006, doi: 10.1111/j.1745-7254.2006.00304.x.
- [66] T. Arai *et al.*, "Introduction of the interleukin-10 gene into mice inhibited bleomycin-induced lung injury in vivo," *Am J Physiol Lung Cell Mol Physiol*, vol. 278, no. 5, pp. L914-22, May 2000, doi: 10.1152/ajplung.2000.278.5.L914.
- [67] J. C. Leemans *et al.*, "The role of Toll-like receptor 2 in inflammation and fibrosis during progressive renal injury," *PLoS One*, vol. 4, no. 5, p. e5704, May 27 2009, doi: 10.1371/journal.pone.0005704.
- [68] W. H. Yiu, M. Lin, and S. C. Tang, "Toll-like receptor activation: from renal inflammation to fibrosis," *Kidney Int Suppl (2011)*, vol. 4, no. 1, pp. 20-25, Nov 2014, doi: 10.1038/kisup.2014.5.
- [69] M. Liu and K. Zen, "Toll-Like Receptors Regulate the Development and Progression of Renal Diseases," *Kidney Dis (Basel)*, vol. 7, no. 1, pp. 14-23, Jan 2021, doi: 10.1159/000511947.
- [70] K. A. Fitzgerald and J. C. Kagan, "Toll-like Receptors and the Control of Immunity," *Cell*, vol. 180, no. 6, pp. 1044-1066, Mar 19 2020, doi: 10.1016/j.cell.2020.02.041.
- [71] H. J. Kim *et al.*, "Inhibition of kidney ischemia-reperfusion injury through local infusion of a TLR2 blocker," *J Immunol Methods*, vol. 407, pp. 146-50, May 2014, doi: 10.1016/j.jim.2014.03.014.
- [72] V. Sepe, C. Libetta, M. Gregorini, and T. Rampino, "The innate immune system in human kidney inflammaging," *J Nephrol*, vol. 35, no. 2, pp. 381-395, Mar 2022, doi: 10.1007/s40620-021-01153-4.
- [73] T. T. Braga *et al.*, "MyD88 signaling pathway is involved in renal fibrosis by favoring a TH2 immune response and activating alternative M2 macrophages," *Mol Med*, vol. 18, pp. 1231-9, Oct 24 2012, doi: 10.2119/molmed.2012.00131.
- [74] D. Paveljsek, K. Ivicak-Kocjan, P. Treven, M. Bencina, R. Jerala, and I. Rogelj, "Distinctive probiotic features share common TLR2-dependent signalling in intestinal epithelial cells," *Cell Microbiol*, vol. 23, no. 1, p. e13264, Jan 2021, doi: 10.1111/cmi.13264.
- [75] Q. Chen, X. Guan, X. Zuo, J. Wang, and W. Yin, "The role of high mobility group box 1 (HMGB1) in the pathogenesis of kidney diseases," *Acta Pharm Sin B*, vol. 6, no. 3, pp. 183-8, May 2016, doi: 10.1016/j.apsb.2016.02.004.

- [76] M. Weitz, M. Schmidt, and G. Laube, "Primary non-surgical management of unilateral ureteropelvic junction obstruction in children: a systematic review," *Pediatr Nephrol*, vol. 32, no. 12, pp. 2203-2213, Dec 2017, doi: 10.1007/s00467-016-3566-3.
- [77] S. Balster, M. Schiborr, O. A. Brinkmann, and L. Hertle, "[Obstructive uropathy in childhood]," *Aktuelle Urol*, vol. 36, no. 4, pp. 317-28, Aug 2005, doi: 10.1055/s-2005-870934. Obstruktive Uropathien im Kindesalter.
- [78] D. I. Williams, "The diagnosis and treatment of obstructive uropathy in childhood," *Bibl Paediatr*, vol. 74, pp. 445-69, 1960. [Online]. Available: <https://www.ncbi.nlm.nih.gov/pubmed/13844838>.
- [79] R. Klaus, T. K. Barth, A. Imhof, F. Thalmeier, and B. Lange-Sperandio, "Comparison of clean catch and bag urine using LC-MS/MS proteomics in infants," *Pediatr Nephrol*, vol. 39, no. 1, pp. 203-212, Jan 2024, doi: 10.1007/s00467-023-06098-3.
- [80] C. Caubet *et al.*, "Advances in urinary proteome analysis and biomarker discovery in pediatric renal disease," *Pediatr Nephrol*, vol. 25, no. 1, pp. 27-35, Jan 2010, doi: 10.1007/s00467-009-1251-5.
- [81] R. L. Chevalier, "Congenital urinary tract obstruction: the long view," *Adv Chronic Kidney Dis*, vol. 22, no. 4, pp. 312-9, Jul 2015, doi: 10.1053/j.ackd.2015.01.012.
- [82] G. Grandaliano *et al.*, "MCP-1 and EGF renal expression and urine excretion in human congenital obstructive nephropathy," *Kidney Int*, vol. 58, no. 1, pp. 182-92, Jul 2000, doi: 10.1046/j.1523-1755.2000.00153.x.
- [83] M. T. El-Sherbiny, O. M. Mousa, A. A. Shokeir, and M. A. Ghoneim, "Role of urinary transforming growth factor-beta1 concentration in the diagnosis of upper urinary tract obstruction in children," *J Urol*, vol. 168, no. 4 Pt 2, pp. 1798-800, Oct 2002, doi: 10.1097/01.ju.0000027231.84450.8f.
- [84] F. Bandin *et al.*, "Urinary proteome analysis at 5-year followup of patients with nonoperated ureteropelvic junction obstruction suggests ongoing kidney remodeling," *J Urol*, vol. 187, no. 3, pp. 1006-11, Mar 2012, doi: 10.1016/j.juro.2011.10.169.
- [85] A. Scalabre *et al.*, "Early detection of ureteropelvic junction obstruction in neonates with prenatal diagnosis of renal pelvis dilatation using (1)H NMR urinary metabolomics," *Sci Rep*, vol. 12, no. 1, p. 13406, Aug 4 2022, doi: 10.1038/s41598-022-17664-4.
- [86] Z. Lin, H. Lin, W. Li, Y. Huang, and H. Dai, "Complement Component C3 Promotes Cerebral Ischemia/Reperfusion Injury Mediated by TLR2/NFkappaB Activation in Diabetic Mice," *Neurochem Res*, vol. 43, no. 8, pp. 1599-1607, Aug 2018, doi: 10.1007/s11064-018-2574-z.

Acknowledgements

I am deeply grateful to Prof. Dr. Lange-Sperandio for the possibility to be part of an amazing research team. Her expert direction, abundant advice, and unwavering enthusiasm have guided me through the challenges and triumphs of this project. I extend my heartfelt thanks to Ursula Keller for her warm reception in the nephrology laboratory. This thesis would not have been possible without the support of several collaborators, whom I am highly grateful for their support. It is an honor to have you as authors on my publications.

Lastly, I express my appreciation to my partner and our families for their unwavering support throughout this journey.